TABLE OF CONTENTS

EXECUTIVE SUMMARY

The development of the reliability based offshore platform design and requalification involves defining the scope (class of structure, load cases, etc.) and code format - including definition of characteristics values; selecting reliability measure; assessing uncertainties in loads and resistance; establishing target reliability level; and accomplishing the calibration itself to determine partial safety factors.

The uncertainty assessment is one of the most important components in the development of the reliability based design and requalification criteria. The nature of uncertainties and methods for their modeling and analysis is the key in any reliability analysis and design. Four types of uncertainty are dominant: a) inherent randomness, which arise from intrinsic variability in materials and environment effects, such as the wave elevation at a given position in the ocean; b) statistical uncertainty, which arise in the course of estimating parameters of probability distributions from observed sample of limit size; c) model uncertainty, which arises from the imperfection of mathematical models used to describe complex physical phenomena, such as models describing loads and capacities of offshore structures and foundation; d) human error which arises from erroneous actions, inaction, and activities of people.

There is another equivalent uncertainty classification system. The uncertainty due to inherent randomness is called Type I uncertainty. The statistical and model uncertainty is called Type II uncertainty. The human error is called Type III uncertainty. Whereas the type I uncertainty due to inherent randomness is irreducible, type II statistical and model uncertainty can be reduced, the former by collection of additional samples, and the latter by use of more refined models.

The objective of this report is to conduct the uncertainty analysis of static strength of tubular joints in assisting the screening methodology in use for offshore platforms reassessment and requalification. Following the introduction of the tubular joint technology development, the basic theory of the joint capacity are summarized. The existing design guidelines are reviewed and evaluated. Based on the evaluation of the existing codes, the uncertainty models of simple joints and complex joints are developed based on the database established during the past decades.

1.0 INTRODUCTION AND BACKGROUND

1.1 BACKGROUND

The first attempt at tubular joint design in the later 1950s were based on elastic analyses of the tubular shell. It quickly became apparent from a few tests in the early 1960s that there was little correlation between ultimate strength and elastic shell analysis. This led to a series of tests in the mid 1960s and covered a limited range of joint types and geometry. These tests were recognized as mainly "pilot" tests to investigate the relative importance such as β (ratio of brace diameter to chord diameter) and γ (ratio of chord radius to chord wall thickness).

The American Petroleum Institute Specification API RP 2A was first published in 1969. The first edition used some 30 test results to define a lower bound capacity based on the punching shear stress concept. The first code was very simple to use; all members framing into the joints were considered separately as T or Y. No K joint were specified.

A large number of tubular joint research programs were undertaken in the 1970s. The database of test results exceeded 300 and size of specimens increased significantly. API RP 2A, however, maintained a single expression with slightly adjustments to the punching shear format. It became apparent in the late 1970s that a single simple expression for joint capacity could not be used to encompass all joint types and load conditions.

At about the same time, offshore tubular joint research was greatly expanded by UK, Norway as North Sea developed. These research programs led to a greater awareness that significant research effort was being expanded on simple joints subjected to unidirectional loading. However, the design problem involved complex loading and complex geometry. Therefore, since later 1970s, research effort has been directed towards area such as determination of joint moment capacities, the interaction of multi-directional brace loading, the interaction of chord load with brace load and the capacity of K joints.

Perhaps the greatest impact on tubular joint design since later 1970s has been the collation and critical assessment of tubular joint data. The databases were generated by experimental studies and numerical studies. The critical assessment of these data led to the development of the design codes such as API, UK HSE Codes. Statistical analysis and lower bound fits to the test data become common practice and more and more 'design' equations appeared in the literature. It is generally recognized that Yura (1980), UK Den (HSE) (1990a), UEG Design Guide (1985), and Wardenier (1982) represent excellent examples of data organization and appraisal.

The draft amendment proposed for the UK Department of Energy (HSE)'s guidance Notes was based on ultimate strength concept. API RP2A, on the other hand, adopted the ultimate strength concept at its 15 edition after some thirteen editions of API RP 2A where a single expression based on the punching

shear stress concept was used together with multipliers to accommodate the various joint types and load cases.

1.2   DESIGN CODE DEVELOPMENT

1.2.1   API RP 2A

The American Petroleum Institute's API RP2A traditionally relied on a single expression based on the punching shear stress concept to define joint capacities for all editions up to and include the 13th. Various multipliers were used to accommodate different joint and load cases. Major changes were made to the 14th edition. However, this edition was withdrawn a few months later due to significant typographical errors inherent in the recommendations. The corrected recommendations were re-issued in the 15th edition in 1984.

In the 15th edition of API RP 2A, the nominal load approach was used as an alternative to the punching shear stress concept. Both approaches are intended to give equivalent results. The code requires that the applied nominal load, which is calculated from design loading, should not be greater than a maximum allowable load. The allowable loads for different joint types and load cases have been derived from a lower bound interpretation of test data and contains a factor of safety against static collapse. Until the 20th edition, the applied nominal load approach was adopted solely in the API RP 2A.

1.2.2   UK HSE CODE

The UK Heath and Safety Executive (HSE, former Department of Energy) first published its Guidance on the design and construction of offshore installation in 1974 in order to provide a basis whereby fixed and mobile offshore installations could be certified as being fit for their purpose. In the first edition, no recommendations for the design of tubular joints were published. In subsequent editions, 1977 and 1984, the guidance given was limited to a report by Kurobane et al (1976) which presented a limited number of ultimate strength formulae with no specific recommendation on the value or application of safety factors. In 1990's edition, subsequent revision has been made based on the review of the published database and JISSP (Joint Industry Static Strength Project) data developed by Wimpey Offshore (1986). The resulting guidance is relatively therefore comprehensive and reflects advanced knowledge in the tubular joint design in 1980s.

1.2.3   ISO CODE

In the 1990s, there has been a major industry initiative to harmonize worldwide, offshore design codes as ISO standards. The ISO code has not only to set up a common set of technical criteria, but also incorporate recent research findings that are not yet included in the API RP 2A or the UK HSE Guidance notes.

Since 1980, there is a dramatically increase in the knowledge of the tubular joint design. Therefore, the new ISO standards are quite different and much more

comprehensive than those in other offshore codes of practice. For the joint static strength, the primary code enhancements have been in the areas of design considerations and capacity of both simple and complex joints. Under design considerations, load-displacement formulation appears for the first time. Furthermore, there is substantive improvements in guidance on material limits, minimum capacity, joint classification, and detailing practice.

The ISO code provides extensive modification to existing guidance of simple joint capacity. The new ISO code also has improved guidance with respect to capacity of complex joints, especially overlapping, grouted, and internally ring-stiffened ones.

1.3   OBJECTIVE AND SCOPE

The objective of this report is to provide a reassessment of the tubular joint databases to evaluate its uncertainty and reliability. Following a summary of the basic theory about tubular joints, it describes a review of data on the static strength of tubular joints in offshore structures. Based on the review, available engineering guidelines, namely HSE Guidance 1991, and API RP 2A 1993, for tubular joints are evaluated to assess their reliability and uncertainty. The evaluation focuses, in turn, on three interrelated problems areas: 1) simple joints, 2) complex joints, and 3) design considerations. Based on the evaluation, uncertainty models and design recommendations are developed to facilitate the development of the screening methodologies for use in platform assessments and requalifications.

This report is divided into eight sections. Section 2 summarizes the basic theory of the tubular joints. The existing design guidance are reviewed in the section 3. Section 4 describes a review of data on the static strength of tubular joints. An evaluation of the existing design guidelines is summarized in Section 5. Based on the evaluation, the uncertainty models associated with the existing design guidelines are developed in Sections 6, 7 and 8. Section 9 summarizes the calibration and verification of the uncertainty models. Section 10 is the summary and conclusions.

2.0 BASIC THEORY

2.1 GENERAL

Joints between panels, and rectangular tubulars with the same width can be designed based on diaphragms to transfer loads by membrane forces, and the ultimate strength may be fairly easily estimated. Joints between cylindrical members have much more complex shell behavior. Such joints can be classified as (HSE, 1991):
- Simple joint, and
- Complex joint.

Simple joints are defined as joints formed by the welding of two or more tubular in a single plane without overlap of brace members and without the use of gussets, diaphragms, stiffened, or grout (Figure 2.1). Overlapping joints are defined as joints in which part of the brace forces are transferred between overlapping braces through their common weld (Figure 2.2).

In simple joint, the joint type usually looks like the letter formed from the brace and chord intersection. Four basic simple joint types exist in offshore structures:
- T or Y Joint
- K Joint
- KT Joint
- X Joint

Although the joint type usually looks like the letter formed from the brace and chord intersection, the joint is actually classified based on load distribution. If the axial load is transferred between the brace and chord by shear, the joint is T or Y joints. If the load is transferred between the braces at a joint without travelling through the joint, it is classified as a K joint. If the load is transferred by some combination of shear through the joint and brace-to-brace, then the joint is KT. The X joint is to transfer the load from one chord side to another side.

2.2 FAILURE MODES OF SIMPLE JOINTS

The mode of failure of a tubular joint is dependent on the type of joint, loading conditions and the geometrical parameters defining the joint . Tests carried out have identified several types of failures, namely
1. Plastic failure of the chord,
2. Cracking and gross separation of brace from chord,
3. Cracking of the brace,
4. Local buckling,
5. Shear failure of the chord between adjacent bracings, and
6. Lamellar tearing of thick chord walls under brace tension loading (often considered as a material - related failure).

Typical load-deformation curves for axially loaded joints are shown in Figure 2.3. For tension loading, yielding of the chord around the brace and distortion of

the chord cross-section occurs. As the load increases, a crack at the 'hot spot' which eventually leads to gross separation of the brace from the chord. Failure in compression loaded T/Y and DT/X joint is usually associated with buckling and plastic deformation of the chord wall. The stiffness and capacity of DT/X joints are less than those of T/Y joints. Although the failure modes are similar with regard to deformations local to the brace/chord intersection, these are clearly differences in the way that brace axial loads are reacted by the chord; global bending of the chord can occur in T/Y joints but not in DT/X joints. In addition, DT/X joints are subjected to a double ovalisation. In general, for braced steel jacket structures, axial stresses make up some 70% of the total brace stress. Therefore, one may expect failure by the plastic deformation of the chord wall to be dominant.

The failure mechanism of balanced axially loaded K joints (tension in one brace, compression in other brace) largely depends on the gap between the two brace members. For large gaps, the joint behaves as two single-brace T/Y joints. As the gap reduces, the strength of the joint can increase due to the increased bending stiffness of the chord between the braces. Chord plastic deformation and 'punching' failure are the two most common modes of failure for these joints. However, for large β ratios, shear failure of the chord section between the two brace members can occur.

Typically, for in-plane moment loaded joints, failure occurs due to fracture through the chord wall on the tension side of the brace and plastic bending and buckling of the chord on the compression side. For out-of-plane moment loaded joints, local buckling of the chord wall in the vicinity of the brace saddle on the compression side occurs, resulting in reduced stiffness. Failure is usually associated with fracture on the tension side of the brace after excessive plastic deformations.

2.3   PRINCIPAL FACTORS

Research and in-service experience leads to the following variables which affect the static strength of a given tubular joint:

(1) Chord outside diameter   (D)
(2) Brace outside diameter   (d)
(3) Chord wall thickness   (T)
(4) Gap (for K, YT, KT joints)   (g)
(5) Included angle between chord and brace   (θ)
(6) Chord material yield stress   (F_y)

The chord and brace diameters are taken here to relate to outside tubular dimensions. The above terms are defined in Figure 2.3.

2.4   DIMENSIONAL ANALYSIS

The static strength of a tubular joint may be expressed in the form

$$(P_u) \text{ or } (M_u) = F(D, d, T, g, \theta, L, F_y, F_t) \tag{2.1}$$

where P_u and M_u are maximum axial and moment capacities respectively.

The effect of brace wall thickness t on joint strength has been examined by Kanatani (1966) and is shown to have little effect. The number of parameters involved can be reduced by introducing non-dimensional geometrical ratios as follows:

$$\alpha = 2\frac{L}{D} \qquad (2.2)$$

$$\beta = \frac{d}{D} \qquad (2.3)$$

$$\gamma = \frac{D}{2T} \qquad (2.4)$$

$$\varsigma = \frac{g}{D} \qquad (2.5)$$

$$\xi = \frac{F_y}{F_t} \qquad (2.6)$$

Thus, the equation (2.1) becomes

$$(P_u) \quad or \quad (M_u) = F(\alpha,\beta,\gamma,\varsigma,\xi,\theta,F_y) \qquad (2.7)$$

The accepted non-dimensional forms of the ultimate capacities P_u and M_u are $\dfrac{P_u}{F_y T^2}$ and $\dfrac{M_u}{F_t T^2 d}$ respectively, the term $F_y T^2$ is based on a theoretical ring analogy and can be related to the plastic moment of a ring model of unit width.

It should be recognized that, so far as chord wall failure is concerned, only the axial load component perpendicular to the chord affects joint strength, which leads to the introduction of the term $\sin\theta$ into the axial capacity equation. For moment loaded joints the two possible loading planes must be considered separately. The in-plane moment load is resisted in full at the intersection, whereas the out-of-plane moment can be resolved into a component causing bending perpendicular to the chord axis and a component causing torsion at the intersection weld. As for axial loading, the latter component for out-of-plane moment load need not be considered in the determination of joint capacities. The perpendicular component to be considered in $M_u \sin\theta$. Therefore, expressions are derived for joint strength to have the following forms:

Axial
$$\frac{P_u \sin\theta}{F_y T^2} = F(\alpha,\beta,\gamma,\varsigma,\xi,\theta) \qquad (2.8)$$

In-plane bending
$$\frac{M_u}{F_y T^2 d} = F(\alpha,\beta,\gamma,\varsigma,\xi,\theta) \qquad (2.9)$$

Out-of-plane bending
$$\frac{M_u \sin\theta}{F_y T^2 d} = F(\alpha,\beta,\gamma,\varsigma,\xi,\theta) \qquad (2.10)$$

The following parameters may also influence joint capacity:

K_a or K_a' (relative length factors)

$K_b, K_{bi},$ or K_{bo} (relative section factors)

Q_β	(sometimes referred to as geometrical factor)
η	$\dfrac{\beta}{\sin\theta}$

2.5 DEVELOPMENT OF DESIGN EQUATIONS

Based on the basic theory presented in section 2.1-2.5. The design equation of static strength of tubular joints can be developed. This section illustrates the development of design equation of compression loaded T/Y joints. The factors affecting the joint capacity are analyzed in developing the design equations.

This development is based on a total of 124 T, Y, DT, YT and K joint test data. This data group consists of over half the total joint data population in the project and as such encompasses more parameter variations than for any other data group used in this project.

The nondimensional equation can be derived as:

$$\frac{P_u \sin\theta}{F_y T^2} = F(\alpha, \beta, \gamma, \varsigma, \xi, \theta) \tag{2.11}$$

EFFECT OF α RATIO (CHORD 2L/D). Insufficient data are available to analysis the effects of change of chord length (i.e. shear span length) for T/Y joints. However, it is commonly accepted that this length should be at least four chord diameters longer ($\alpha \geq 8$) apart from a few tests conducted by Kanatani (Tables A.1, and A.4)

EFFECT OF INTERSECTION ANGLE θ, K_a', AND K_a. For simple Y, X, and K joints, the effect of the intersection angle θ manifests itself in two ways. First, the brace axial load is resolved into two perpendicular directions and only the component perpendicular to the chord wall is considered. Thus, the term $\sin\theta$ appears as a multiplier to the load P_u. Second, the length of the intersection is increased as θ. The exact length of the intersection, as measured on the outer surface of the chord, is a complex function of the brace diameter, the chord diameter, and the angle of intersection.

It is convenient to non dimensionalize the length of the intersection by expressing it as a multiple of the nominal brace perimeter (π, d). This exact 'relative length factor' is referred to as K_a' and is the non dimensionalization a function of the brace to chord diameter ratio α and the intersection angle θ.

AWS D.1-84 gives a formula for K_a' as:

$$K_a' = x + y + 3\left(x^2 + y^2\right)^{0.5} \tag{2.12}$$

where, $x = \dfrac{1}{2\pi \sin\theta}$, and $y = \dfrac{1}{3\pi} \dfrac{\left(3 - \beta^2\right)}{\left(2 - \beta^2\right)}$

The maximum value of K_a' for a T joint is 11.167 and occurs at $\beta = 1$. K_a' is asymptotic to a value of unity at $\beta = 0$.

The relative length factor curve can be obtained by using an approximate value, denoted by K_a as:

$$K_a = \frac{1 + \dfrac{1}{\sin\theta}}{2} \qquad (2.13)$$

This value is not a function of β and therefore has a value of unity for all T joints. K_a approximates the ratio between the brace perimeter measured on a plane parallel to the chord axis to that measured on a plane perpendicular to the brace axis.

A total of fifteen results are available to investigate the justification for K_a. These comprise 3 Y joint tests and 12 K joint tests with gap parameter ζ greater than 0.15. K joints with $\zeta \leq 0.15$ are significantly influenced by the gap between braces. These 15 tests all relate to the same intersection angle $\theta = 45°$ and all have β ratios of less than 0.6.

It will be shown that the general formula for the mean strength of T, Y, and K joints is:

$$\frac{P_u \sin\theta}{F_y T^2} = (2.37 + 23.60\beta)\sqrt{Q_\beta'}\, Q_g K_a \qquad (2.14)$$

Using this equation, the predicted strength of each Y and K joint was computed and compared to the actual test result. The comparison shows that on average the above formula predicts the error which would have been caused by omitting K_a would be 17%. The inclusion of K_a appears justified within the limits of experimental accuracy, limited test data and the scatter of test results.

EFFECTS OF γ RATIO ($\dfrac{D}{2T}$). Existing design codes differ in the effect on strength conducted by γ. Early publications by Yura et al (1980) as well as the API RP 2A codes suggest that γ has no effect on the strength of a tubular joint, when it is expressed in terms of non-dimensional strength.

The test data for compression loaded T joints are illustrated in Figure 2.5 against γ for groups of data points with approximately equal β values. The figure confirms that γ has no significant effect on joint strength for compression loaded T/Y joints. It should be noted that the range of γ included in the assessment greatly exceeds that used by others who have concluded different power law relationships for γ. This analysis uses results for γ as high as 46.5; different conclusions can be obtained from statistical analysis if a restricted range of γ is considered.

EFFECT OF β RATIO ($\dfrac{d}{D}$). For ease of equation format the term Q'_β is defined as

$$Q'_\beta = 1 \text{ for } \quad \beta \le 0.6$$

$$Q'_\beta = Q_\beta \qquad \text{for} \quad \beta \ge 0.6$$

Q_β is given by the formula $Q_\beta = \dfrac{0.3}{\beta(1 - 0.833\beta)}$ \hfill (2.12)

An illustration of non-dimensional strength against β is given in Figure 2.6. It includes the results of three large gap ($\zeta \ge 0.6$) K joints. The relationship is approximately linear for $\beta \le 0.6$ but strength increases at a higher rate above this value. Many design codes introduce the term Q'_β to account for this nonlinear relationship. Q'_β has a value of unity for $\beta \le 0.6$ and is equal to Q_β for higher values. Yura et al (1980) and hence API RP 2A eliminate the available tests results at $\beta = 1.0$ as being from small specimens and therefore do not introduce the term Q_β into their design equations. It is evident from Figure 2.6 that introduction of the term Q'_β would provide a greater correction factor than required, the square root of the term is introduced to ensure that correction applied is not excessive. When the test results are plotted in terms of $\sin\left(\dfrac{F_y T^2}{\sqrt{Q'_\beta K_a}}\right)$ against β a clear linear relationship results (Figure 2.7). It concluded that the introduction of the term $\sqrt{Q'_\beta}$ gives a small coefficient of variation.

The mean line does not pass through the original and thus a relationship of the following form can be used to describe the strength of compression loaded T/Y joints:

$$\frac{P_u \sin\theta}{F_y T^2 \sqrt{Q'_\beta K_a}} = A + B\beta \hspace{3cm} (2.15)$$

A least squares fit to the data gives values for A and B of 1.614 and 24.890 respectively for the mean line. Thus, the mean strength of a T/Y joint loaded in compression is given as:

$$\frac{P_u \sin\theta}{F_y T^2} = (1.61 + 24.89\beta)\sqrt{Q'_\beta}K_a \hspace{2cm} (2.16)$$

The above equation is modified as:

$$\frac{P_u \sin\theta}{F_y T^2} = (2 + 20\beta)\sqrt{Q'_\beta}K_a \hspace{2.5cm} (2.17)$$

Which is used in the UK HSE design code.

The low bound equation can be fitted by:

$$\frac{P_u \sin\theta}{F_y T^2} = (3.4 + 19\beta)$$

(2.18)

which is used in the API design guidelines.
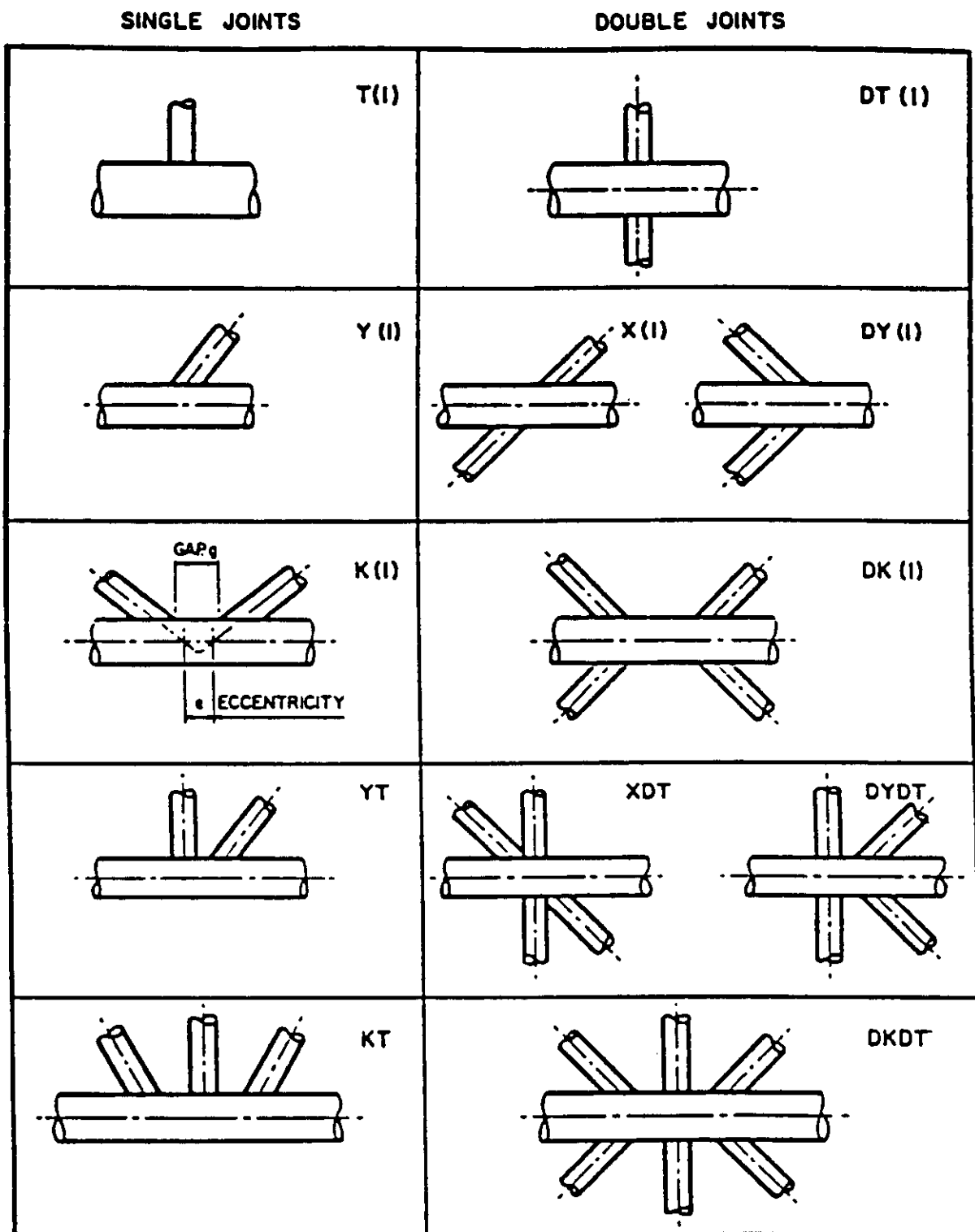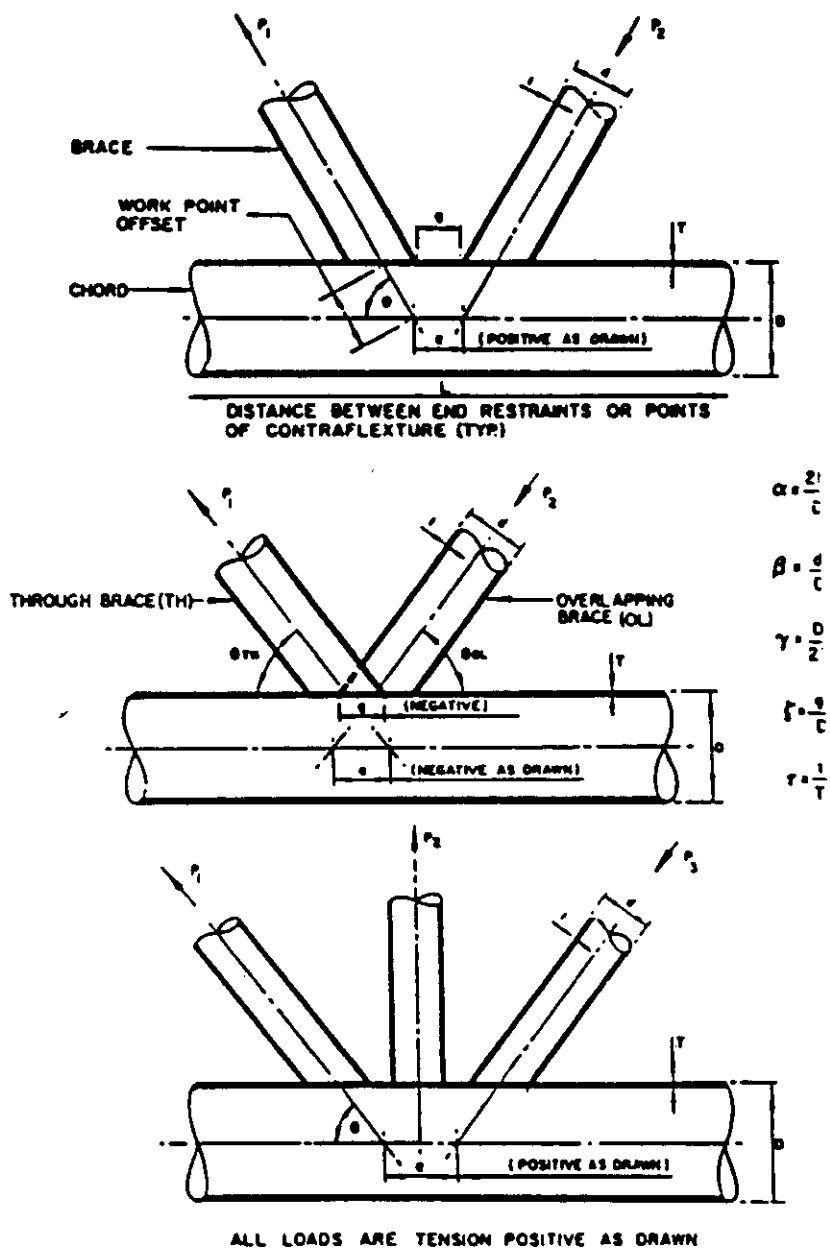
Figure 2.1 Joint Classification
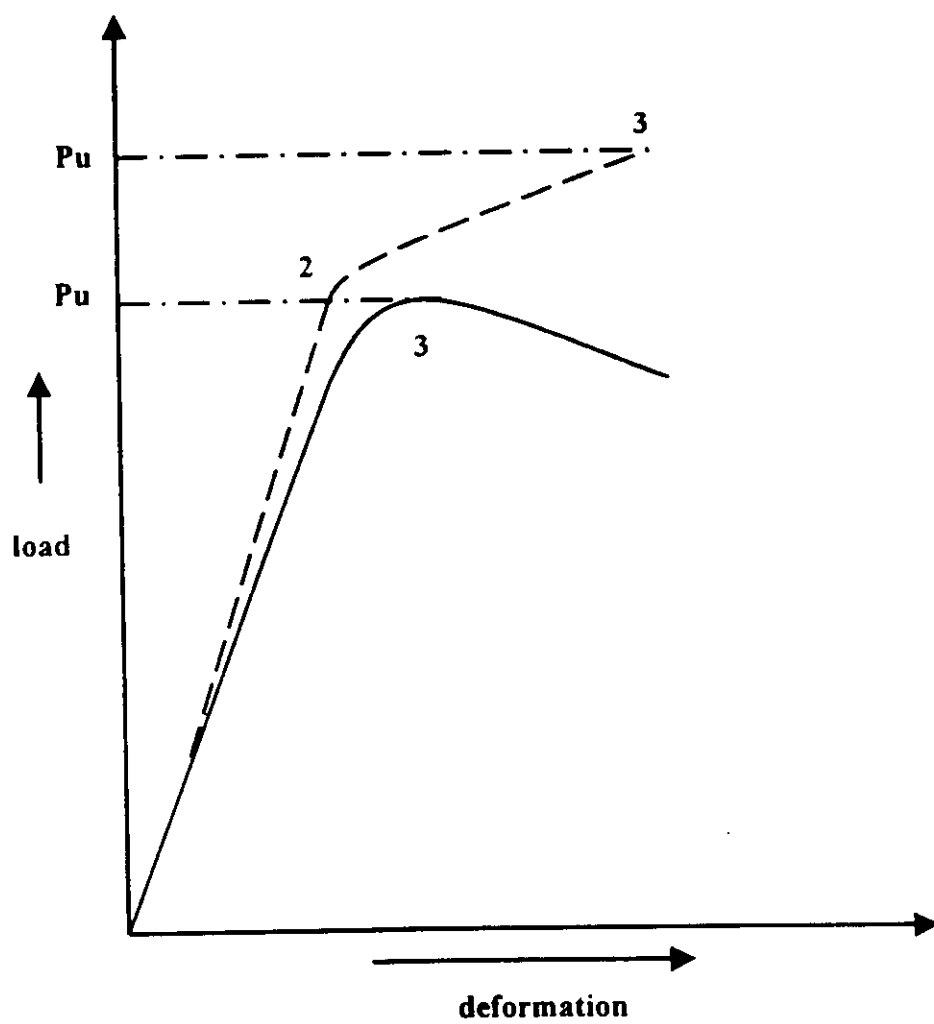
Figure 2.2 An Illustration of Overlapping Joints

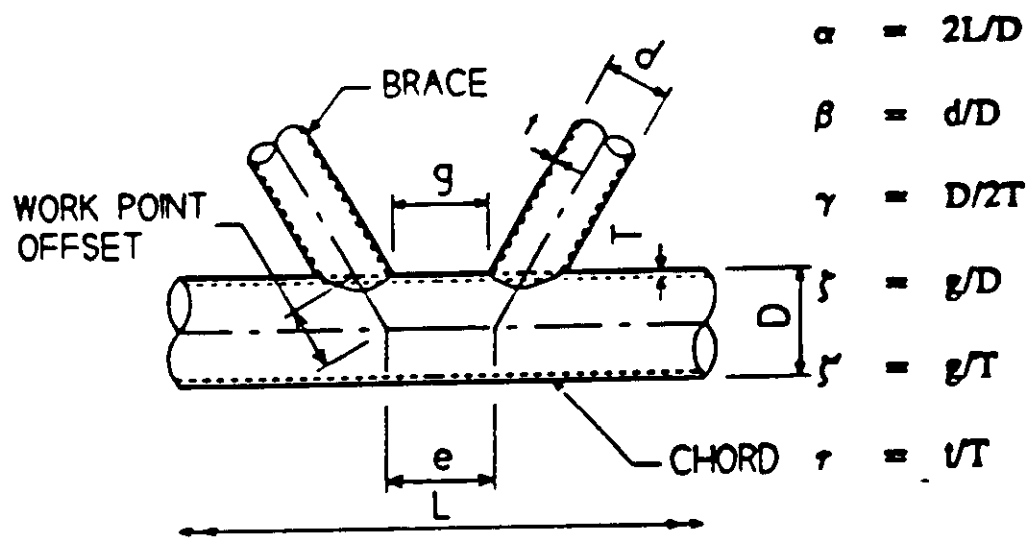Figure 2.3 A Typical Load-Deformation Curve for Tubular Joints
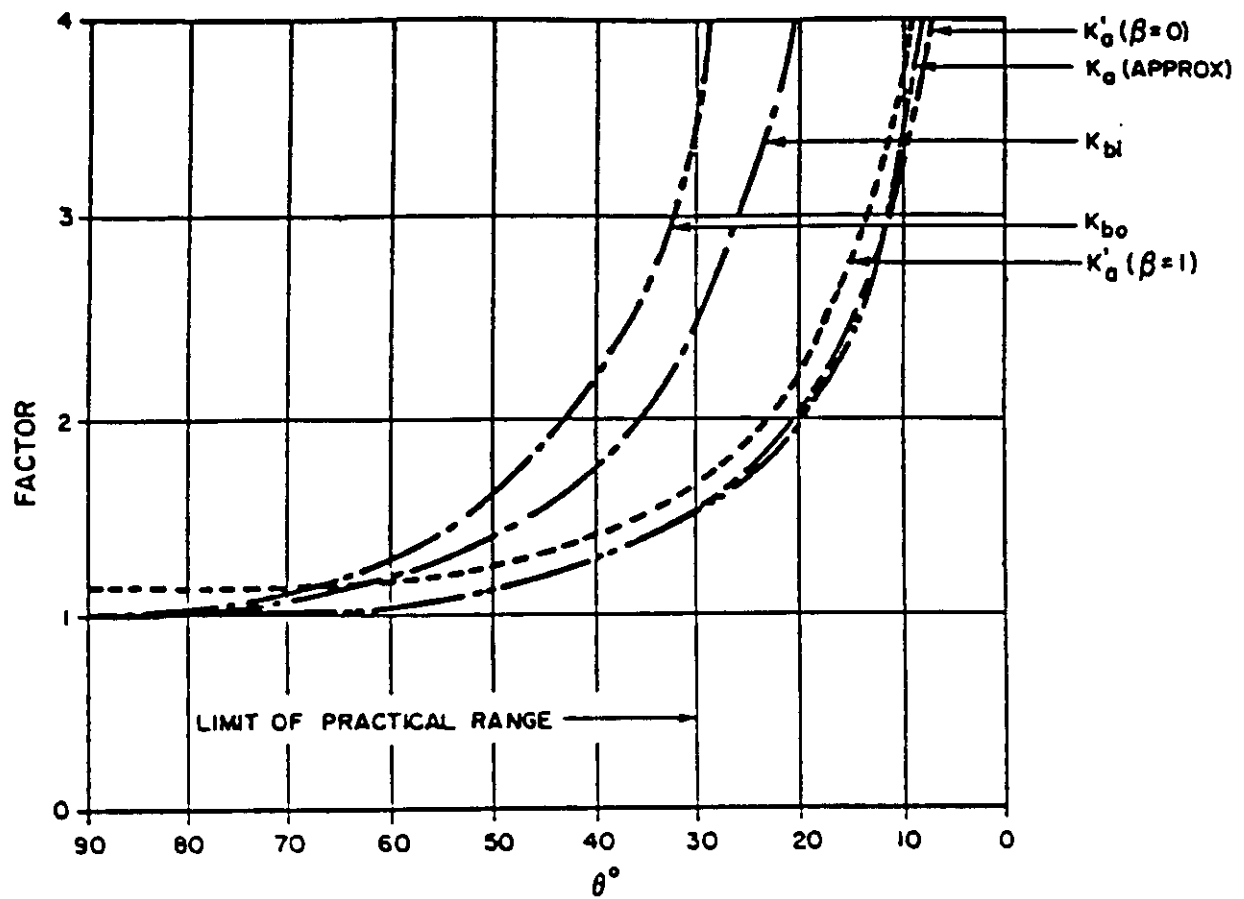
Figure 2.4 Definition of Tems in Tubular Joint Technology
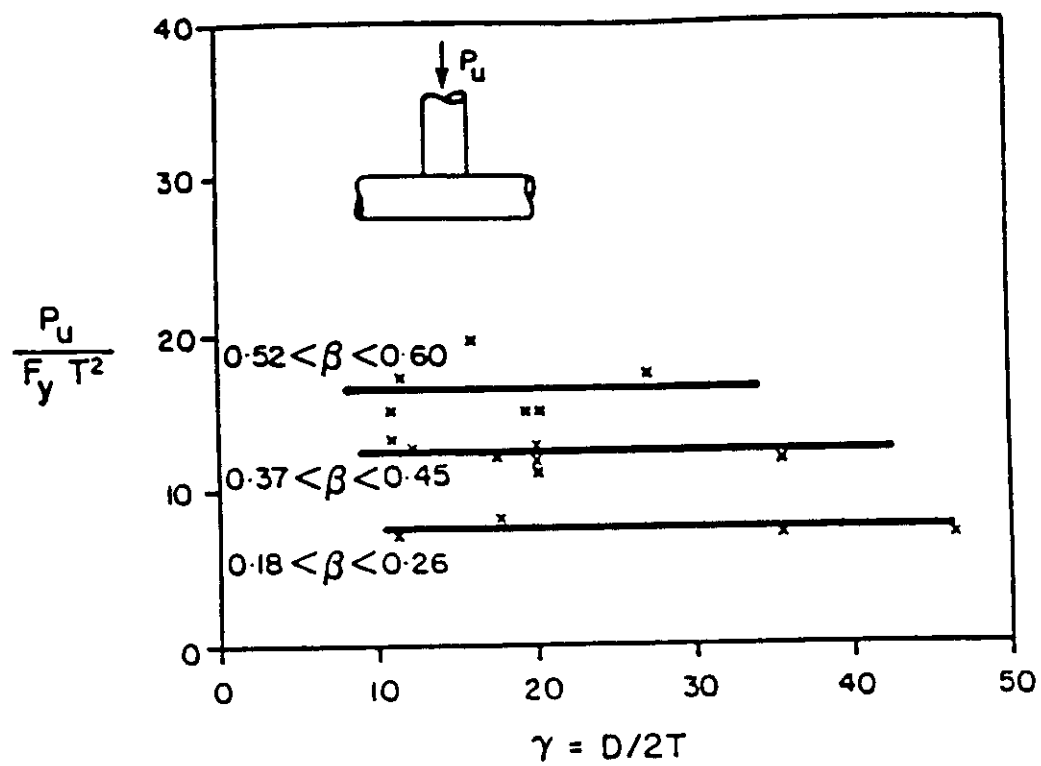
Figure 2.5 Relative Length and Section Factors
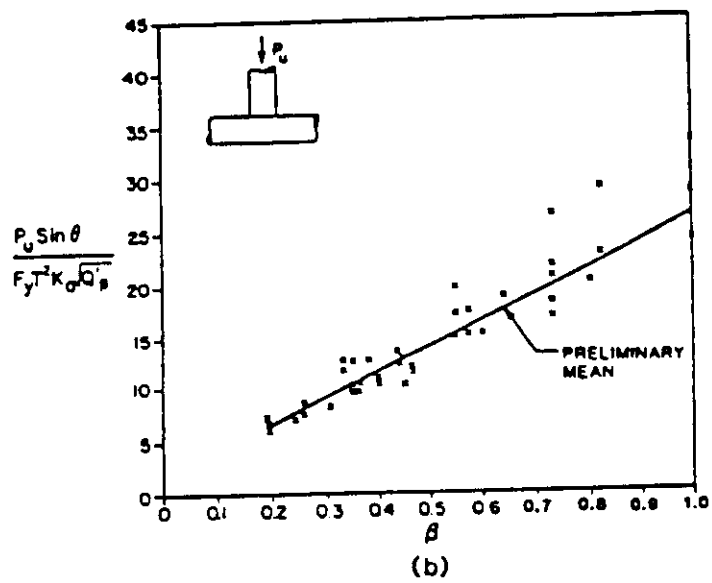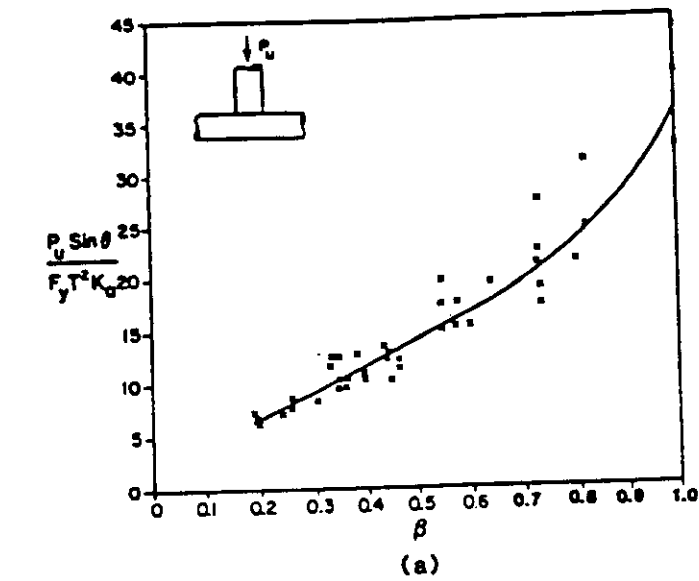
Figure 2.6 T joints - Compression Strength against γ ratio

Figure 2.7 T/Y joints - Compression Strength aganist β ratio

3.0 REVIEW OF DESIGN CODES

3.1 GENERAL

Current design codes (HSE, 1990. NPD, 1993, API, 1991, 1993) specify parametric formula for unstiffened, plane K, T, Y, X shaped joints, calibrated by tests. Other joints, e.g., plane KT, DT, and multiplane joints, need to be considered on a case basis. These joints are usually classified based on the geometry and loading as discussed in Section 2.0.

The design codes have been established by fitting parametric formulae to experimental data or numerical data. While API uses a pragmatically determined lower bound of test data, European codes are based more on statistical analysis to determine mean and 5% fractile curves.

The objective of this section is to review the API design codes for the static strength of tubular joints. Following the definition of joint classification, the design equations for the static strength of simple joints are presented. The static strength of complex joints are addressed.

3.2 SIMPLE JOINTS

Simple tubular joints without overlap of principal braces and having no gussets, diaphragms, or stiffeners should use the following guidelines. Terminology is defined in Figure 3.1.

Joint classification as K, T & Y, or cross (X) should apply to individual braces according to their load pattern for each load case. To be considered a K joint, the punching load in a brace should be essentially balanced by loads on other braces in the same plane on the same side of the joint. In T and Y joints the punching load is reacted as beam shear in the chord. In cross joints the punching load is carried through the chord to braces on the opposite side. For braces that carry part of their load as K-joints, and part as T & Y or cross joints interpolate based on the portion of each in total. Examples are shown in Figure 3.2.

Many properly designed tubular joints, especially those with brace to chord diameter ratios approaching 1.0 will exhibit different failure mechanisms and strength properties than the empirically based formulae contained herein. At present, insufficient experimental evidence exists to precisely quantify the degree of increased strength. Therefore, in lieu of the recommendations contained in the Section herein, reasonable alternative methods may be used for the design of such joints.

The adequacy of the joint should be determined on the basis of factored loads in the brace. Brace axial loads and bending moments essential to the integrity of the structure should be included in the analysis.

STRENGTH CHECK. Joint capacity should satisfy the following:

$$P_D < \varphi_j P_{uj} \tag{3.1}$$

$$M_D < \varphi_j M_{uj} \tag{3.2}$$

where:

P_D = the factored axial load in the brace member, in force units,

P_{uj} = ultimate joint axial capacity, in force units,

M_D = the factored bending moment in brace member, in moment units,

M_{uj} = the ultimate joint bending moment capacity, in moment units, and

φ_j = resistance factor for tubular joints (See Table 3.1)

For combined axial loads and bending moments in the brace, Equation 3.2 should be satisfied along with the following interaction equation:

$$1 - \cos\left[\frac{\pi}{2}\left(\frac{P_D}{\varphi_j P_{uj}}\right)\right] + \left[\left(\frac{M_D}{\varphi_j m_{uj}}\right)^2_{IPB} + \left(\frac{M_D}{\varphi_j m_{uj}}\right)^2_{OPB}\right] \leq 1.0 \qquad (3.3)$$

where:

IPB = in-plane bending
OPB = out-of-plane bending

The ultimate capacities are defined as follows:

$$P_{uj} = \frac{F_y T^2}{1.7 \sin\theta} Q_u Q_f \qquad (3.4)$$

$$M_{uj} = \frac{F_y T^2}{1.7 \sin\theta}(0.8d)Q_u Q_f \qquad (3.5)$$

1.7 is the safety factor, and Q_f is a design factor to account for the presence of longitudinal factored load in the chord.

$$Q_f = 1.0 - \lambda \gamma A^2 \qquad (3.6)$$

where:

λ 　　=0.030 for brace axial stress
　　　　=0.045 for brace in-plane bending stress
　　　　=0.021 for brace out-of-plane bending stress

$$A \quad = \frac{\left(\bar{f}^2_{ax} + \bar{f}^2_{IPB} + \bar{f}^2_{OPB}\right)^{1/2}}{\varphi_q F_y}$$

$\bar{f}_{ax}$, $\bar{f}_{IPB}$ and are the factored axial, in-plane bending, and out-of-plane bending stresses in the chord.

φ_q = yield stress resistance factor =0.95

Set $Q_f = 1.0$ when all extreme fiber stresses in the chord are tensile. Q_u is the ultimate strength factor which varies with joint and load type, as given in Table 3.2.

For braces which carry part of their load as K-joints and part as T & Y or cross joints, interpolate Q_u based on the portion of each in total.

DESIGN PRACTICE. If an increased wall thickness in the chord at the joint is required, it should be extended past the outside edge of the bracing a minimum of one quarter of the chord diameter or 305 mm (12 in.) including taper, whichever is greater. See Figure 3.3. The effect of joint can length on the capacity of cross joints is discussed in Section 3.4.

Where increased wall thickness or special steel is used for braces in the tubular joint area, it should extend a minimum of one brace diameter or 610 mm (24 in.) from the joint, including taper, whichever is greater.

Nominally concentric joints may be detailed with the working points (intersections of brace and chord centerlines) offset in either direction by as much as one quarter of the chord diameter in order to obtain a minimum clear distance of 51 mm (2 in.) between non-overlapping braces or to reduce the required length of heavy wall in the chord. See Figure 3.3. For joints having a continuous chord of diameter substantially greater than the brace members (e.g. jacket leg joints), the moments caused by this minor eccentricity may be neglected. For K and X joints where all members are of similar diameter, the moments caused by eccentricity may be important and should be assessed by the designer.

Simple joints which can not be detailed to provide 51mm (2 in.) minimum clear distance between braces within the limits of allowable offset of the working point, as established above, should be designed for stress transfer as discussed in Section 3.1 below and specially detailed on the drawings.

3. 3   OVERLAPPING JOINTS

Overlapping joints, in which brace moments are insignificant and part of the axial load is transferred directly from one brace to another through their common weld, may be designed as follows:

The factored axial force component perpendicular to the chord,

$$P_{D\perp} < \left(\varphi_j P_{uj} \frac{l_1}{l} \sin\theta \right) + \left(2 v_w t_w l_2 \right) \qquad (3.7)$$

where:

$v_w = \phi_{sh} F_y$

ϕ_{sh} = the AISC resistance factor for the weld,

t_w = the lesser of the weld throat thickness or the thickness, t, of the thinner brace.

l_1 = circumference of the brace which contacts the chord (actual length)

l = circumference of the brace contact with the chord neglecting pressure of overlap

l_2 = the projected chord length (one side) of the overlapping weld, measured perpendicular to the chord.

These terms are illustrated in Figure 3.4.

The overlap should preferably be proportioned for at least 50% of the acting $P_{D\perp}$. In no case should the brace wall thickness exceed the chord wall thickness. Moments caused by eccentricity of the brace working lines and exceeding that in Section 3.1 may be important and should be assessed by the designer.

Where the braces carry substantially different loads and/or one brace is thicker than the other, the heavier brace should preferably be the through brace (as illustrated in Figure 3-4) with its full circumference welded to the chord.

3. 4   CONGESTED JOINTS

Where bracing members in adjacent planes tend to overlap in congested joints, the following corrective measures may be considered by the designer. Where primary braces are substantially thicker than the secondary braces, they may be made the through member, with the secondary braces designed as overlapping braces per Section 3.2. See Figure 3.5, detail A.

An enlarged portion of the through member may be used as indicated in Figure 3.5, detail B, designed as a simple joint per Section 3.1.

A spherical joint, Figure 3.5, detail C, may be used, designed on the basis of ultimate joint strength per Section 3.1 assuming:

$$\gamma = \frac{D}{4T} \tag{3.8}$$

$$\theta = arc\ cos(\beta) \tag{3.9}$$

$$Q_u = 1.0 \tag{3.10}$$

$$Q_f = 1.0 \tag{3.11}$$

Secondary braces causing interference may be spread out as indicated in Figure 3.5, detail D, provided the moments caused by the eccentricity of their working lines are considered in the design analysis.

3.5   LOAD TRANSFER ACROSS CHORDS

Cross joints, launch leg joints, and other joints in which load is transferred across the chord should be designed to resist general collapse. However, for such joints reinforced only by a joint can having increased thickness Tc and length L (for cases where joint cans are centered on the brace of interest L is defined as shown in Figure 3-6a) and having brace chord diameter ratio less than 0.9, the allowable axial branch load shall be taken as:

$$P = P(1) + \frac{L}{2.5D}\left[P(2) - P(1)\right] \qquad \text{for } L < 2.5D \tag{3.12}$$

$$P = P(2) \qquad \text{for } L > 2.5D \tag{3.13}$$

where:

$P(1) = P_a$ from equation 3.1-4 using the nominal chord member thickness

$P(2) = P_a$ from Equation 3.1-4 using thickness Tc

Special consideration is required for more complex joints. For multiple branches in the same plane, dominantly loaded in the same sense, the relevant crushing load is $\sum_i P_i \sin\theta_i$. An approximated closed ring analysis may be employed, including plastic analysis with appropriate safety factors, using an effective chord length as shown in Figure 3.6b. Any reinforcement within this dimension (e.g., diaphragms, rings, gussets, or the stiffening effect of out of plane members) may be considered in the analysis, although its effectiveness decreases with distance from the branch footprint.

Joints having two or more appropriate located diaphragms at each branch need only be checked for local capacity. The diaphragms shall be at least as thick as

the wall thickness of the corresponding branch member. The capacity may be calculated using Table 3.1 or E. 3.2 for cross joints with diaphragms.

3.6   OTHER COMPLEX JOINTS

Joints not covered by Section 3.1 through 3.4 may be designed on the basis of appropriate experimental or in-service evidence. In lieu of such evidence, an approximate analytical check should be made. This check may be done by cutting sections which isolate groups of members, individual members, separate elements of the joints (e.g., gussets, diaphragms, stiffeners, welds in shear, surface subjected to punching shear), and verifying that a distribution without exceeding the allowable stress of the material.
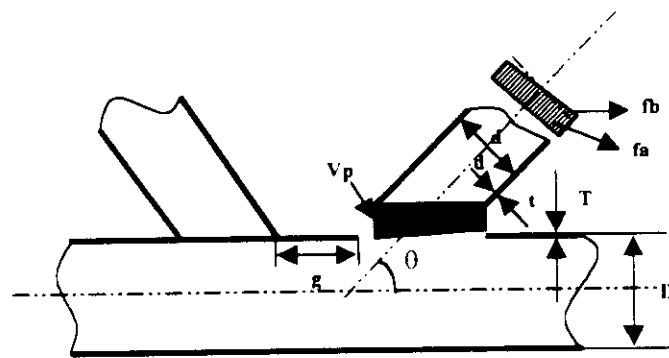
θ = brace angle (measured from chord)
g = Gap
t = Brace Thickness
T = Chord Thickness
d = Brace Diameter
D = Chord Diameter

$$\tau = \frac{t}{T}, \quad \beta = \frac{d}{D}, \quad \gamma = \frac{D}{2T}$$

Figure 3.1 Terminology and Geometric Parameters for Simple Tubular Connections
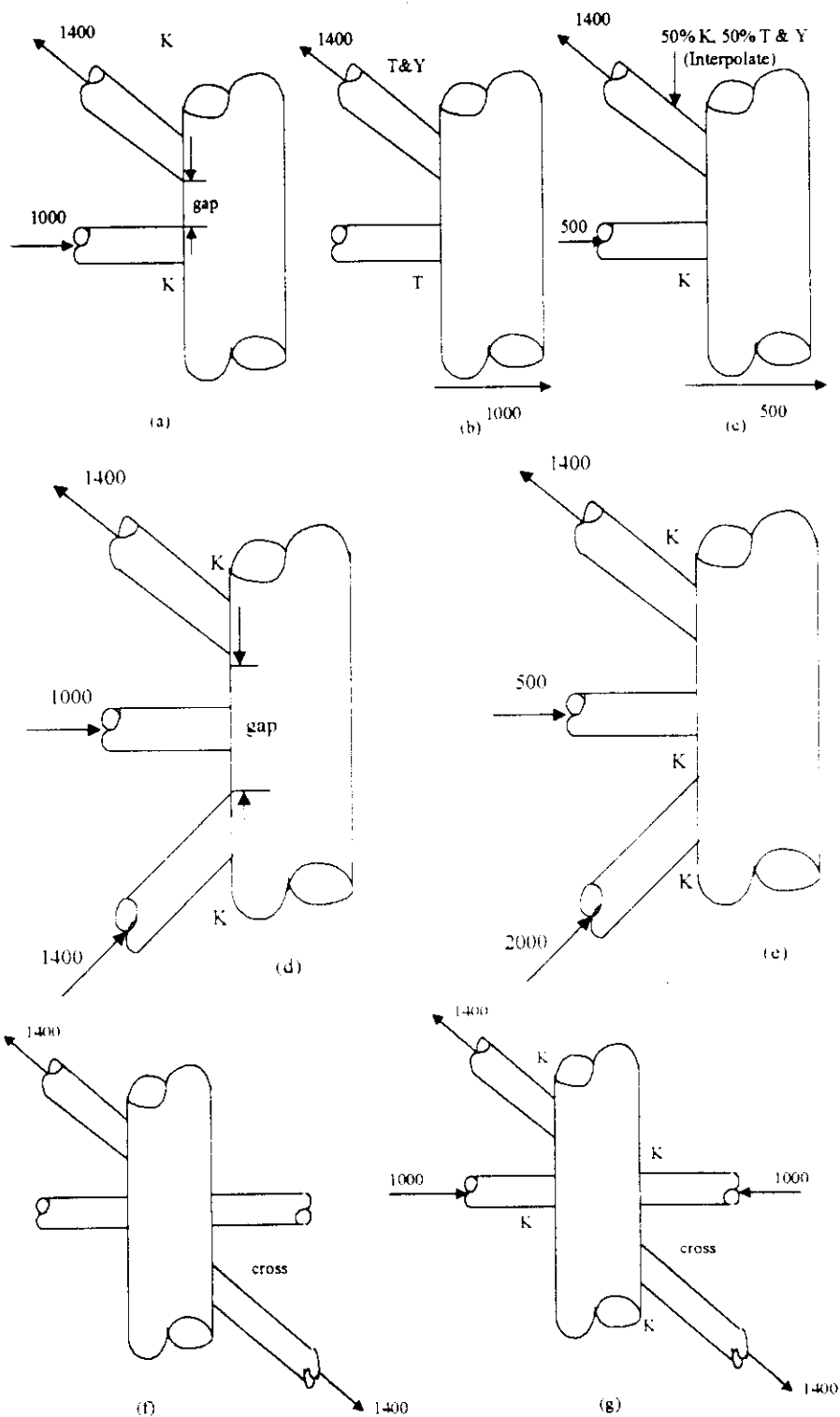
Figure 3.2 Examples of Joint Classification

HEAVY WALL SECTION OF CHORD

OFFSET NOT TO EXCEED ± D/4

D/4 OR 12" MINIMUM

D/4 OR 12" MINIMUM

D OR 24" MINIMUM

SEPARATION 2" MINIMUM

STUB OF HEAVY WALL OR SPECIAL STEEL IN BRACE (OPTIONAL)
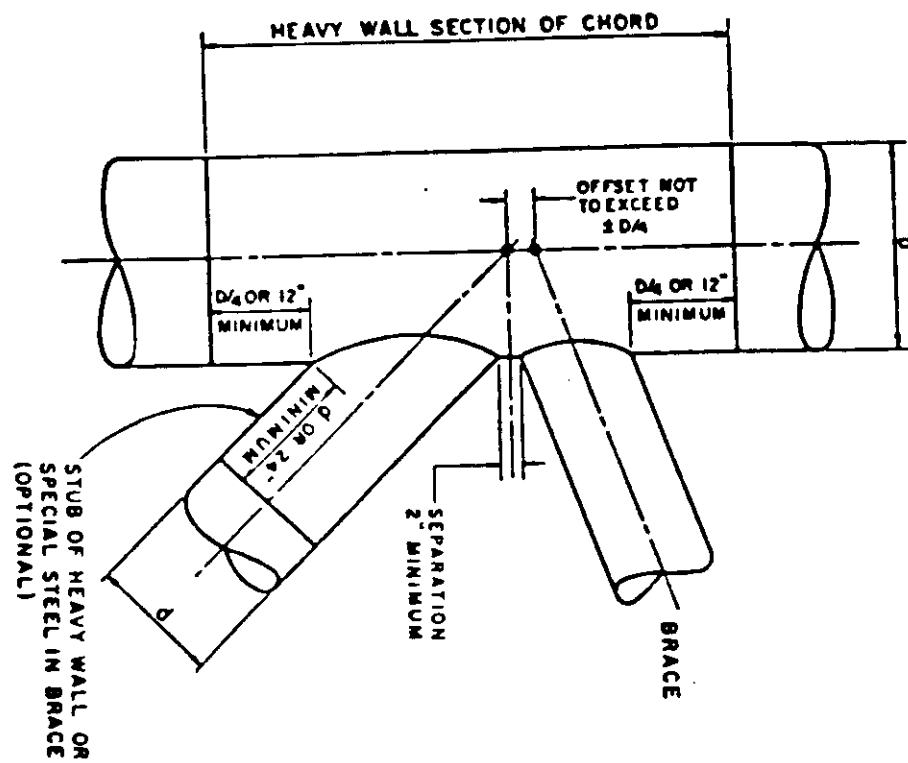
BRACE

Figure 3.3 Detail of Simple Joint
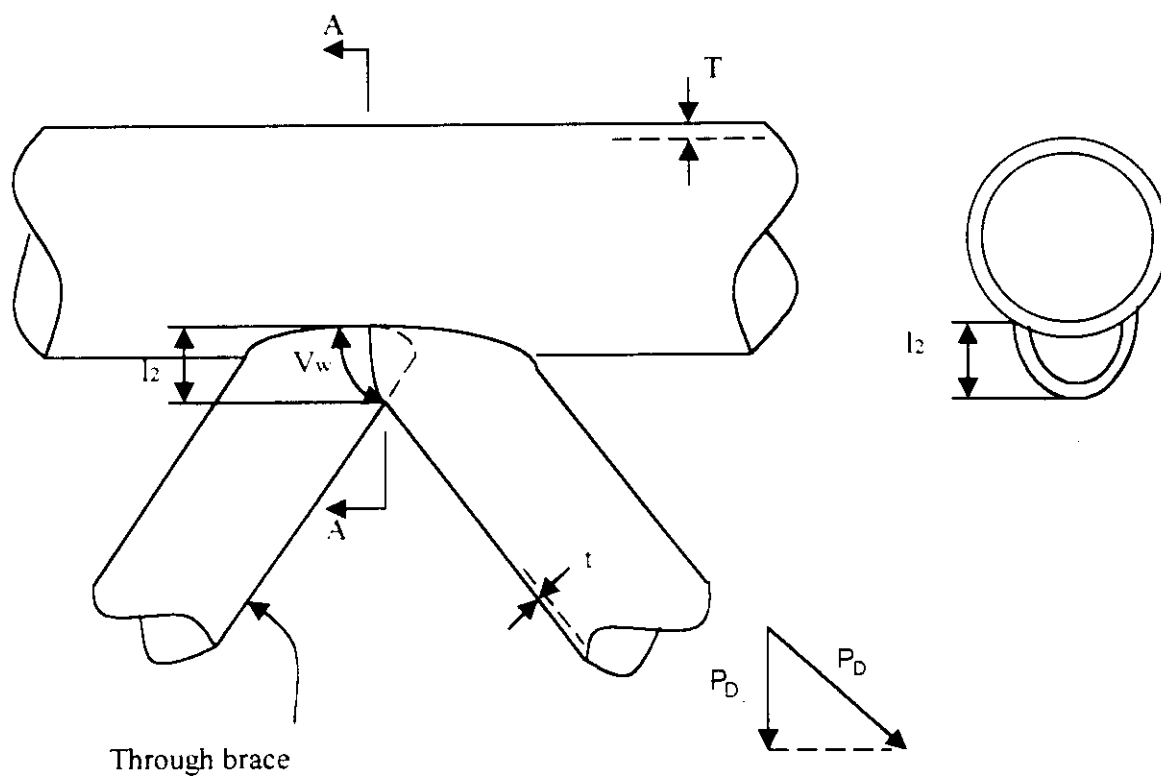
Figure 3.4 Detail of Overlapping Joint

Detail A

t_1

t_2

PRIMARY BRACES

OVERLAPPING SECONDARY
BRACE WITH $t_2 < t_1$

Detail B

ENLARGED JOINT
SECTION

INTERSECTION LINES FOR
SECONDARY BRACES

Detail C

SPHERE

Detail D

OFFSET SECONDARY BRACES
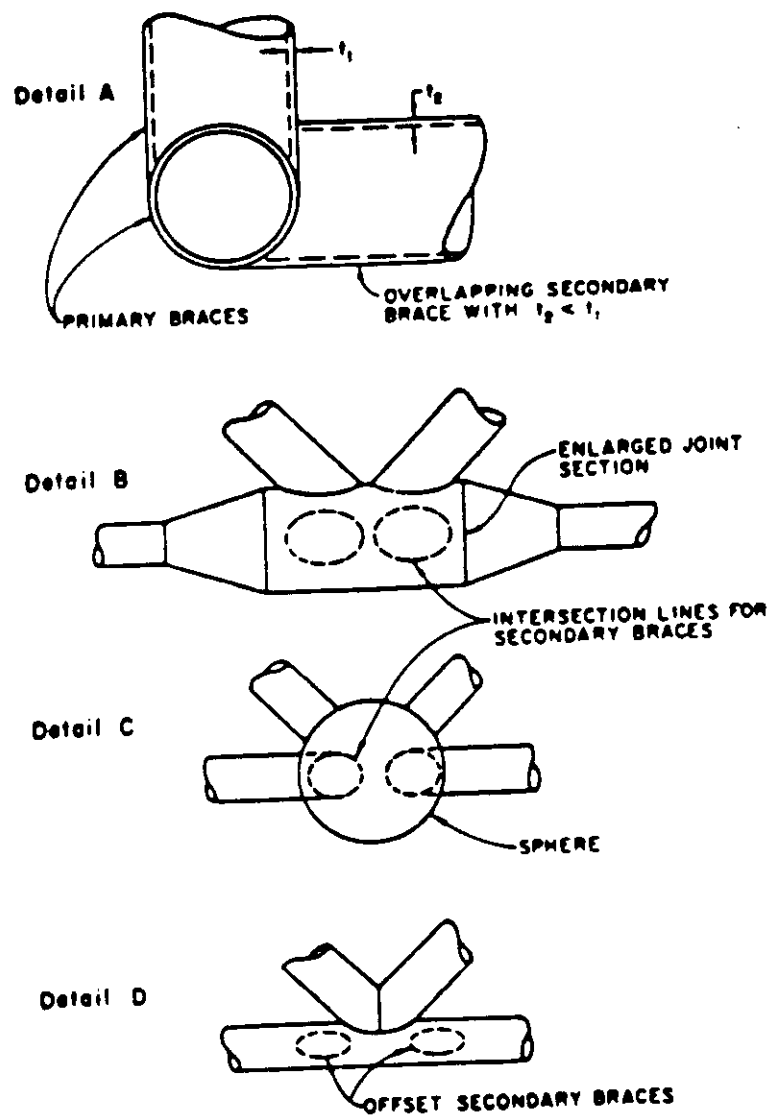
Figure 3.5 Secondary Bracing
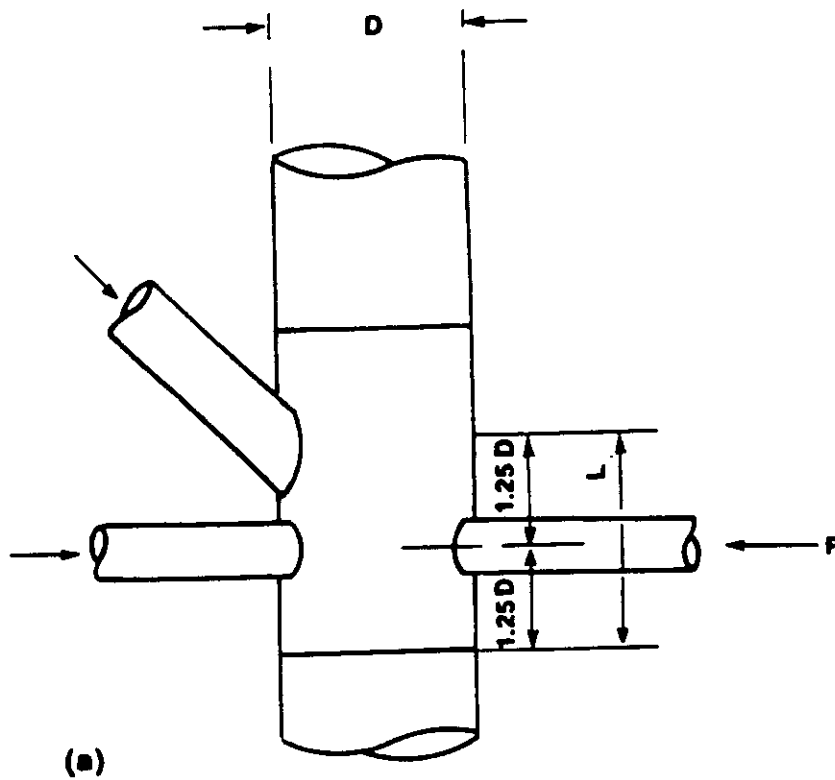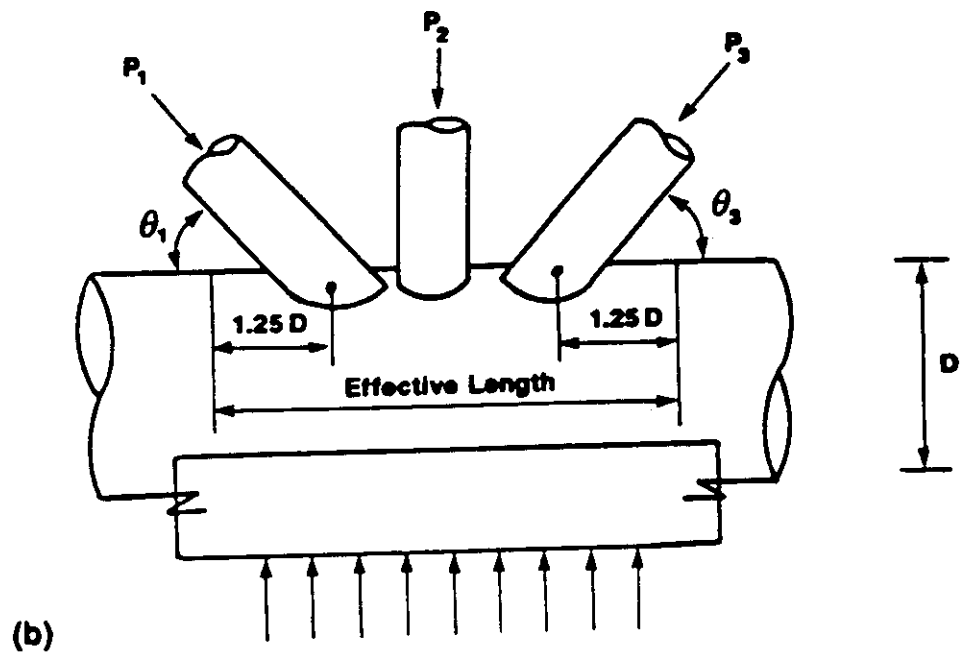
Figure 3.6 Definition of Effective Cord Length

Table 3.1 Connection Resistance Factor - φ_j

Typical of Load in Brace Member				
Type of Joint and Geometry	Axial Tension	Axial Compression	In-Plane Bending IPB	Out-of-Plane Bending OPB
K	0.95	0.95	0.95	0.95
T and Y	0.90	0.95	0.95	0.95
Cross (X)	0.90	0.95	0.95	0.95

For braces which carry part of their load as K-joints and part as T & Y or cross joints, interpolate φ_j based on the portion of each in total.

Table 3.2 Values for Q_u

Typical of Load in Brace Member				
Type of Joint and Geometry	Axial Tension	Axial Compression	In-Plane Bending IPB	Out-of-Plane Bending OPB
K	$(3.4 + 19\beta)Q_g$		$3.4 + 19\beta$	
T and Y	$3.4 + 19\beta$		$(3.4 + 7\beta)Q_\beta$	
Cross Joint W/O diaphragms	$3.4 + 19\beta$	$(3.4 + 13\beta)Q_\beta$		
W/diaphragms	$3.4 + 19\beta$			

$$Q_\beta = \frac{0.3}{\beta(1 - 0.833\beta)} \text{ for } \beta > 0.6$$

$Q_\beta = 1.0$ for $\beta \le 0.6$

Q_g is a gap factor defined by:

$$Q_g = 1.8 - 0.1\frac{g}{T} \text{ for } \gamma \le 20$$

$$Q_g = 1.8 - 4\frac{g}{T} \text{ for } \gamma > 20$$

but in no case shall Q_g be taken as less than 1.0.

4.0 EVALUATION OF EXISTING CRITERIA

During the past three decades, a number of design codes provide recommendations which relate to the design, construction, and maintenance of tubular joints. These recommendations have been derived from an interpretation of research results and in-service performance experience.

The objective of establishing tubular joint design criteria is to dimension the joints so that they perform satisfactorily in service and achieve a balance between economic and risk of failure. Generally, these requirements are implicitly met by satisfying the tubular joint provisions contained in documents such as API RP 2A (1993) and UK HSE Guidance (1990).

The objective of this section is to review the current status of the tubular joint research to examine some problems in the design codes such as API RP 2A and UK HSE Guidance Notes. These problems are the main source of the uncertainties associated with the existing design codes. It is intended to present the physical picture of the uncertainty models developed in the next sections.

4.1 EVALUATION OF DESIGN CODES

Design codes for structural components have historically been based on the elastic design of members where the approach is limit the applied stress on a member to a value below its yield capacity. These codes have an inherent safety factor, which although calculable, is generally taken for granted by the designer. The application of classic elastic design criteria to tubular joints would lead to grossly over conservative design, since the stress distribution along the joint is complicated and local "hotspot" stresses greater than yield can occur without any apparent distress to the joint or the structure. Therefore, design criteria for tubular joints have generally been based on an empirical approach which is expressed in limit state terms. In the case of static strength, permissible loads are based on interpretation of ultimate load test data and consideration of an adequate safety factor.

A number of design guidance are available which contain approaches based on an interpretation of research data and field experience. API RP 2A (1993) and the UK HSE (1991) are used in the offshore industry, while the IIW (1989), AWS (1991) and CIDECT (1991) recommendations are applied extensively for land-based structure. Examination of these documents, the databases developed in this project, the research conducted, and in-service experience reveal the following observations:

1. The large majority of the research has been directed towards simple joint configurations (T/Y, DT/X and K), subjected to unidirectional brace loads. The reasons are two-fold, first, the experimental modeling under these arrangements is simple, and secondly, it allows the basic response characteristics to be understood prior to investigations concerning complex joint load cases and types. The research on simple joint configurations subjected to complex, combined brace and chord loads in 1980s, and on complex joint configurations subjected to simple loads in 1990s, therefore, represented a natural extension of the approach.

2. It comes no surprise that the API RP 2A recommendation and HSE Guidance notes concentrate on simple planar joints, in light of the research

conducted to date. The guidance covers strength formulation of different simple joint types subjected to unidirectional brace loading. Influence functions for the effects of chord load are presented, together with brace load interaction equations which essentially allow joint utilization ratios to be calculated.

3. The research has also been a proliferation of statistical analyses and lower bound fits to the available tests data, and more and more 'design' equations have been appeared in the literature. The findings of these data analyses have had led to design practices specified by API, HSE, IIW, CIDECT for steel structures.

4. While the simple joint recommendations in various design documents are derived from an interpretation of test data, a significant number of difference exist in the recommendations, leading to designs which are appreciably different, depending on the applied design code, as discussed by Lalani (1987). These difference exists for a number of reasons:
   - Data available to the code drafting committees at the time of preparation of guidance,
   - Data screening, acceptance and rejection criteria,
   - Data interpretation, in respect of the manner and degree of influence of each parameter considered,
   - Lack of information and knowledge, leading to extrapolations to cover the practical range.

5. The static strength of overlapping joints, relative to simple joints, has received little attention. Recently, there is the trend in the offshore industry to avoid the use of overlapping joints to minimize fabrication effort, or to reduce the perceived problems associated with in-service inspection of hidden welds. However, overlapping joints continue to be used, either consequentially as a result of congestion, or deliberately as a result of design requirements. The later is interesting in that the need of reinforcement (thicker cans, stiffeners, grout, etc) could be avoided through the judicious sizing of overlapping joints. Under static loads, part of the load is transferred through the common weld between the brace members. This results in a more efficient load transfer, as the chord is not required to transmit the entire load.

   The design recommendations contained in API RP 2A and UK HSE Guidance Notes are based on an engineering mechanics approach utilizing an approximate ultimate strength model, in which the load carrying capacity for that portion of the brace welded to the chord, and the shear capacity of common weld between braces, are assumed to act simultaneously. Some of the early tests in this field were conducted on specimens constructed using land-based fabrication models at that time, while resulted in the omission of the hidden welds. Therefore, specific care needs to be taken in the establishing of data screening and validity procedure in this respect.

6. Multiplaner joints are an unavoidable feature of steel jacket structure. By definition, the joint have brace members in more than one plane, and can be overlapping and non-overlapping. In the design of multiplanar joints, each plane is treated in isolated and designed accordingly, with no reference to the effect of presence of, and loads in, out-of-plane braces. Neither API RP 2A nor HSE Guidance notes present any guidance on multiplanar joints. The behavior of multiplanar joints has been studied recently due to an

increasing awareness that the present design treatment of multiplanar joints as a series of uniplanar connections may be conservative (potential cost saving) or unconservative (potential safety implications) depending on the configuration, geometry and applied load.

7. Internally stiffened tubular joints are used in offshore installations to enhance static capacity and to reduce chord wall flexibility for stress analysis. Ma et al (1992) indicated that at least 2000 ring stiffened joints were in service in the North Sea. In designing such joints, a number of aspects such as stiffener shapes, sizes and locations, construction sequence, economy, etc require careful attention. None of the offshore design codes provide any substantial guidance on stiffened joints; this is not surprising since available information on such joints is scare and codification becomes a difficult task. S

Stiffened joints can permit a reduction in joint-can thickness, an important consideration as the forming limit of fabrication is approached. The increase in static strength is a function of type, size, number and location of stiffeners. Observations of the failure modes of stiffened joints under axial load application suggest that the maximum load the joints can sustain are reached at roughly the same deformation levels as equivalent unstiffened connections. This indicates that carefully selected ring stiffener size and positions do not affect the ductile properties of the joint. Failure usually occurs either by elastoplastic buckling of the ring stiffener or local buckling of the brace wall in the vicinity of the joint. This second form of failure would suggest that, for heavily stiffened joints, brace buckling could be the limiting criteria in design.

In the following sections, some important issues which is believed to be the main uncertainty sources are discussed in some detail.

4.2   DATA SCREENING AND VALIDITY

In the formulation of API RP 2A and HSE Design Guidance Notes, screening procedures were established for data acceptability in order to avoid the use of inconsistent or inappropriate data within the framework of the basic intent of developing design criteria for specific applications. The acceptability (or rejection) of data has resulted in significant difference in design recommendations, as well as the uncertainty models. Some of the screening factors are discussed below:

- **GEOMETRICAL EFFECTS.** Perhaps the most important issues relates to size effect. Some 1000 test results are currently available, encompassing, a wide range of geometric variations. The potential influence of size has been debated extensively. In the preparation of HSE Guidance notes, all steel model test results with chord diameters less than 125 mm were omitted from the database. The equivalent cut-off limited adopted in API RP 2A was 140 mm. The argument for a cut-off limit is from a concern that small scale specimens are not representative of fabricated joints in offshore installations, from a material, weld and tolerance standpoint. It is also argued that failure modes for tubular joints subjected to predominantly static loading are generally dominated by gross, plastic ovalisation of the chord cross-section, and size effects would be therefore expected to be less dominant when compared with joints subject to fatigue loading. However,

the uncertainty models developed by large scale tests are significant different for that of small scale tests.

Other issues which require consideration in selecting a cut-off limit for size include the following

1. Associated β and γ ratios for the small chord diameter joints. The effect of such small brace diameters on joint strength therefore needs consideration. Similar comments apply to joints with high γ ratios for small chord or brace diameter joints.

2. It is understood that many of the small scale specimens were fabricated using fillet welds as opposed to full penetration welds. The fillet leg length has the potential impact of increasing the effective β ratio (the dominate joint strength parameter), thereby leading to a measured strength which may be different from that which would be expected for joints fabricated using standard offshore practice.

The technical issues related to size effects are not simple. In the uncertainty research, all original source documents which contain test data are being collected, and investigations of size effects are considered which recognize the need to consider different joint type, different load cases, manner of tubular forming, method of welding and final weld profile, and inter-related limiting values of β, γ, d , t and T. The effort being expanded in substantial and reflects the need to formulate a rational basis for data acceptance or rejection and statistical appraisal and reliability assessments can be addressed using a consistent database.

MATERIAL PROPERTIES. It has long been recognized that the measured chord yield stress value should be used to evaluate and interpret test data. However, it has also been recognized that the manner of yield stress measurement may impact on the actual value obtained and, consequently, on data interpretation. Many of the test results wrongly rely on measured chord yield stress values generated for other nominally identical specimens which may form part of the same test program. (Note, this is synonymous with SCF measurements for one specimen, and the inappropriate assumption that this SCF distribution is equally applicable for other nominally identical specimens within the same test program).

Yield stress measurement should be carried out on tubulars used to construct the specimen. For fabricated tubulars, this approach rightly and implicitly requires yield stress measurements to be taken on samples from the tubular, rather than from the plate material used in forming the tubulars. The primary intent in any yield stress measurement is to gauge the yield condition of each element with accuracy. It is therefore important that each element of the joint (chord, braces, stiffening) is individually evaluated and subjected to individual tests to define the yield criteria.

Yield stress measurements for the large majority of the test data have been conducted on standard tensile coupon specimens (dynamic yield), in order to maintain consistency with mild certificate which guarantee minimum yield strengths for the tubulars. However, static strength tests on tubular joints follow a quasi-static test procedure and, therefore, a better assessment of the yield condition of any joint element can be expected to be obtained using static yield procedures. Static yield tests have been carried out in a number of recent test programs and therefore, in the current HSE research (MSL, 1995), the original reports are being screened to identify:

- where the yield stress is measured,
- how many coupons have been tested, and their relative locations around the tubular circumferences,
- what method has been adopted,
- the results of sub-column tests, if any.

It should be noted that difference of 10% - 15% in measured yield stress values can be obtained between the dynamic yield test and static yield test method. It should also be noted that variations of up to 10% in static yield stress values can be obtained depending on the strain rates and stoppage procedures adopted when conducting a static yield test.

CHORD/BRACE LENGTH AND BOUNDARY CONDITION EFFECTS. For axially loaded T and Y joints, the chords resist in-coming brace axial loads through a combination of shear and bending. The chord deflects in a beam-bending sense as increasing brace axial loads are applied. It follows that, at long chord lengths, chord yielding and failure may occur prior to joint failures as the plastic moment of the chord cross-section at the crown locations is reached. At shorter lengths, the chord resists the brace axial loads increasingly through shear transfer (i.e., the chord begins to act as a deep beam).

For high β ratio T/Y joints ($\beta > 0.8$) subjected to axial loads, it is not possible to achieve joint failure unless the chord lengths are short. However, at short chord lengths, the influence of end effects and stiffening due to end plates or diaphragms may result in unusually high measured capacities. The majority of the test results to date for axially loaded $\beta=1.0$ T/Y joints can be shown to fall within one of the two following categories:
1. short chord lengths, unexpectedly high joint strengths
2. long chord lengths, unexpectedly low joint strengths as the chord portion in the vicinity of the brace is "softened" due to yielding or. even more severe, · chord M_p is attained from bending-induced deflection.

For axially loaded T/Y joints, across the range of β ratios, the attainment of chord Mp will restrict the capacity of the joints. The following closed form expression for the brace load at which chord failure occurs, in the beam-bending sense, has been derived (Lalani, 1992):

$$\frac{P_u}{F_y T^2} = \frac{15\gamma}{\alpha - 2\beta} \tag{4.1}$$

P_u is the brace axial load which chord Mp is attained, and has been derived on the basis of simple beam theory with the chord ends pinned.

Figure 4.1 shows a plot of equation 4.1 for compression loaded T joints with $\beta=0.8$, $\gamma=20$ and varying $\alpha/2$ values. Superimposed on Figure 4.1 are a series of comparable results obtained through non-linear FE analysis reported by Zettlemoyer (1988) and van der Valk (1988). It can be observed that capacity increases with decreasing chord length (assuming constant chord diameter). With increasing chord length, the joint capacity converges to the limiting brace load at which chord M_p is attained. It can also be observed that the rate of gain in strength for short chord length increases significantly due to the presence of stiff rings at chord ends. These boundary conditions are often unavoidable, and are typical of conditions under which the large majority of tests on axially loaded T/Y joints have been conducted.

Figure 4.2 shows an equivalent plot for DT joints subjected to compression loads. The two curves related to data generated through nonlinear FE analyses reported by Lalani et al (1989) and Vegte et al (1991). It appears from the Lalani data that capacity increases with decreasing chord length. However, this does not occur with expected behavior trends. For an axially loaded DT joints, the chord is not required to resist net shear across the cross-section, i.e. the brace loads are equal in magnitude and opposite in direction. It would, therefore, be expected that, as the chord length reduces, capacity reduces for small to intermediate β ratio joints where a greater part of the chord is mobilized to provide resistance to the incoming brace loads. The dominant effect indicated is the chord boundary condition effect, for the Lalani data, a stiff diaphragm was placed at the chord ends. Hence, the expected reduction in capacity for the $\beta=0.67$ joint as chord length reduces is more than compensated by the presence of end diaphragms which constraint the double ovalisation. The Vegte data, on the other hand, relate to $\beta=0.73$ DT joints with no chord length restraints. A general trend of an increase capacity with increasing chord length can be observed, although the rate of increase is small. This observation is comparable with the findings reported by Zettlemoyer (1988). For unrestrained chord ends, the behavior of axially loaded DT joints with $\beta=1.0$ has been shown to be insensitive to chord length variations (Sauders, et al 1987), as expected, since the chord resists the brace loads in membrane rather than local bending action and, therefore, the chord material away from the brace footprint offers little additional resistance.

For balanced axially loaded K joints, the effect of chord length on joint strength is more difficult to isolate from the available data as the number of dependent variables is greater than for other joint types. Nevertheless, a chord length effect would be expected, in line with the above observations, although this effect is unlikely to be significantly different, from a sensitivity standpoint, than the effect described above for axially loaded DT joints. This reflects the manner in which K joint brace loads are reached by the chord; the available test data all relate to balanced axial loading where the net shear across the chord cross-section is essentially zero, and therefore, beam-bending of the chord in a manner noted above for T joints does not occur.

Apart from a chord length effect, an influence of boundary conditions on K joint strength would be expected. Under balanced axial brace load conditions, the resolved brace load in a direction parallel to the chord introduces a chord axial load which is reacted at the chord ends by one of two methods that have almost exclusively been adopted in all K joint tests to date:

- provision of a pin support at one chord end (usually at the end where the pin is required to provide compressive reaction), with the other chord end free,
- Provision of pin supports at both chord ends.

The choice of test arrangements (and hence boundary conditions) has usually been dictated by the nature of the testing facilities available to the research. It becomes clear that the effects of boundary conditions on joint strength in these instances may be appreciable.

Neither the API RP 2A recommendations and HSE Guidance Notes recommendations reflect any chord length effects, although the need for this has been recognized by both committees. Some investigations in this respect have been conducted in the report.

In developing the database for the uncertainty models in this report, an attempt is made to be along the following criteria:

- For each test result, identify and catalogue the chord length, and the resulting α parameter,
- For axial or moment loaded T/Y and K/TYT joints, the chord is called upon the resist the incoming brace loads in a manner which requires the chord ends to be provided with reactive restraints. Under axial or in-plane moment loads, chord pin support restraints are usually specified, while the out-of-plane brace moment loads impose the need for torsional supports. It is, therefore, necessary to identify and catalogue the chord end restraints provided for each test. In addition, and equally important, is the need to identify the manner of restraint. For example, a large number of the test specimens have been provided with cap (or internal) diaphragms or rings at the chord ends, which are used as attachment points for pin supports to the test rigs. These diaphragms and ring vary in size, and in many instances additional end stiffeners are provided. The conditions at the brace ends are similar, i.e. provision of cap diaphragms, ring and/or stiffeners to allow the brace loads to be applied.
- Using the information collated in the above manner, carry out investigations and statistical assessments to evaluate chord length and boundary condition effects. A number of different evaluations are considered:

1. Assessment of data based on member length and/or chord stress influence functions
2. Assessment if the data to explore the potential of introducing an α ratio correction term
3. Assessment of the data to investigate the need to impose a limit α ratio and/or a chord end ovalisation restraint ratio beyond which the test results are deemed to be significantly influenced by chord length, boundary condition or boundary restraint effects (or combination of all three), to the extent that these test results would be considered to be unrepresentative of the behavior of tubular joints in practical offshore applications.
4. For all test results, assessment of the data to examine the influence of brace length and end conditions on joint strength
5. For K/Y joints, assessment of the data to examine the effects of the provision of one chord end support versus both chord end supported.

The discussion on chord length and boundary condition effects raise a number of other potential concerns. First, the present joint detailing practices in respect of the D/4 or 300 mm minimum rule for chord can length specification has been shown to be neither sufficient or consistent with the assumptions made in the derivation of current offshore design code provisions (Zettlemoyer, 1988, and Vegte et al 1991). Second, both API RP 2A and HSE Guidance Notes contain design formulations for axially loaded K/YT joints which default to T/Y joint capacity at large gaps. This may not be necessary given the expected, and relatively greater, chord length on one side for K/YT joints. This differential is expected to be the greatest at large β values. Third, the ability of isolated joint tests to adequately capture space frame conditions has been questioned. Some investigations in this field have recently been conducted, Connelly et al (1989), Lalani et al (1990) van der Valk (1991) highlighting one of the dominant requirements of the care needed to ensure that the idealized loading, chord length, boundary conditions, and chord ovalisation constraints are consistent with the needs to accurately reflect actual frame conditions. This is often not only difficult to achieve but also impossible to attain. For example, the brace ends in isolated joint tests are able to deflect and/or rotate under load, and may attain an equilibrium position significantly different from frame-mounted joints

where the braces may be highly restrained (e.g., braces of X-framed structures). These difficulties in data interpretation are amplified when post-peak performance is addressed, from the standpoint of isolated joint test results and actual performance under frame mounted conditions.

JOINT FLEXIBILITY. The discussion noted above recognized that codes do not always give best estimates of joint strength, for example, API RP 2A and HSE Guidance Notes essentially represent 1980 and 1985 technology, respectively, and no fundamental changes have been made since that time. It is also recognized that a number of technological advances have taken place regarding the ultimate limit state of tubular joints since 1980 to date, including the generation of pertinent new data and information.

Information on joint stiffness has to be available. For most options, this implies that knowledge of the full nonlinear load deformation ($P\delta$, and $M\theta$ and their interaction) is required, although elastic local joint flexibility suffice for applying elastic analysis and code check. Nonlinear load deformation data, in the form of $P\delta$ and $M\theta$ curve, is only reported in the literature. It is not, therefore, always possible to identify a load deformation curve from the literature closely corresponds (i.e. having similar joint parameters) to the joint being designed or studied. Even then, it is not clear how reliable or representative the reported curve is.

4.3   MULTIPLANAR JOINTS

Neither API RP 2A nor the HSE Guidance Notes present any guidance on multiplanar joints, which are common in offshore structures. AWS D.1.1 present design criteria with the flexibility to extend beyond simple planar joints to multiplanar joints with an arbitrary member of intersecting braces.

AWS introduces a chord ovalisation parameter a_0 which is calculated using procedure defined in Figure 4.3. AWS requires a_0 to be evaluated separately for each brace for which joint capacity is checked (denoted the 'reference' brace), and for each load case, with summation being carried out for all braces present at the joint. In the summation, the cosine term expresses the influence of braces as a function of position around the circumference, and the exponential decay term expresses the lessening influence of braces as distance L_a increases; these terms are both unity for the reference brace which appears again in the denominator.

Table 4.2 presents the results of some example calculation of a_0 for T joints, corner T joints (multiplanar joints with T braces at 90 degree out-of-plane positions) and DT joints to demonstrate the ovalisation severity indicated by these criteria. This table shows that compression loaded DT joints have a 45 % increased severity in ovalisation over compression loaded T joints, a difference which is expected in light of evidence from simple joint data. For corner T joints with equal but opposite loads, the degree of ovalisation severity is similar to compression loaded DT joints. However, for corner T joints with equal loads of the same sign, the a_0 value is 1.0, indicating that the ovalisation tendency of one brace load is counteracted by the other brace such that the reference brace joints has a greater capacity than the capacity of a simple T joint. A number of further observation can be made with respect to the AWS criteria:

- The length L_a in Figure 4.3 represents the distance between adjacent planar brace center lines. The use of a gap parameter , i.e. correlation with distance between brace ends (appropriately non-dimensionalized) may be more relevant than the exponential decay function adopted by AWS, based on planar K joint performance implied in both the API RP 2A and HSE Guidance notes.
- The out-of-plane effects are essentially accommodated in the AWS criteria by the cosine φ term. The use of out-of-plane non-dimensional gap and angle terms, perhaps along the lines postulated by Paul et al (1991) may provide a more appropriate representation of capacity variations.
- The capacity of multiplanar joints subjected to in-plane or out-of-plane moment loads is not treated in any rigorous manner.
- AWS suggests that capacity increases with increasing a_0, the ovalising term, for joint with large β ratios. This obviously does not represent expected trends. Further unexpected trends can also be demonstrated for variations in a_0 with changing g ratios.
- On the positive side, the AWS criteria does not require the designer to make decisions regarding joint classifications. This aspect is embodied within the calculations for the ovalising parameters.

In recent times, the need to develop technology for multiplanar joints has increasingly been recognized. A number of investigations have been conducted, in Canada, the Netherlands, and Japan. Mirti et al (1987) reported on the findings from a total of seven tests on compression loaded V joints, i.e. two planes each comprising a T joint. The nineteen test results reported by Makino et al (1984) relate to multiplanar K joints, subjected to balanced axial loads in the planar sense. More recent testing work has related to multiplanar DT joints reported by Vegte et al (1991) and a series of axial load tests on V and multiplanar K joints (Paul, et al 1991, 1993).

Perhaps the most significant of all test results related to the Delft University /TNO effort reported by Vegte et al (1991), as some of these tests encompass investigations for moment loading. Figure 4.4 shows a plot of all multiplanar, compression loaded, DT joint results generated from these Delft University/TNO investigations. The enhancement in compression capacity due to compression pre-load in the out-of-plane braces is evident. The two results at a compression pre-load ratio of 1.0 relate to two different β ratios, and the beneficial effects of increasing capacity with increasing β ratio for this joint configuration can be noted. The detrimental effect of tension pre-load can also be observed, although this detrimental effect is limited due to the positive effect of the presence of out-of-plane braces in constraining ovalisation (note the results at zero pre-load). Superimposed on Figure 4.4 is the CIDECT (1991) recommendation to account for multiplanar effects on joint configurations and load cases considered in this research program. The CIDECT recommendation provides a reasonable lower bound fit to the data presented in Figure 4.4, which have been normalized to the HSE Guidance Notes mean strength recommendations.

Figure 4. 5 presents the related multiplanar, moment loaded, DT joint data. The presence of out-of-plane braces and tension pre-load in these braces has little effect on the in-plane moment capacity. The beneficial effects of compression pre-load in this case is also limited. This is perhaps not surprising as the chord resistance to in-plane brace moment loads is concentrated around the chord crown locations. This notation is supported by the data for out-of-plane moment

loaded joints; it can be observed that the presence of out-of-plane braces (with no pre-load) in this case has a major beneficial effect, and this effect dominates irrespective of the presence of pre-load.

4.4   SUMMARY AND CONCLUSIONS

This sections presents a general discussion of the existing criteria. It reflects the current status of tubular joint technology and examines some major uncertainty sources which have been received, and continue to receive the significant research and development attentions.

Given the discussion, it is recognized that the uncertainty associated with tubular joints of the existing design codes should be carefully examined in establishing the risk-based design and requalification criteria for offshore structures.
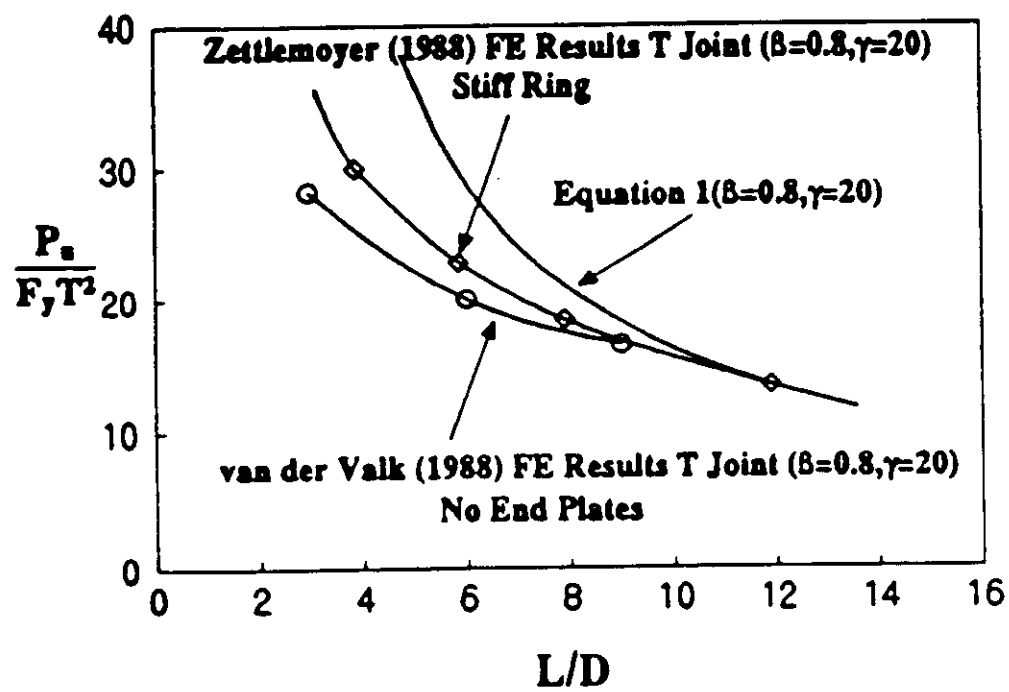
Figure 4.1 Effects of Chord Length and Boundary Conditions for T Joints
Subjected to Axial Compression
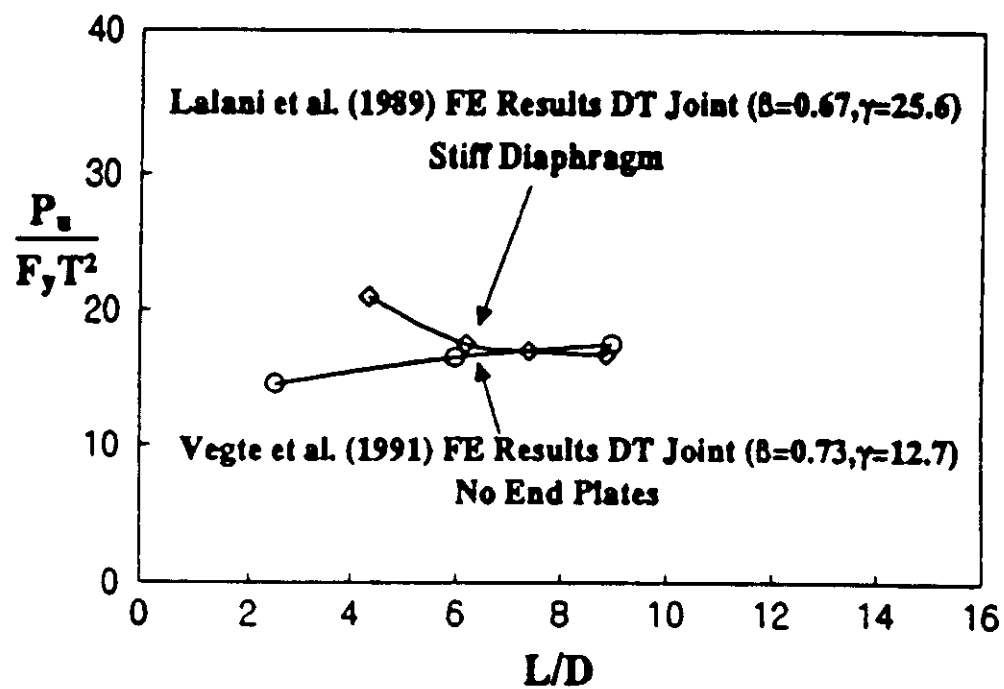
Figure 4.2 Effect of Chord Length and Boundary Conditions for DT Joints
Subjected to Axial Compression

4.12

$$Z = \frac{L_\alpha}{\sqrt{RT}}$$

$$\gamma = \frac{R}{T}$$
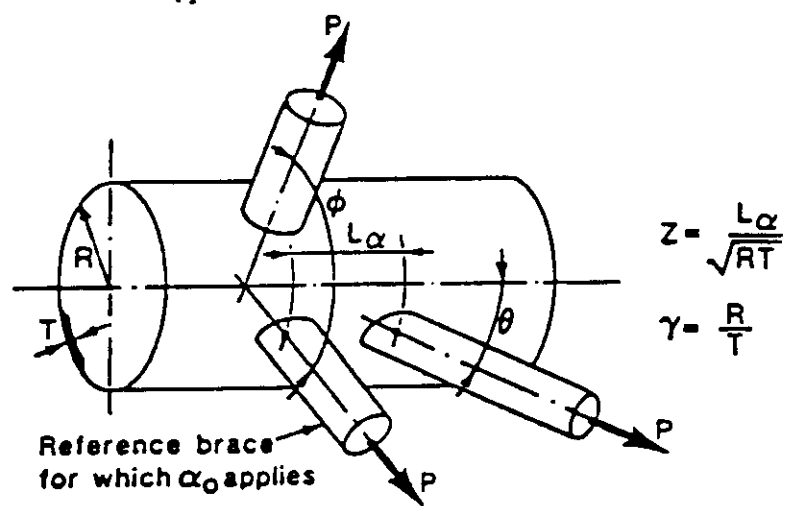
$$\alpha_0 = 1.0 + 0.7 \frac{\underset{\substack{\text{All braces} \\ \text{at a joint}}}{\sum} P \sin\theta \cos 2\phi \exp - \frac{Z}{0.6\gamma}}{[P \sin\theta] \underset{\substack{\text{Reference brace for} \\ \text{which } \alpha_0 \text{ applies}}}{}}$$

$$\alpha_0 \geq 1.0$$

Figure 4.3 Definition of Ovalising Parameters α_0
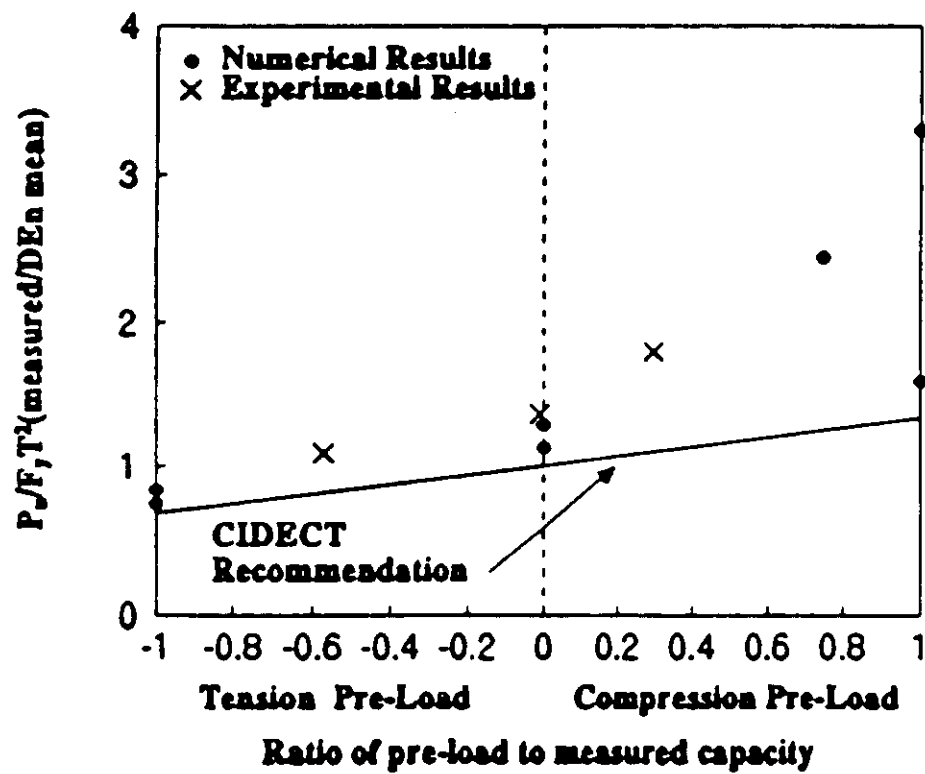
Figure 4.4 Multiplanar, Compression-Loaded DT Joint Results from Delft
University/TNO
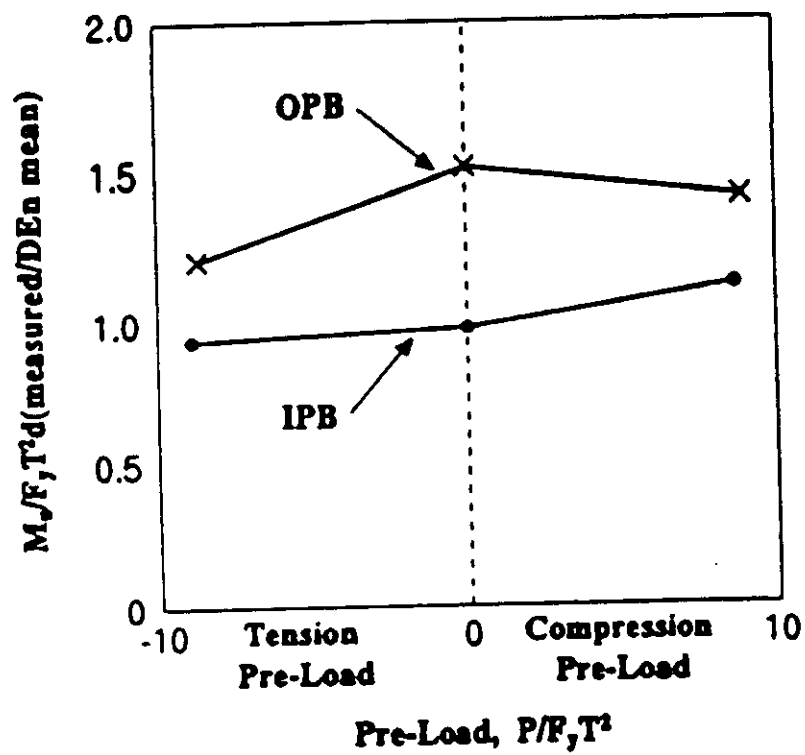
Figure 4.5 Multiplanar Moment Loaded DT Test Results from Delft
University/TNO
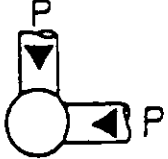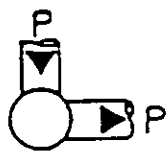
Joint type and load case	Value of α_0
	1.7
	1.0
	2.4
	2.4

Table 4.1 Example Calculation Using Ovalising Parameters α_0

Brace Loading	API	ISO
Axial Compression (AXc)	$3.4 + 19\beta$	$(1.9 + 19\beta)\sqrt{Q_\beta}$
Axial Tension (AXt)	$3.4 + 19\beta$	30β
In-Plane Bending (IPB)	$0.8(3.4 + 19\beta)$	$4.5\beta\sqrt{\gamma}$
Out-of-Plane Bending (OPB)	$0.8(3.4 + 7\beta)Q_\beta$	$3.2\gamma^{(0.5\beta^2)}$

$$Q_\beta = 1.0 \ \text{ for } \ \beta \leq 0.6 \ \text{ and } \ Q_\beta = \frac{0.3}{\beta(1 - 0.833\beta)} \ \text{ for } \ \beta > 0.6$$

$$K_a = \frac{1 + \dfrac{1}{\sin\theta}}{2} \qquad \beta = \frac{d}{D} \qquad \gamma = \frac{D}{2T}$$

Table 4.2 Q_u Values for Y Joints

5.0 UNCERTAINTY OF TUBULAR JOINT CAPACITY

Figure 5.1 summarizes laboratory tests results on a full scale K joints (Lalani, 1995). The test data are summarized as the brace axial load versus the brace axial displacement for a monotonically increasing loading. Note the load at which the first major propagating cracks occurred in the tests specimen and the test ultimate load. Also note that after the maximum capacity was reached that the brace was cycled at the maximum sustained loading.

The joint was able to sustain repeated ultimate state loadings without catastrophic reduction in the load carrying capacity. The joint demonstrated a large amount of ductility and a significant source of bias between the ultimate strength specified in the design codes and the true ultimate strength. The bias is a factor of 2.0.

Figure 5.2 summarized the results of a X joint in a large frame test (Bolt, H. M., 1994). Figure 4.2 is the global response for frame, in which the top bay X joint was the critical component. The $\beta=1.0$ compression X joint gradually softened until the peak capacity was achieved. A bias factor of 2.0 can be found between the predicted ultimate joint capacity and test joint capacity (10). However, An additional load path was developed in the X-braced panel (load shedding) to compensate by carrying a greator portion of the global load giving no perceptible influence on the linearity of the overal response until the yield capacity of the tension chord was also exceeded (12). With increasing global deflection the joint continued to compress until 18 when the braces came into contact across the flattened chord creating a new stiff load path through the panel. The global load sustained by the frame continued to increase until the buckling resistance of the compression brace was exceeded and load was rapidly shed. A bias factor of 4.0 of the joint capacity can be seen in the redundant structural system.

Figures 5.1 and 5.2 show the large variability of the tubular joint tests. Given the variability of the test data and design value, it is necessary to conduct a detailed analysis of the uncertainty associated with the existing design criteria.
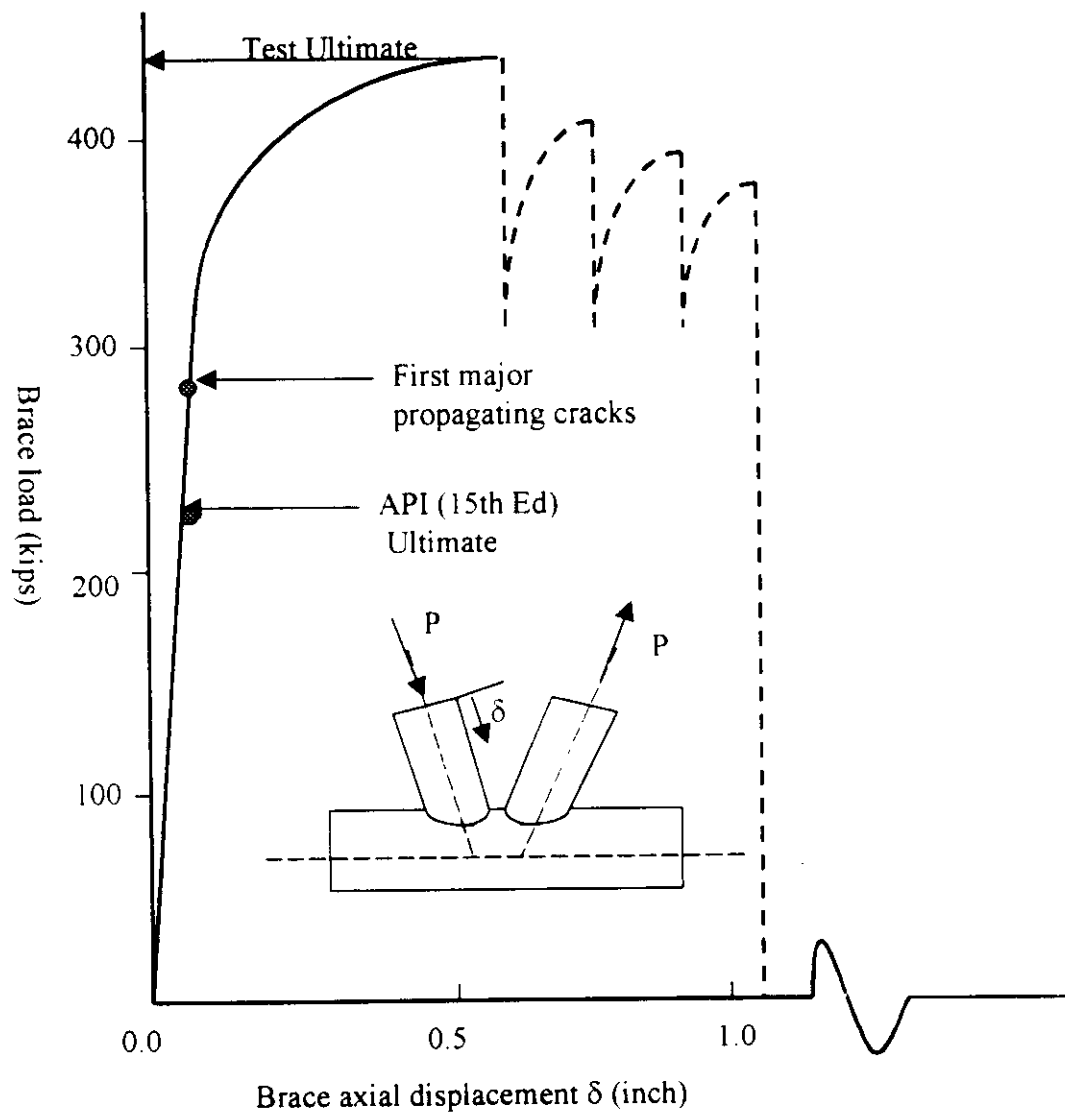
Figure 5.1 Full Scale Test of Tubular Joint

Upper compression
brace in top bay buckles

22

LATERAL LOAD

X joint failure

18

10

API RP 2A

Allowable
Design Load

Λ

LATERAL DISPLACEMENT
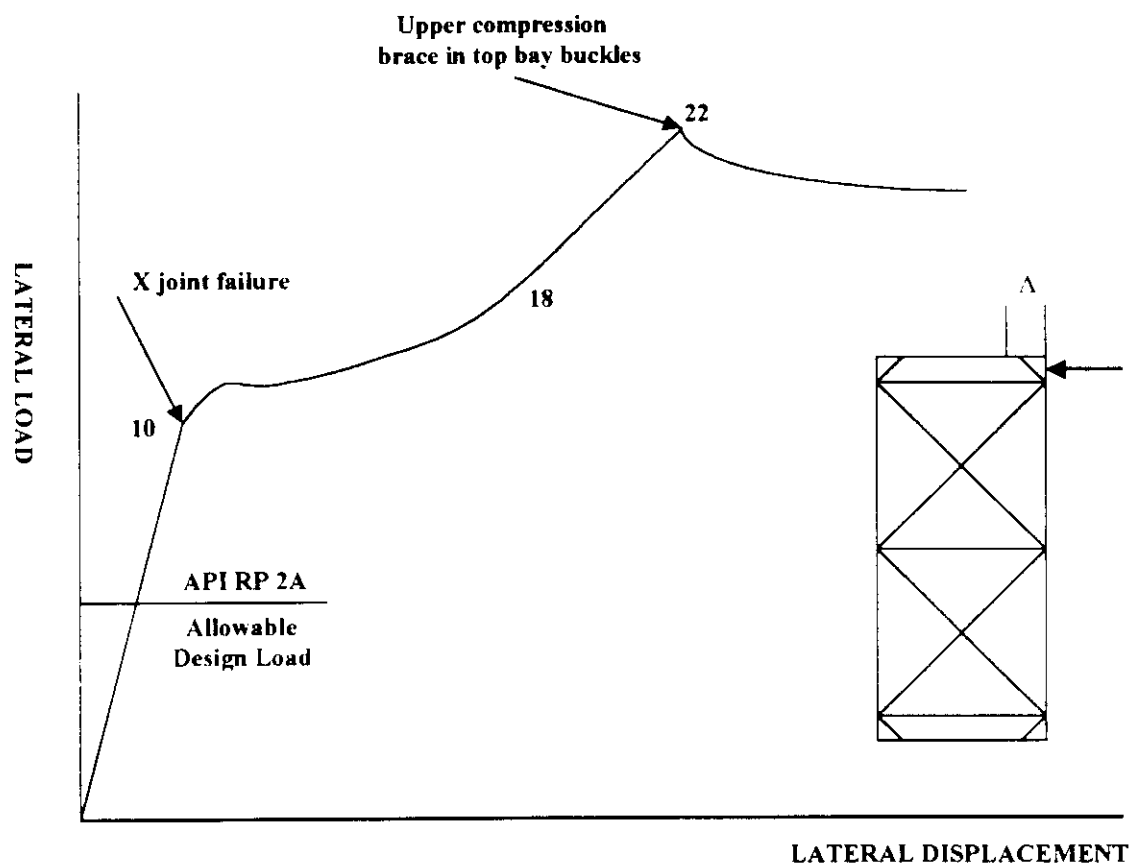
Figure 5.2 Overall Load-Displacement Resposne in a Large Scale Frame Tests

6.0 REVIEW OF THE DATABASE

Some 400 references area available on the static strength of tubular joints. Many of these present the experimental test results. Some of the early review papers give summaries of the test data available at that time. However, careful studies of these summarizes reveals a number of minor inconsistencies.

In order to develop consistent uncertainty models of static strength of tubular joints. An evaluation of existing database is conducted. In evaluating the existing database, an attempt is made to maintain consistency with the API RP 2A database where appropriate.

6.1 DATA SCREENING AND ACCEPTABILITY

For the database established to develop the uncertainty models in this report, the following constraints have been applied:

- Test results for joints with chord diameters less than 125 mm have been omitted from the database. This cut-off point has been chosen to limit the scale effects and to allow sufficient data to be accepted. Approximately 300 test results, mostly K joints with chord diameter of 60 mm or 100 mm have been omitted on size restrictions.
- Where material properties (i.e., F_y) were not measured and only minimum specified yield strength are given, the results are omitted. The inclusion of such results could lead to uncertainty models to be inconsistent with the API design equations.
- Test reports have been carefully studied to identify the failure mechanisms of the test specimens, the test rigs and test procedures. A number of test results have been omitted where insufficient information was presented or where inadequate testing procedures were adopted. Test results for which failure of the specimen did not occur at the joint, such as brace yielding, have been eliminated from the database.
- The limit state design approach differentiates between the two limit states of strength and serviceability. The former is taken as the maximum load achieved during the test and the latter as some local damage criterion. Thus for tension tests, the 'first crack' load is related to a serviceability criterion and not to ultimate strength which is defined as maximum achieved load.
- Test results for axially loaded specimens with $\alpha \leq 5.0$ have been omitted from the database. The effects of chord end conditions on joint capacity may be significant for these joints. The majority of joints in the database have $\alpha \geq 0.8$.
- For some tests, the same results have been reported in different papers using different specimen reference numbers. Therefore, duplications of results have been avoided.

6.2 DEVELOPMENT OF THE DATABASE

Five databases have been developed in this project: 1) Yura/API database, 2) UK HSE database, 3)JISSP database, 4) database for multiplanar joints, and 5)

database for cracked joints, and 6) other data collected from recent studies (1995-1997).

YURA/API DATABASE. The Yura/API database includes:

- tension loaded: 13 T, 3Y and 3 DT joints tests,
- compression loaded: 37 T, Y and DT joints tests,
- in-plane moment loaded: 14 T joints and 2 K-joints tests,
- out-of-plane moment loaded: 11 T-joints, 2 Y-joints, and 4 K-joints tests, and
- 48 axially loaded K-joint tests.

HSE DATABASE. The UK HSE database represents the results from a total of 211 tests. These relate to a variety of joint configurations and load cases and consists of:

- 38 T joints loaded in compression,
- 3 Y joints loaded in compression,
- 29 DT joints loaded in compression,
- 26 K joints loaded in compression,
- 26 T joints loaded in tension,
- 2 Y joints loaded in tension,
- 16 DT joints loaded in tension,
- 31 T joints loaded in in-plane bending,
- 12 T joints loaded in out-of-plane bending,
- 2 Y joints loaded in out-of-plane bending,
- 4 K joints loaded in out-of-plane bending,
- 2 DT joints loaded in in-plane bending, and
- 2 DT joints loaded in out-of-plane bending.

JISSP DATABASE. The JISSP database includes 35 joint tests:

- 4 T joints under compression,
- 3 Y joints under compression,
- 4 Y joints under in-plane bending,
- 2 Y joints under out-of-plane bending,
- 1 T joint under out-of-plane bending,
- 3 X joints under compression,
- 6 K joints under in-plane bending,
- 4 K joints under out-of-plane bending,
- 1 YT joint under out-of-plane bending,
- 6 T joints under the combined brace and chord load, and
- 1 DT joint under combined brace and chord load.

MULTIPLANAR DATABASE. The database for multiplanar joints include:

- 39 axially loaded KK joints,
- 18 axially loaded TT joints,
- 3 axially loaded XX joints, and
- FEA numerical data for KK, TT, and XX joints.

DATABASE OF CRACKED JOINTS. The database for cracked joints and other complex joints include:

- 19 large scale cracked T joints under axial loading
- 2 large scale cracked T joints under out-of-plane bending,

- 1 large scale cracked Y joint under axial loading,
- 14 small scale cracked K joints under axial loading,
- 9 small scale cracked DT joints under axial loading,
- 16 small scale cracked T, 6 small scale cracked Y under axial loading,
- 13 small scale cracked T, 2 small scale cracked Y under out-of-plane bending , and
- 5 small scale cracked YT joints under axial loading.

RECENT DATA. The recent test data includes:
- 3 T joints under combined axial load, in-plane bending, and out-of-plane bending,
- 3 cracked X joints,
- XX joint under in-plane compression and out-of-plane compression,
- XX joint under in-plane compression and out-of-plane tension,
- T joints with the chord can,
- X joints with the chord can, and
- XX joints with the chord can.

6.3 SUMMARY

The established database is presented in Appendix. Appendix A1 summarizes the Yura/API data. A total of 137 Test results are summarized. However, when the joints under axial tension load in the test, the failure condition is taken as the initiation of the first crack.

The HSE simple joint database is presented in Appendix A2 in terms of the joint geometry, material yield strength, geometrical ratios and non-dimensional strength. It should be noted that for joints with two or more brace members (e.g. K and YT joints) in HSE database, the available test data all relate to the case in which the net force perpendicular to the chord is zero. Under such considerations and unless the braces are of significantly different geometry, the failure is always associated with the brace loaded in compression. The results are therefore presented in terms of the load in the compression brace and K joints are identified as compression loaded joints.

The Appendix A3 represents the HSE database of joints subjected to either chord loads or multi-directional brace loads. While the major constraints defined above for data acceptance have been imposed, the constraint on size of specimen has been relaxed for joints where a baseline result of the same specimen is available. The implication of relaxing this constraint is small since the chord load effects and brace load interaction effects are relative effects with respect to the baseline results. The database consists of 61 tubular joints of K/YT and DT configurations subjected to chord loads and 74 T and DT joints subjected to multi-directional brace loads.

The Appendix A4 summarizes the JISSP data. Test results of 35 ultimate load tests on the welded tubular joints are presented. The results are presented in terms of geometry, nondimensional parameters, measured strength and non-dimensional strength. In the Appendix A4, the measured load represents the

maximum load achieved during the test. The load at a pre-defined deformation limit has not been considered in the tests due to difficulties in selecting an appropriate limit. It is argued in Yura et al (1980) that in some cases, particularly for moment loaded joints, the maximum load achieved is sometimes achieved well beyond "functional deformation". The difficulty here is the definition of a global practical deformation limit to cover all joint types in a service within the constraints of a jacket frame which may be of K configuration, inverted K configuration, X configuration or combination of these. Therefore, only the maximum load is addressed in the Appendix A4 while the deformation is not discussed in detail there.

The Appendix B presents the data of multiplanar joints. Since the API RP 2A or HSE design guidance notes didn't provide any recommendations for multiplanar joints strength, the data is compared with the AWS design code.

The Appendix C summarizes data of cracked joints. The data for complex joints including overlapping joints, stiffened joints, and others are summarized in Appendix D.

A total of more 500 tests results are presented in Appendix A, B, C, D and used in the following sections as the basis for deriving the uncertainty models of the joint capacity in the development of the reliability or risk based design and requalification criteria.

7.0 UNCERTAINTY OF SIMPLE JOINTS

7.1 GENERAL

Design codes (HSE, 1990, API, 1991, 1993) specify parametric formula for unstiffened, plane K, T, Y, X shaped joints, calibrated by tests. Other joints, e.g., plane KT, DT, and multiplane joints, need to be considered on a case basis. The unstiffened joints are usually based on the geometry and loading, see, e.g., Figure 7.1.

Depending on material and geometrical properties, ultimate failure of a joint may occur due to buckling (due to compressive loading), excessive deformation, fracture or gross separation, shear failure of the chord-brace joint, lamellar tearing of thick chords.

For Y- and T-joints, it is therefore, distinguished between compression and tensile loading. Different definitions of crack size that implies tensile failure have been used. While API use first crack, HSE (1990) refers to ultimate load capacity. Therefore, two failure criteria should be addressed: 1) the first visible crack, and 2) ultimate failure. The former criteria is conservative for static loading, but is convenient to avoid consideration of interaction between tension and in- or out-of-plane bending, the joint does not exhibit a distinct limit capacity in the load-defection behavior and the limit state should be given by maximum deformation, and possible maximum strain to avoid fracture.

By merging all failure modes in one ultimate limit state, it is important to ensure ductility, especially for material with yield stress S_0 more than 400 Mpa. Different codes specify the ratio S_0/S_u in the range of 0.70-0.83.

Design codes have been established by fitting parametric formulae to experimental data. Recently, schematic analyses using nonlinear finite element have also been used to generate a data basis for fitting ultimate limit state equations. While API uses a pragmatically determined lower bound of test data, European codes are based more on statistical analysis.

7.2 DESIGN CODES AND STANDARDS

Strength provision in the API WSD/LRFD codes are most widely used. They contain parametric formulae established on the basis of a lower bound on experimental data selected in (Yura, et al 1980). The formulae are generally of the form(API, RP-2A, WSD, 1991):

$$P_u = Q_u Q_f \frac{S_0 T^2}{\sin\theta}$$

(7.1)

$$M_u = Q_u Q_f \frac{S_0 T^2}{\sin\theta} (0.8d)$$

(7.2)

in which S_0 and T are chord yield stress and thickness; and Q_u and Q_f are nondimensional factors for brace load and chord stress effects, respectively. These factors are functions of the ratios of the diameters of the tubulars, of diameter to plate thickness etc.

The following interaction equation is recommended by API RP 2A (1991, 1993):

$$1-\cos\left[\frac{\pi}{2}\frac{P}{P_u}\right]+\sqrt{\left(\frac{M}{M_u}\right)^2_{IPB}+\left[\frac{M}{M_u}\right]^2_{OPB}}=1.0 \qquad (7.3)$$

where IPB and OPB refer to in- and out-of-plane bending.

Since the review (Yura, et al 1980) was accomplished, new data have become available and data used before, have been found obsolete. New data bases have been established by (UEG, 1985). Other code formulation have been proposed by e.g., CSA, HSE, DnV, and NPD. In particular, improved formulations have been introduced for X-joints and in-plane bending. However, it should be noted that the strength formulae given in various codes have different range of validity.

In view of harmonization of offshore codes, a new data base was established by a critical screening of existing data, and recommendations on selection of formulae were given in (MSL, 1992).

In particular, API LRFD (1993) applies a Q_u in Eq. (7.1) for in-plane bending, which is $Q_u = 3.4 + 19\beta$, where β is the ratio of brace and chord diameters. Other codes (e.g., DnV, HSE, NPD) apply a formula of the type $Q_u = k\sqrt{\gamma}\beta$ (where γ is the chord radius to thickness ratio), However, with different values of k. Recently, these formulations have been reviewed (Healy, et al 1993) in view of a new experimental and numerical data basis for T and Y joints. While the latter form of Q_u with k=4.75, fits the mean numerical data generated by nonlinear shell analysis, it represents a lower bound on experimental data.

A close look at the data for axially loaded T/Y joints reveals that the strength factor Q_u is determined from tests with loads in the chord, which makes Q_u smaller than it otherwise would be. However, when using Eq. (7.1) with this Q_u, also a Q_f factor is applied. To avoid that the effect of load in the chord is accounted for twice the initial Q_u should be adjusted to correspond to zero beam-bending (Birkinshaw, M., et al 1993).

7.3   DATA BASE

Some more than 400 tests are available on static strength of simple tubular joints. They are detailed in the Appendix. As discussed in section 3.0, an attempt has been made to maintain consistency with API in developing the database. It is generally grouped as:
• Yura's database,
• JISSP database,
• HSE database, and
• Recent database.
It should be addressed that HSE database includes some data from Yura's database which is used in establish the compression loaded joint capacity in API RP 2A. The Yura's database is grouped because it is the main database in establishing the design guidelines when the failure criteria is referred to initial crack occurrence.

7.4   Y, T, AND DT JOINTS

Typical load-deflection behavior of T and DT joint joints subjected to axial compression and axial tension is illustrated in Figure 7.2. The behavior of the test specimens is characterized by a gradual increasing rate of deformation caused by yielding of the chord around the branch and distortion of the cross section (ovaling) until a first crack has formed. The branch load continues to increases until gross separation occurs. The DT joint behavior in tension is similar to the T-joint, but both the stiffness and capacity are reduced.

Compression loading produces the lowest joint capacity. Failure is usually associated with yielding, buckling, and gross distortion of the chord wall. The DT joint is usually weaker than the T joints except possibly at β values near 0. The initial stiffness of the joint is similar for both compression and tension.

TENSION LOADED T,Y AND DT JOINTS. The uncertainty models of tension loaded T, Y, and DT joints, two sets of data is used:
- API/Yura Data (19 tests) for first crack criteria
- HSE Data (34 tests) for ultimate strength criteria, and

First Crack Criteria. API/Yura's database includes 13 test data of T-joint, 3 test data of Y joint, and 3 test data of DT joint. The test capacity, P_T, is the first crack load in all tests. Therefore, the uncertainty model developed based on the API/Yura's data is referring to initial crack occurrence which is different from ultimate strength of the tubular joints.

Figure 7.3 illustrates the test load vs β. At best, the data can only be described as scattered. Various attempts were made to organize the data in a tighter arrangement using other test variables, such as γ, but little improvement was observed (Yura, et al 1980). The reason may be twofold. First, its is due to the fracture characteristics. When failure are due to fracture of the steel, considerable scatter should be expected. Second, the API/Yura formula neglects the effects of intersection angle θ, K_a, and K_a. The error caused by omitting K_a would be 17%.

The test data histograms are shown in Figure 7.4. The range in each histogram is considerable larger. However, it is interesting to note that the early API RP 2A 9th edition provide better estimate. The bias and COV for the tension loaded joints are 1.411 and 42.7% for API RP 2A 20th edition based on Yura's database. However, the bias and COV for the tension loaded joints are 0.978 and 39.8% for API RP 2A 9th edition.

Ultimate Strength Criteria. UK HSE database includes T, Y and DT joints tests results. This database consists of 16 T joints, 2 Y joints, and 16 DT joints. The test capacity, P_T, is the ultimate maximum load in all tests. Therefore, the uncertainty model developed based on the UK HSE data is referring to ultimate strength of the tubular joints.

Figure 7.5 is the test results histograms for tension loaded T/Y and DT joints. The bias is 2.33 for T/Y joints and 1.72 for DT joints. The COV is 14.1% for T/Y joints and 17.3% for DT joint

COMPRESSION LOADED T, Y AND DT JOINTS. The compression loading usually produces the lowest joint capacity. Failure is associated with yielding, buckling, and gross distortion of the chord wall. Four databases are considered in developing the uncertainty model:

- Yura's Database,
- HSE database,
- JISSP database, and
- Recent database.

The Yura's database includes 37 T, Y and DT joints tests. The bias and COV of the API design equations based on the Yura's database are 1.067 and 7.1% which are shown in Figure 7.6.

The HSE database includes 38 T joint tests, 3Y joint tests, and 29 DT joint tests. The bias and COV are 1.236 and 19.8% for DT joints The bias and COV are 1.13 and 7.73% for DT joints. The data is shown in Figure 7.7.

The JISSP database includes 7 Y & T joint tests. The test data is shown in Figure 7.8. The bias is 2.025. The COV is not presented because of insufficient data. The recent test data (Kim, J. D. et al 1996) indicated that the bias was about 1.63. The JISSP data is the large full scale test data. It is believed that the results will represent the better field performance. However, JISSP doesn't include all the β range. It only considers β=0.8 or 1.0.

MOMENT LOADED SIMPLE JOINTS. The response of a joint to applied in-plane bending (IPB) and out-of-plane bending (OPB) moment is illustrated in Figure 7.9. Typically, the joint subjected to in-plane bending reaches a maximum load at moderate deformation with actual failure due to plastic bending and buckling of the chord wall on the compressive side of the branch, and fracture through the chord wall on the tension side. For out-of-plane bending, the chord wall distorts locally resulting in lower joint stiffness and strength. Fracture may occur, but only after excessive deformation.

Out-of-plane bending are apt to be more sensitive to β than in-plane results. At high β values the branch transfers load to the chord primarily through membrane action in the chord as opposed to wall bending. Improved capacity and stiffness are expected, just as for the DT compression specimens. On the other hand, the mode of load transfer for in-plane bending is not altered significantly by β.

Four databases are considered in developing the uncertainty model:
- Yura's Database,
- HSE database,
- JISSP database, and
- Recent database.

The Yura's database includes 14 in-plane moment loaded T joints and 2 K-joints tests. The bias and COV of the API design equations based on the Yura's database are 1.227 and 17.3% for in-plane bending moment. They are shown in Figure 7.10.

The Yura's database includes 11 out-of-plane moment loaded T-joints, 2 Y-joints, and 4 K-joints test data. The bias and COV of the API design equations based on the Yura's database are 1.171 and 15.3% which is shown in Figure 7.10.

The HSE database includes 31 T joint and 2 DT joint tests under in-plane bending moment, and 12 T joints, 2 Y-joints, 2 DT joints, and 4 K-joints under

out-of-plane bending moment. The bias and COV are 1.18 and 17.3% which is shown in Figure 7.11.

The JISSP database includes 4 Y-joint under in-plane bending moment. The bias factor is about 2.4. In addition, six JISSP K-joint tests data are available. The bias factor can not be determined since the API design equation of K joint is not available. Two T-joint and one Y-joint test under out-of-plane bending moment are available in JISSP database. The bias factor is 1.145.

The recent database includes 3 large scale T joint tests under in-plane bending moment. The bias factor is 1.54.

7.5   AXIALLY LOADED K AND YT JOINTS

Researches on K-joints have indicated that the gap, g, between the intersecting branches has a significant influence on the capacity, as do the variables which affect single branch joints. If the gap is larger relative to the members, the joint performs like a single branch joint. As the gap approaches zero, the overall joint strength is increased because the bending stiffness of the chord wall between the branches is increased. For large gaps, the joint capacity is usually controlled by plastic bending and buckling of the chord wall in the vicinity of the compression branch. For small gaps, the joint strength depends on considerations in the gap.

Some axial K-tests have had one 90 degree branch loaded in compression and a 45 degree branch loaded in tension. In these cases the gap was in tension and failure was governed in part by fracture of the chord or welds in this region. Therefore, considerable scatter of results can be expected.

Two databases are reviewed to develop the uncertainty model:
- Yura's database,
- HSE database, and

The Yura's database includes 48 test results. The bias and COV are 1.310 and 26% which is shown in Figure 7.12. The HSE database includes 36 test results. The bias and COV are 1.32 and 20%. The test data are shown in Figure 7.13.

7.6   SIMPLE JOINT UNDER COMBINED LOADS

While some qualitative information about uncertainty of interaction equation is given in (Healey, et al 1993) more work is necessary to quantify the uncertainty and choice of interaction equation. Test data indicated that the uncertainty was in the range of 1.0-1.2 which is illustrated in Figure 7.14. However, the limited tests data doesn't allow us to develop a reliable uncertainty model. Therefore, recommendations have been made to conduct the detailed research here.

7.7   SUMMARY

This section presents a uncertainty analysis of API design equations for simple joints. The uncertainty model is developed based on various database. Table 7.1 summarizes the results. It can shown in Table 5.1 that large uncertainty is associated with the API design equations. The bias and COV are in the range of 1.2-2.3 and 7% and 30%.

The wide range in B and COV reflects differences in the types, sizes, loadings, and failure mechanism of the test specimens. These bias characterizations are a mixture of Type I and Type II uncertainties. There is an inherent variability contributed by steel strength and so on, and a variability contributed by the analytical model used to determine the capacity.

Table 7.1 Uncertainty of API Design Codes for Simple Tubular Joints

Joint Type	Load Type	Yura Database		HSE Database		JISSP
		B	COV(%)	B	COV (%)	B
T & Y	Tension	1.41	42.7	2.71	14.1	-
X & DT	Tension			1.72	17.3	-
T & Y	Compression	1.07	7.1	1.236	19.8	2.025
X & DT	Compression			1.13	7.73	1.49
K & YT	Compression	1.31	26	1.32	20	-
All	In-Plane Bend	1.23	13.3	1.18	17.8	2.4
All	Out-Plane Bend	1.17	15.3	1.18	17.8	1.145
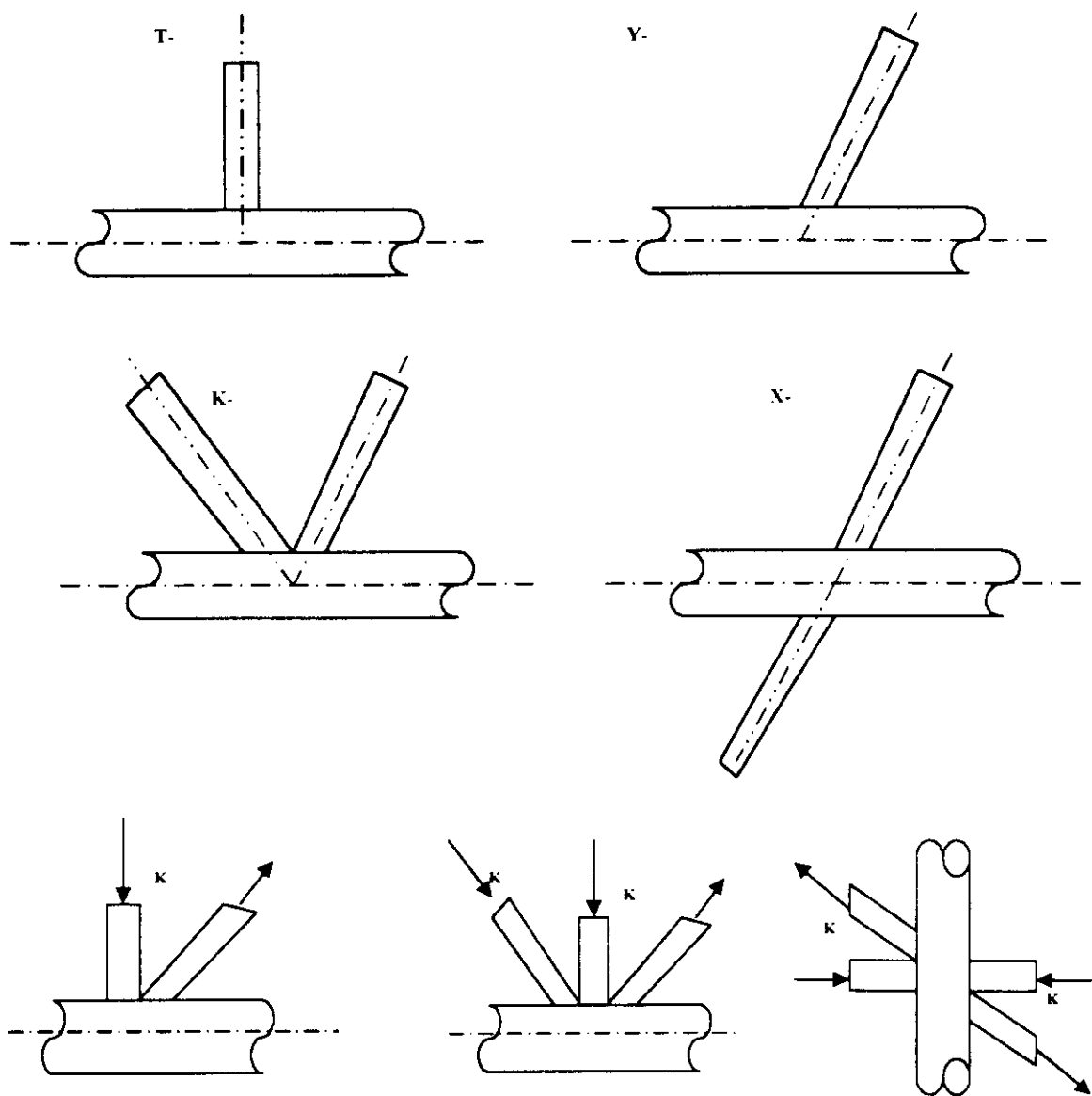
Figure 7.1 Joint Classification
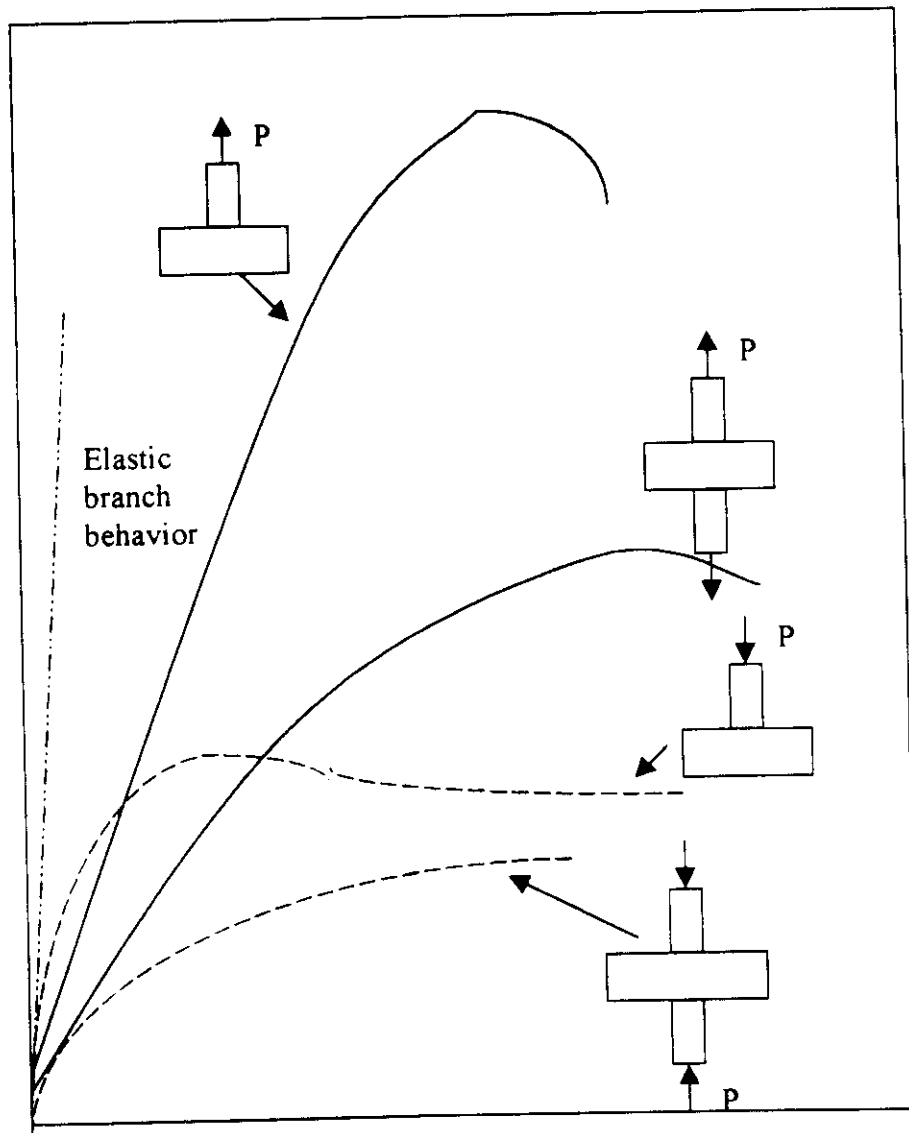
Figure 7.2 Load Deflection Behavior of Axially Loaded T and DT joints
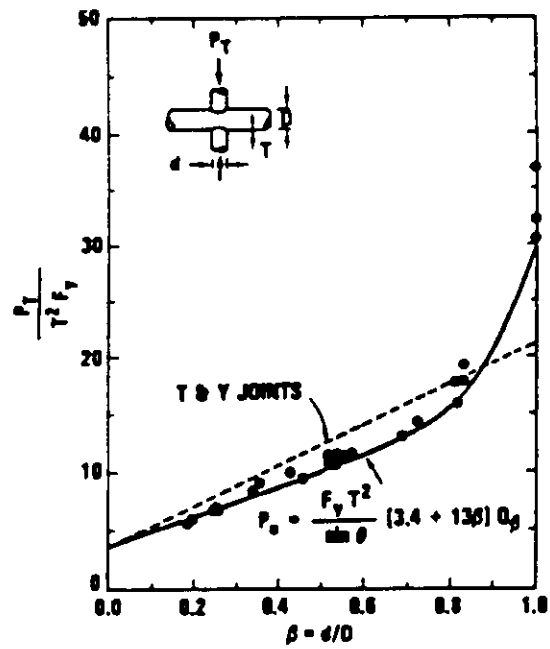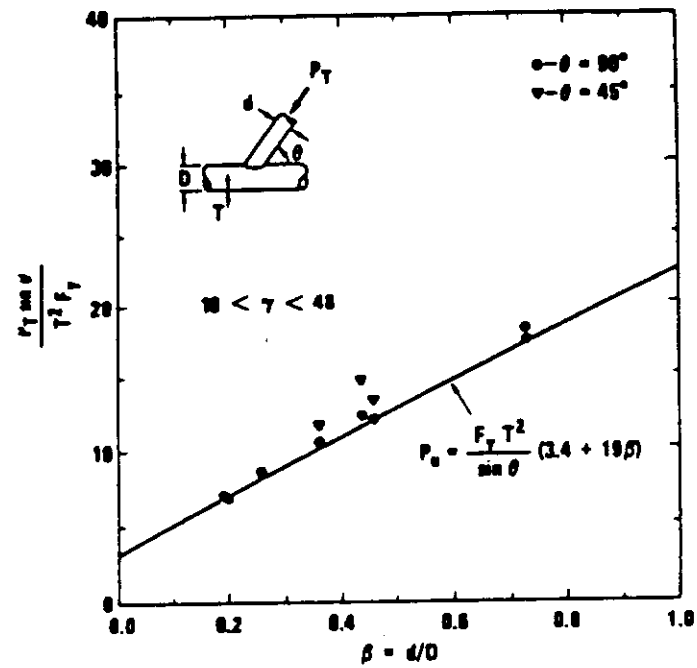
Figure 7.3 Compression Loading of T, Y, and DT Joints
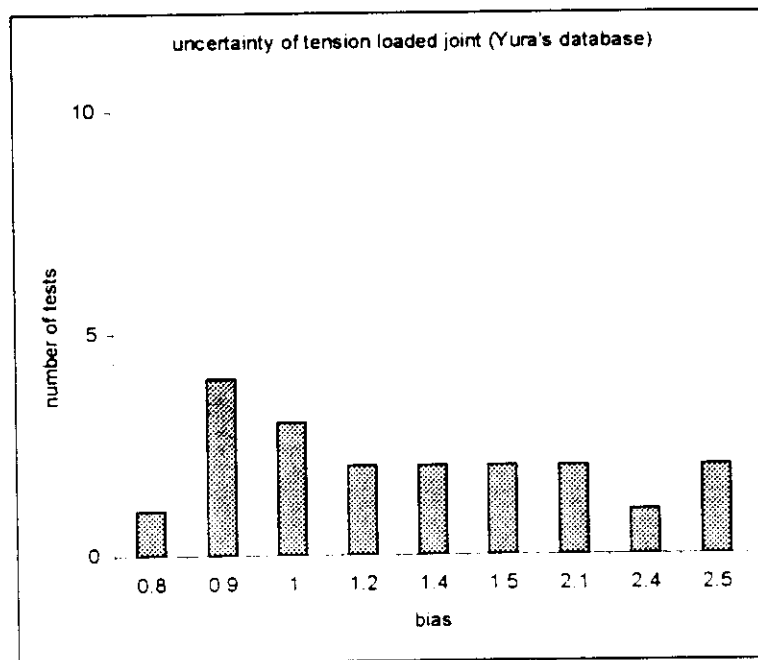
Figure 7.4 Uncertainty of Tension Loaded T, Y and DT Joints Based on Yura's

Database (First Crack Criteria)
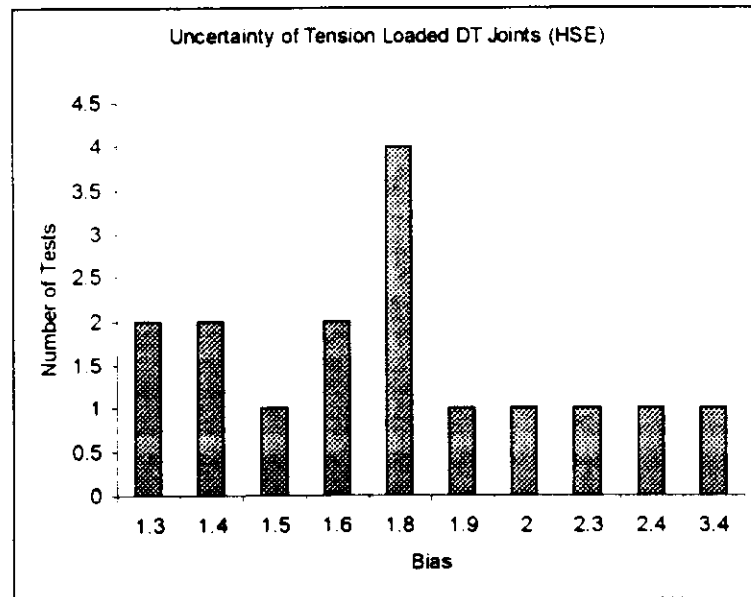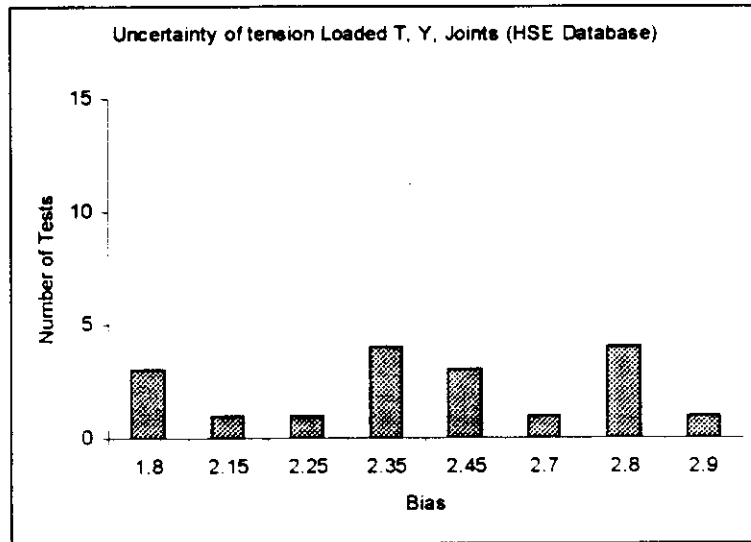
Figure 7.5 Uncertainty of Tension Loaded T, Y and DT Joints Based on HSE

Database (Ultimate Strength Criteria)

Uncertainty Model for Compression Loaded T, Y & DT Joints
Based on Yura's Database
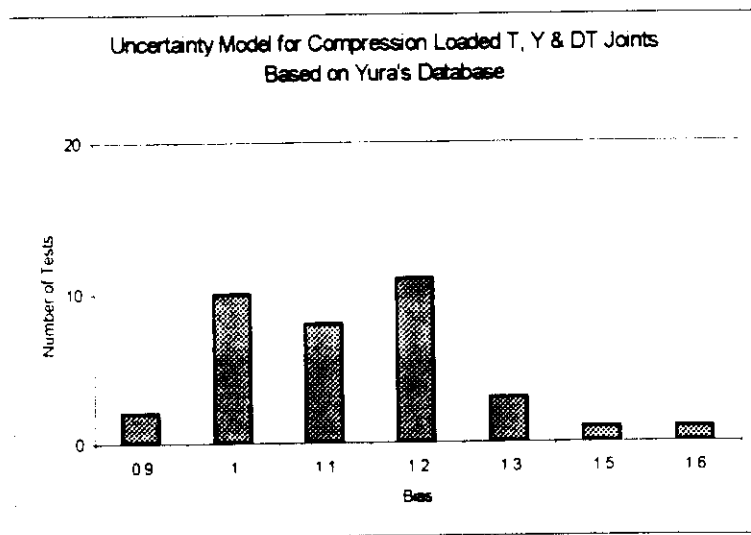
Figure 7.6 Uncertainty Model of T, Y, and DT Joints Based on Yura's Database

Compression Loaded T and Y Joints based on HSE Database

Uncertainty for Compression Loaded DT Joint based on HSE Database
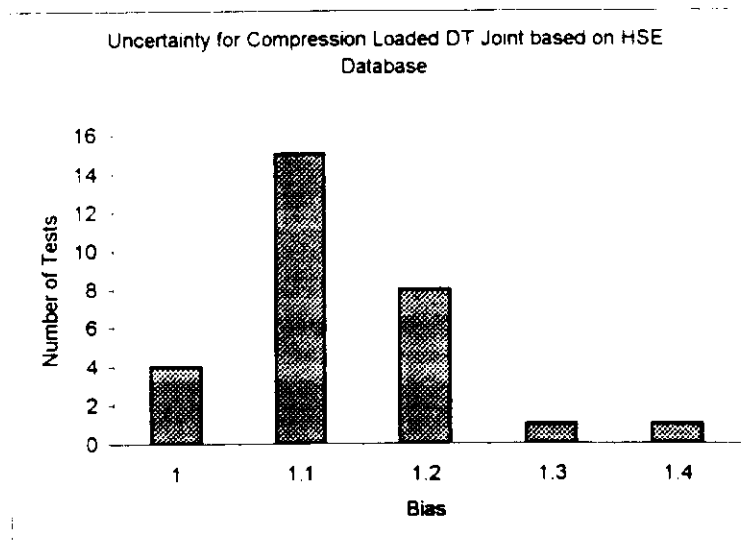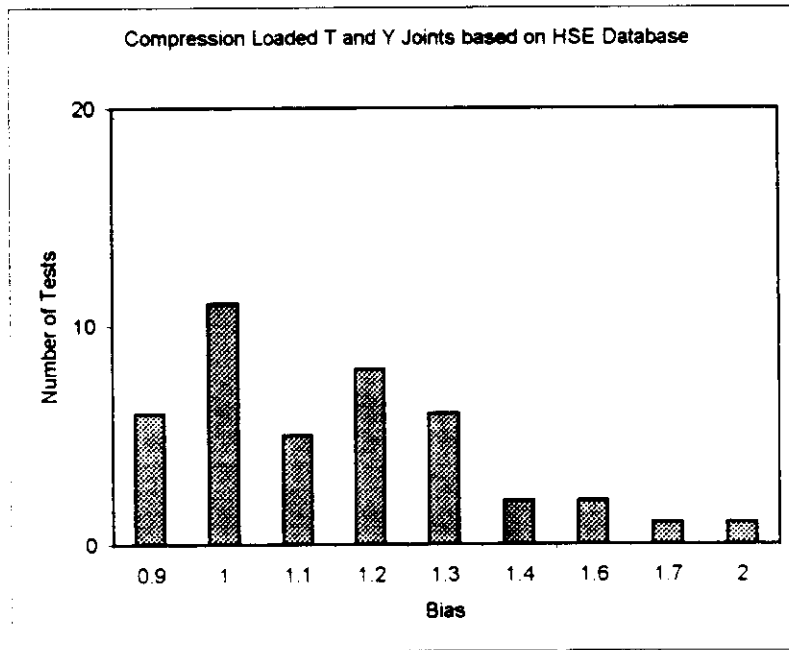
Figure 7.7 Uncertainty for Compression Loaded T, Y, and DT Joints Based on

HSE Database

Uncertainty for Compression Loaded T & Y

Number of Tests

15 -

10 -

5 -

0

| 1 68 | 1.6 | 2 | 1.8 | 2 6 | 1.9 | 2 6 |

Bias
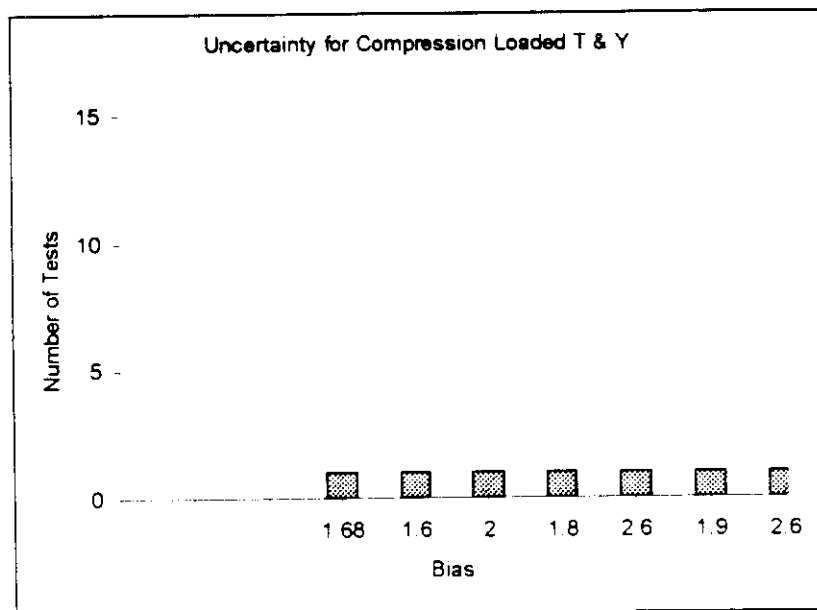
Figure 7.8 Uncertainty of Compression Loaded T and Y Joints Based on JISSP

Database
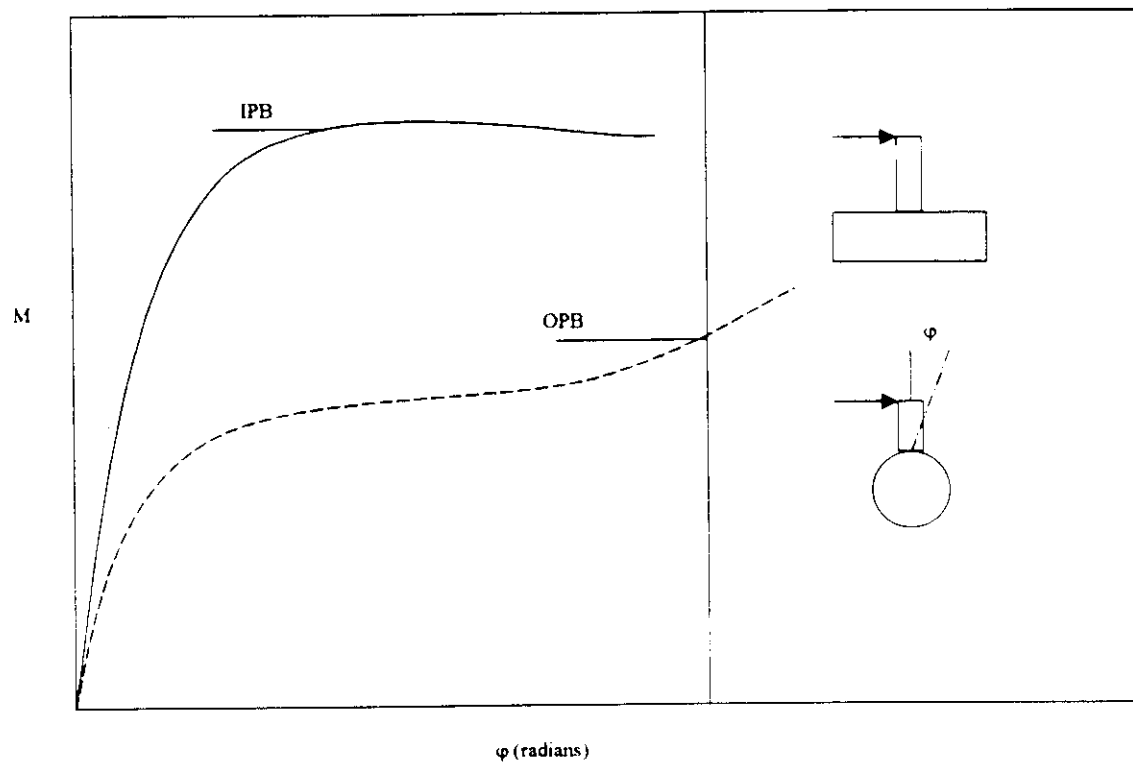
Figure 7.9 Load-deflection Behavior of Tubular Joints subjected to Bending
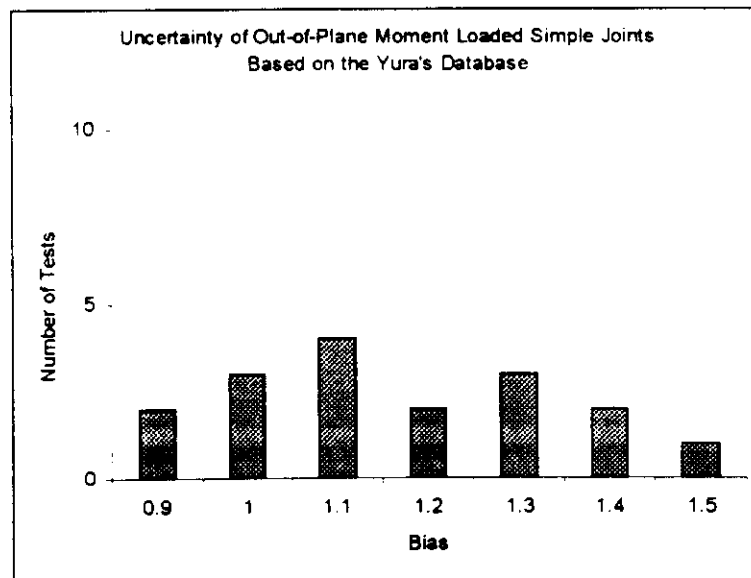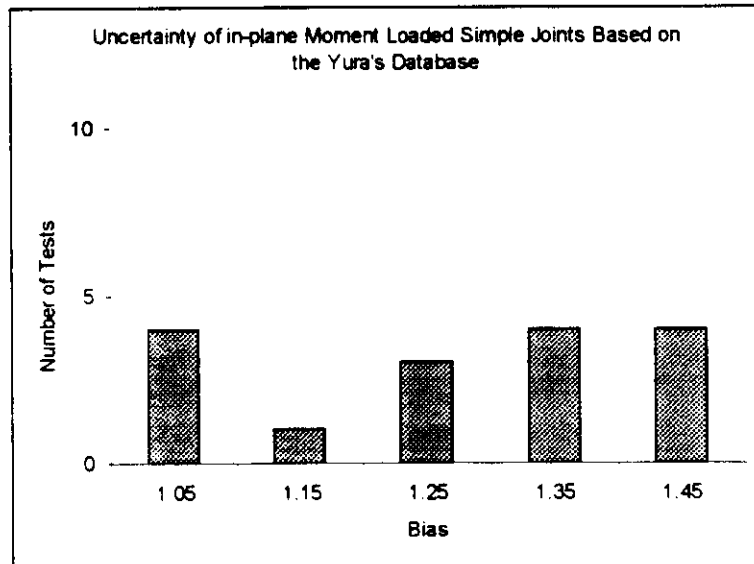
Figure 7.10 Uncertainty of Moment Loaded Simple Joints Based on Yura's
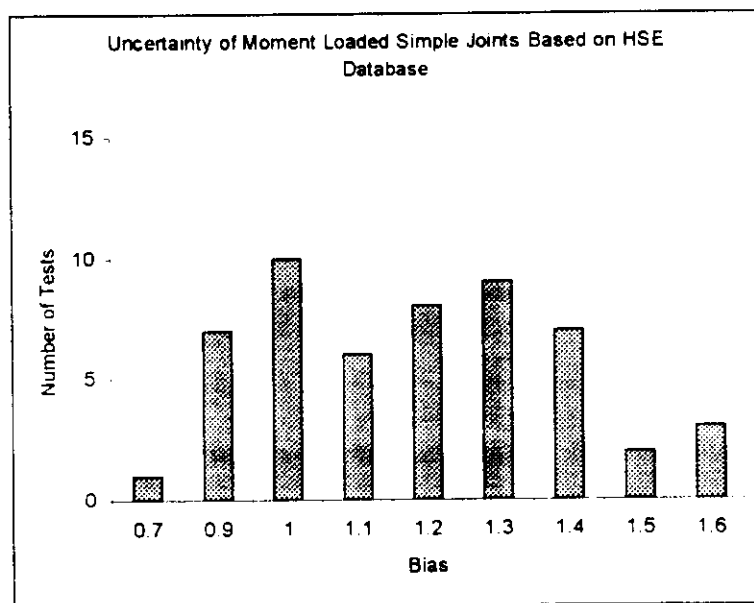
Database

Figure 7.11 Uncertainty of Moment Loaded Simple Joints Based on

the HSE Database
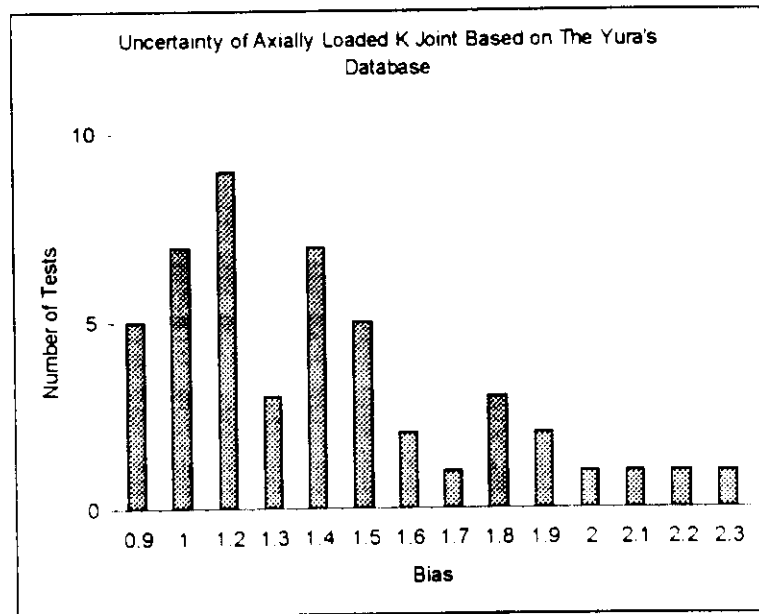
Figure 7.12 Uncertainty of Axially Loaded K-Joints Based on

the Yura's Database
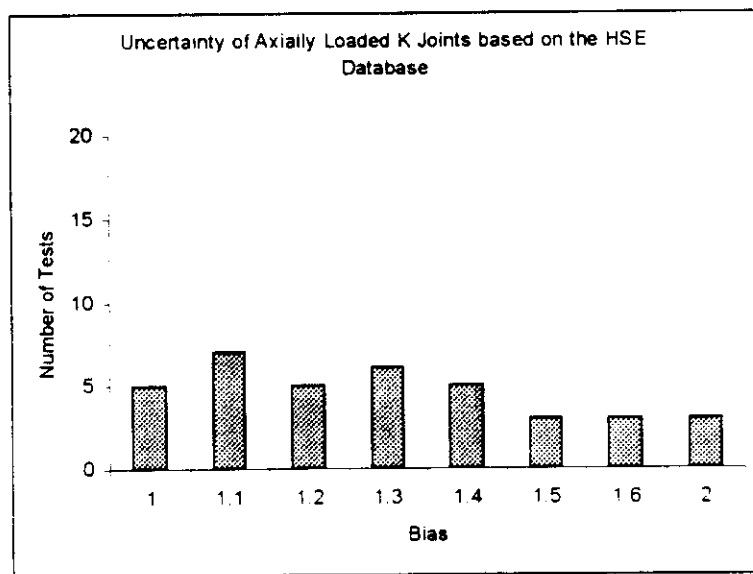
Figure 7.13 Uncertainty of Axially Loaded K-joint Based on

the HSE Database

8.0 UNCERTAINTY OF MULTIPLANAR JOINTS

8.1 GENERAL

Welded joints are common features in offshore structures. Many of these joints are multiplanar in configuration - they are composed of brace members lying in different planes. As discussed early, API and other design documents provide guidelines for the analysis and design of tubular joints. However, such codes are almost exclusively derived from interpreting test results on uniplannar joints and the possible multiplanar effects on strength have not been included in their formulations.

The exception to this is the design formula given in the AWS D1.1 structural welding code (1985) which incorporates a unique overalisation parameter α_0 in accounting for the ovalisation of the chord member due to the position of and loading in the out-of-plane braces. The AWS formulation has the further advantage of providing a single set of equations for all joint types, thus eliminating the often rather arbitrary and subjective joint classification required in other codes.

Since the mid eighties there has been growing attention in understanding multiplanar behavior of tubular joints and many research program mainly experimental have been carried out worldwide. The results of the research have shown that the AWS equation although relatively easy to use and promising in many respects, are lacking in reliability for some joint geometry. Predictions obtained from the AWS code have been found to be either too conservative or unsafe (Lalani and Bolt, 1990, Wilmshurst and Lee !993) to result in large uncertainty associated with the AWS equations.

8.2 OVERVIEW OF THE AWS CODE

The AWS formula is based on a lower bound interpretation of test data on uniplanar joints. Connections are designed such that the acting punching shear stress on a potential failure surface does not exceed allowable shear stress. The punching shear format can be easily rewritten in allowable force format, which is presented here as a lower bound with the safety of 1.8 removed is

$$P_{lower\ bound} = 6\pi\beta \frac{F_y T^2}{\sin\theta}\left[\frac{1.7}{\alpha_0} + \frac{0.18}{\beta}\right]Q_\beta^{0.7(\alpha_0 - 1.0)} \tag{8.1}$$

$$Q_\beta = 1.0 \qquad\qquad for \qquad\qquad \beta \leq 0.6 \tag{8.2}$$

$$Q_\beta = \frac{0.3}{\beta(1 - 0.8333\beta)} \qquad for \qquad\qquad \beta > 0.6 \tag{8.3}$$

$$\alpha_0 = 1.0 + 7.0\frac{\sum_{all\ brace} P\sin\theta\cos2\phi e^{\frac{-z}{0.6\gamma}}}{(P\sin\theta)_{reference\ brace}} \geq 1.0 \tag{8.4}$$

The formula allows the design of multiplanar connections with an arbitrary member of intersecting non-overlapping braces. This is achieved using ovalisation parameter α_0 shown in Equation (8.4), the terms for which are shown in Figure 8.1. α_0 is calculated for each brace at the connection, checking the joint capacity for a different brace each time. It is a measure of ovalisation of the chord member due to the loading in and position of the brace members. The

cosine term signifies the effects of the out-of-plane braces as a function of their position around the circumference from the reference brace. The exponential decay term incorporates the lessening effect of the in-plane braces as a function of the longitudinal distance along the chord member from the reference brace.

8.3   EVALUATION OF AWS CODES

Although the AWS formulation represents a pioneering attempt at analyzing multiplanar capacities, it has to be noted that:

- the derivation of the ovalisation parameters was based on elastic consideration (Marshall and Luyties, 1982).
- at the time of development, it has not been calibrated against multiplanar test results due to a lack of test data.

As data on multiplanar joints became available, the accuracy and reliability of the AWS formulation has been extensively assessed. Such assessments leads to the following revelations:

KK JOINTS. Following observations have been made in the reassessment of KK joints.
1. the joint capacity increases as the in-plane gap decreases. The original AWS formulation did not adequately account for the sharp increase of strength with very small in-plane gaps. Lalani and Bolt (1990) proposed modifiers for joints with small in-plane and out-of-plane gaps. Paul (1992) recommended the use of the small in-plane gap modifier but showed that trend produce by the out-of-plane modifier were contradictory to those observed in experimental and analysis.
2. the failure modes of this joint can be classified into two types (Makino et al 1984):
- Failure Type 1 - applying to joints with small out-of-plane gaps, $\zeta_t \leq 0.2$. The two compression braces act as a single compression brace with effective diameter, with no apparent deformation of the chord wall between braces, Figure 8.2(a)
- Failure type 2 - applying to joints with large out-of-plane gaps, $\zeta_t \geq 0.2$. The two compression braces act independently producing a 'harmmock effect' of the chord cross-section due to the deformation between the braces, Figure 8.2(b).
- For both failure types the AWS formula becomes more conservative with increasing γ (Wilmshurst and Lee, 1993). However, for failure type 1 the code is less conservative with smaller β for a particular value of γ. The trend is reversed for joint failing in type 2 mode. This difference indicates that perhaps the two failure mechanisms should be treated separately with respect to ultimate load prediction.
3. the unmodified AWS formula gives good predictions for both failure types for joints with $\gamma = 12$. Joints with $\gamma < 12$ are overpredicted by the code for both failure types (Wilmshurst and Lee, 1993).
4. application of the small gap modifiers enhanced the reliability of the prediction at higher γ ratios but otherwise the under-prediction amounted to over 40% for type 1 and 60% for type 2. Joints with lower ☐ ratio (below 12) were overpredicted by up to 20%. The modifiers require further examination and the trend suggested that they may be γ dependent.

XX JOINTS. Paul (1988) investigated the effect of unloaded braces on static strength and found that they restrained the ovalisation of the chord wall. This

effect is not accounted for in the AWS formulation. Van der Vegte, G. J., et al (1991) conducted a numerical simulation of experiments on multiplanar XX joints. Four failure modes are used in the analysis: 1) plastic deformation leading to failure of chord cross section, 2) plastic deformation leading to failure of chord cross section and initiation of cracks at the weld toes, 3) plastic deformation leading to failure of chord cross section and through cracks at the weld toes, and 4) squash load or full plastic moment of braces. Their numerical results indicated that there are considerable bias in the AWS codes and the application of API's uniplanar X joint formula in multiplanar XX joints.

TT JOINTS. Scola et al (1990) reported that the α_0 parameter appeared to be too generous in its prediction of increase in strength for TT joints in comparison to their uniplanar counterparts. The above observation indicates that the large uncertainty is associated with AWS design codes. The two uncertainty sources which require immediate attention are those due to γ and gaps.

8.4   REVIEW OF THE DATABASE

A database of axially loaded multiplanar joints was constructed including the finite element analysis (Wilmshurst, and Lee, 1994, van der Vegte, G. J., et al 1991). and experimental data on KK-, XX- and TT-joints. Table 8.1 illustrates the database used in developing the uncertainty models. It includes the 39 TT test data, 18 KK test data, 3 XX test data, 58 FEA data. Appendix B summarizes the data.

8.5   DEVELOPMENT OF UNCERTAINTY MODELS

The basis for the design of multiplanar joints is still insufficient and the commonly accepted design codes do not provide extensive guidance on multiplanar joints except the AWS codes. The API recommendation is to design multiplanar joints as a series of uniplanar joints ignoring the interaction between the different planes. Therefore, application of the API recommendation of uniplanar joints will result in conservative and unconservative uncertainties depending on the geometry and loading configurations.

Uncertainty analysis is more important for multiplanar joints. However, the uncertainty models have not been rationally established due to the limited test data.   This section first gives the explicit assessment of the uncertainty of multiplanar joints based on the available test and numerical data.

KK JOINT. For planar K joint, the parameters β, γ, ζ_t, and θ are known to have an effect on the static strength. These parameters also have an effect on the static strength of multiplanar KK joints, which are also influenced by φ and ζ_l defined in Figure 8.1.

For KK-joints, experimental data were concentrated on test specimens with relatively high γ ratios (>17). Numerical data are established to:
- extend the database of multiplanar KK-joints with low γ,
- study the effects of γ and τ, and
- establish the boundary between failure types 1 and 2.

39 test data are used to develop the uncertainty models. In addition, 40 FEA data are used to calibrate the test data. The test data are compared with the

AWS codes to develop the uncertainty models. The bias and COV is 1.378 and 15% for AWS codes.

In Figure 8.3, the test/AWS capacity ratio is given as a function of ζ_t. The test/AWS capacity ratio varies from 1.15 to 1.94. The uncertainty associated with the exclusion of ζ_t in AWS codes is reflected in the increase of the over prediction with the decrease of ζ_t when $\varphi_1 = 90^0$ as long as failure mode 2 governs. An opposite trend is seen for the joints with failure mode 1 when $\varphi_1 = 60^0$.

The use of small gap correction factors for small longitudinal and transverse gaps in combination with the AWS codes as developed by Lalani et al (1989) is illustrated in Figure 8.4. The test/AWS capacity ratio varies from 0.95 to 1.70.

API RP 2A proposes no multiplanar coefficients for KK-joints to be used with formulae for uniplanar K-joints. Therefore, the K-joint equation is used in API to predict the capacity of KK-joints. Analysis of the available data indicated that the uncertainty of API RP 2A equations is in the range from 1.22 to 2.08 with a mean bias 1.642 and a COV of 12.1%. Figure 8.5 summarizes some test data. In Figure 8.5, the test to API prediction ratio are given as functions of $\zeta_t(a)$ and $\zeta_i(b)$.

TT JOINT. Similar to uniplanar T-joints, failure for multiplanar TT-joints is caused by a combination of local failure and overall chord bending and shear. Paul et al (1989) conducted a series of 11 tests on multiplanar TT-joints. The influence of the diameter ratio β, the out-of-plane gap to chord diameter ratio $\frac{g_t}{d_0}$ and the out-of-plane angle between the two braces φ were investigated. In addition, G. J. van der Vegte (1995) conducted the numerical analysis for the influence of overall chord bending.

In Figure 8.6 the experimental ultimate capacity to AWS lower bound prediction ratios are given for TT-joints, as function of ζ_t. The test to AWS prediction ratios of TT-joints vary from 0.95 to 1.71 and lower than 1.0 for two joints with small values of β and $\varphi = 90^0$. The bias is 1.214 with a COV of 17%.

In Figure 8.7 the test to AWS prediction ratios are given for TT-Joints, as a function of ζ_t, using the out-of-plane small gap correction factor developed by Lalani and Bolt (1989). For TT-joints the test to AWS prediction ratios vary from 0.92 to 1.61, when the out-of-plane gap factor is used, indicating a small decrease in the COV of 12%.

In Figure 8.8, the test capacity to API lower bound prediction ratio are given for TT-joints as a function of ζ_t. The ratios vary from 1.26 to 2.37 with a mean bias of 1.591 and COV of 0.188.

XX-JOINT. Limited data test data are available for the XX-joints. A large amount of the numerical data have been generated based on finite element analysis. However, only limited numerical data are reliable since most of the FE results are not obtained by a fully calibrated and validate model.

Based on the data analysis, the test/AWS predicted capacity ratios vary from 1.36 to 1.54 with the mean bias of 1.47 and COV of 11.7%.

8.6 SUMMARY AND CONCLUSIONS

This section summarizes the uncertainty analysis of the multiplanar joints. Table 8.2 summarizes the uncertainty models associated with AWS codes and API RP 2A recommendations.

Due to the limited available data, it is believed that the multiplanar joint research should be further conducted and the uncertainty models can be further refined. However, on the basis of the models developed in this section, significant increase of the reliability of multiplanar joint strength can be achieved, leading to more rational risk based design and requalification criteria of offshore platforms in the bay of campeche where joints constitute the weak joints.

Table 8.1 Multiplanar Joint Database

Joint Type	Range of Parameters	Origin of Database	Test or FEA	Number of Data
KK	$60^0 \le \varphi \le 90^0$	Paul et al (1992)	Test	18
	$49.1^0 \le \theta_c \le 90^0$	Makino et al (1984)	Test	19
	$0.224 \le \beta \le 0.471$	Makino et al (1992)		
	$9 \le \gamma \le 40$		Test	2
	$0.82 \le \xi_l \le 16.85$	Wilmshurst et al (1993)		
	$0.037 \le \xi_t \le 0.524$		FEA	40
TT	$60.3^0 \le \varphi \le 120.4^0$	Paul et al (1991)	Test	11
	$0.222 \le \beta \le 0.732$			
	$17.2 \le \gamma \le 18.3$	Scola et al. (1989)	Test	7
	$0.037 \le \xi_t \le 0.732$			
XX	$\varphi = 90^0$		Test	12
	$\beta = 0.602$	Van der Vegte et al		
	$\gamma = 20.32$	(1991,1993)	FEA	18
	$\xi_t = 0.39$			

Table 8.2 Uncertainty of Multiplanar Joint

Joint Type	Load Type	Design Code		Mean	COV
TT Joint	Axially Loaded	AWS	unmodified	1.214	0.17
			In-plane modifier	-	-
			Out-of-plane Modifier	1.179	0.15
			Both Modifier		
KK Joint	Axially Loaded	AWS	unmodified	1.378	0.151
			In-plane modifier	1.310	
			Out-of-plane Modifier	1.239	0.108
			Both Modifier	1.178	0.122
XX Joint	Axially Loaded IPB OPB	AWS	unmodified	1.47	0.167
			unmodified	-(2)	-(2)
			unmodified	-(2)	-(2)
TT Joint	Axially Loaded	API	T-joint formula	1.594	0.188
KK Joint	Axially Loaded	API	K-joint formula	1.642	0.121
XX Joint	Axially Loaded	API	X-joint formula	2.07	0.27

(1) - unavailable due to limited data
(2) - design equation is not available
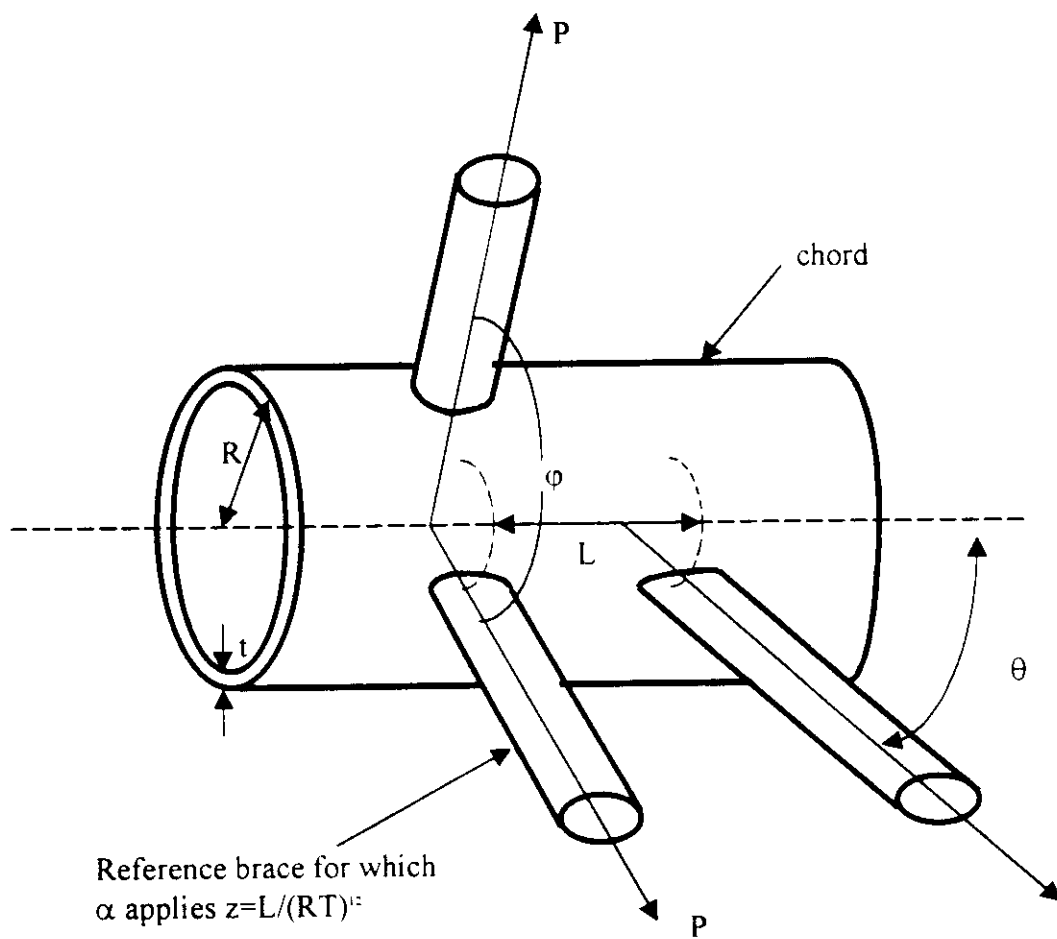
Figure 8.1 Definitions of Terms In Multiplanar Joints
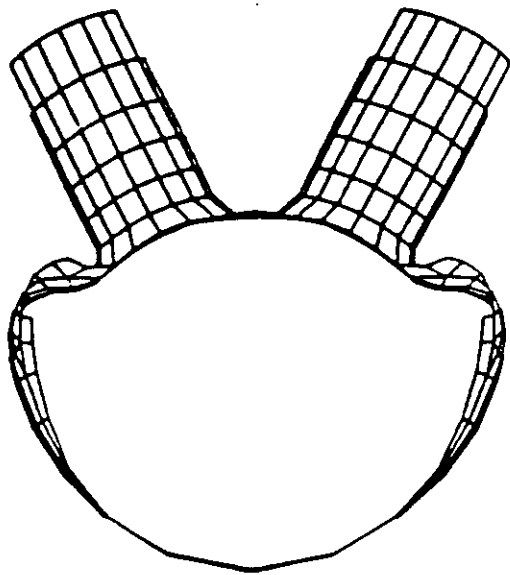
(a) Type 1 failure
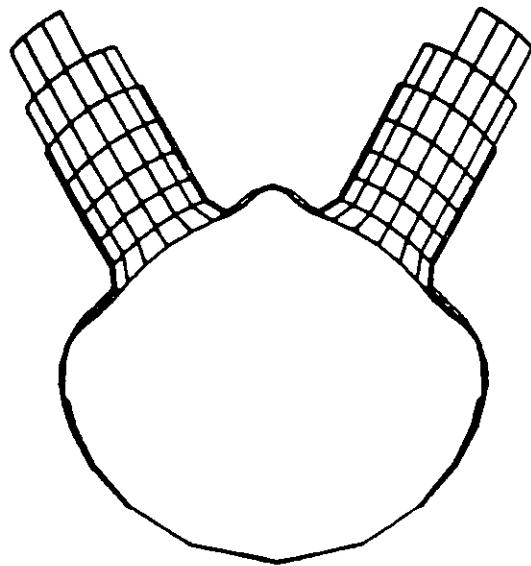
(b) Type 2 failure

Table 4.1 Example Calculation sing Ovalising Parameters α_0
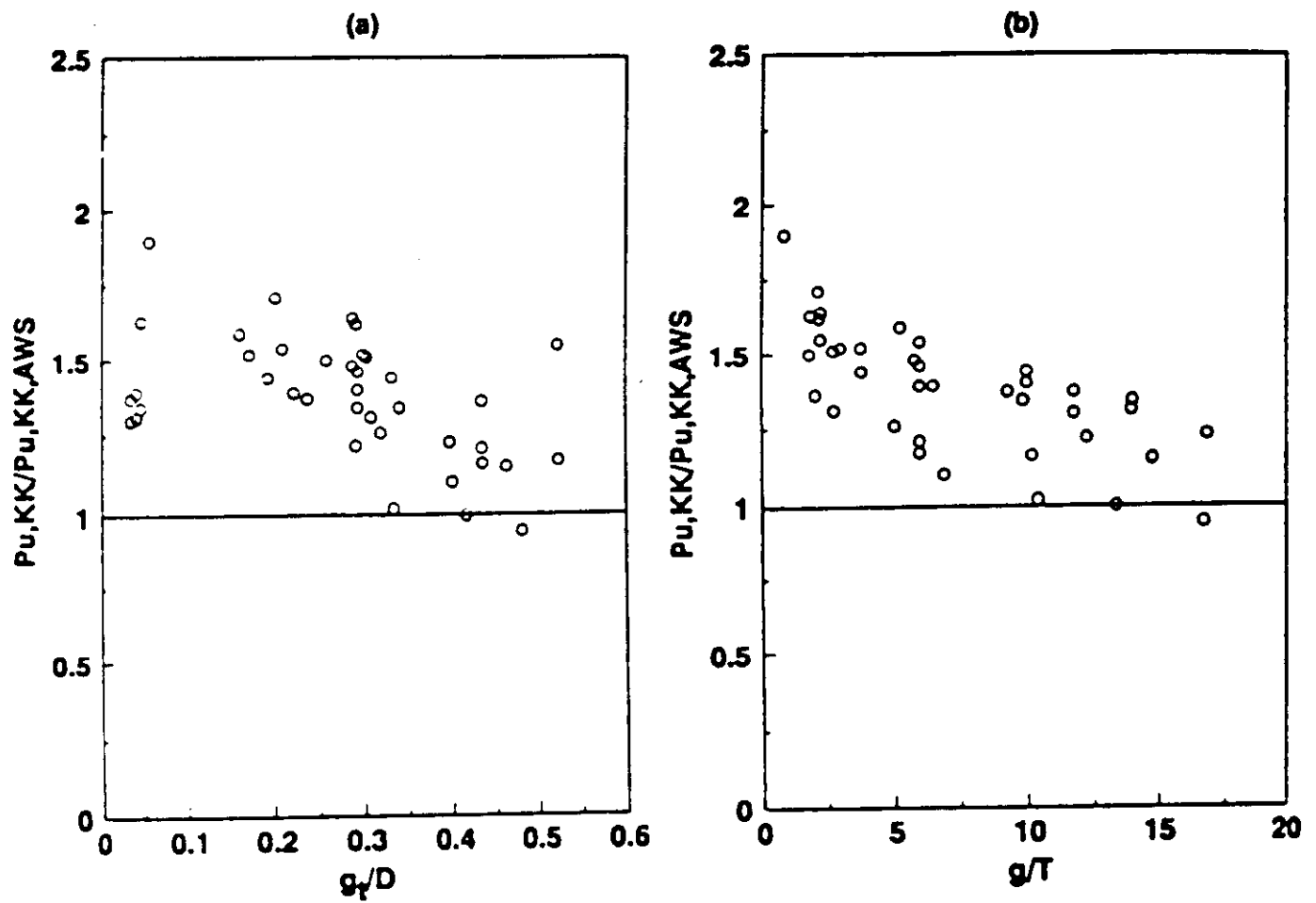
Figure 8.3 Test to Prediction Ratios for KK Joints using Predictions by AWS as a Function of (a) ζ_t, (b) ζ_l
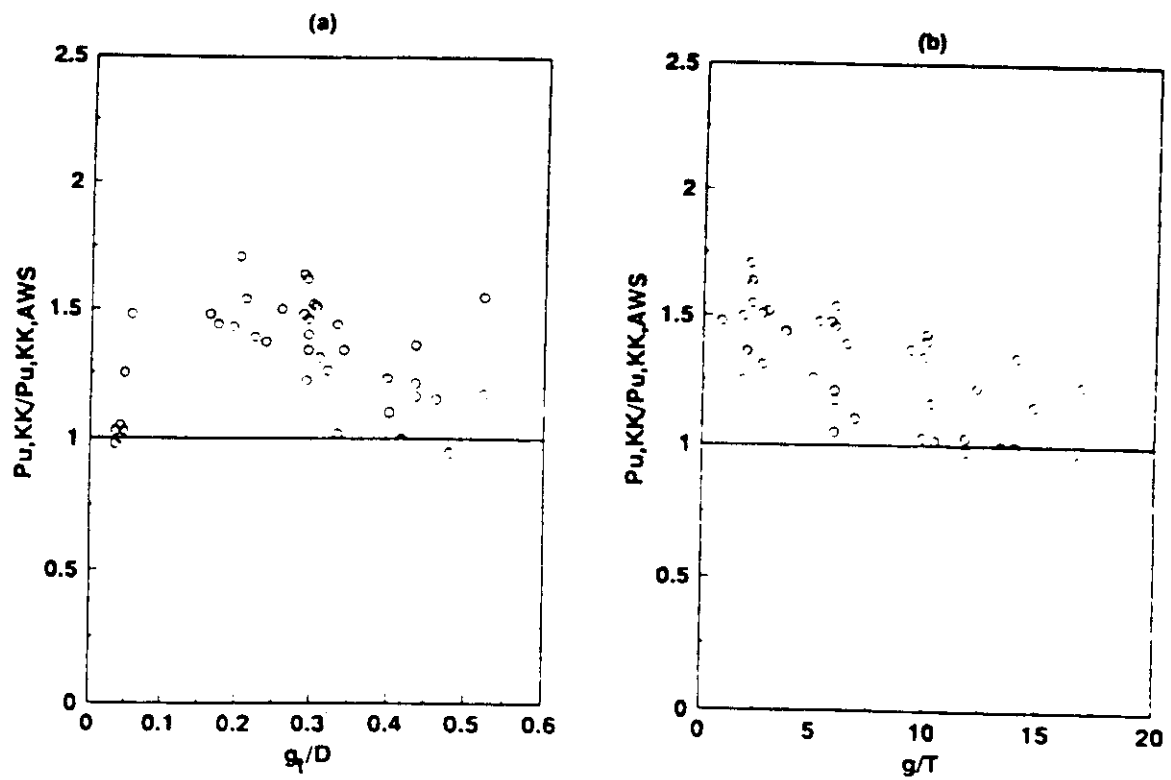
Figure 8.4 Test to Prediction Ratios for KK Joints using Predictions by AWS while Employing the Small out-of-plane Gap Factor of Lalani et al (1989) as a Function of (a) ζ_t, (b) ζ_l

9.0 UNCERTAINTY OF COMPLEX JOINTS

9.1 OVERLAPPING JOINTS

In overlapping joints subjected to static loads, part of the load is transferred through the common shared weld between the brace members. One advantage of such joints is that, since the chord no longer transfers the entire load, its thickness can be reduced. This would generally result in a more efficient load transfer but with added fabrication effort.

The treatment of overlapping joints can be illustrated in Figure 9.1. With zero eccentricity (i.e. e=0) and for a unique b value, the braces of the YT joint may overlap. Here, part of the load is transferred in shear across the common brace weld. For negative eccentricity YT joints, the overlap may be larger (Figure 9.1). The design code API RP 2A is used to check the joints for load transfer perpendicular to the chord member. The loads parallel to the chord are carried by the brace/chord intersection weld and hence the weld and brace wall thickness are designed to transmit this load.

In developing the uncertainty models of overlapping joints, the through brace capacity and the overlapping brace capacity are treated separately due to the lack of reliable data and design codes.

THROUGH BRACE MEMBER. A number of published test results are available in the literature. However, many of the test results are of joints with D < 110mm. In analyzing the existing data, it reveals that the UK HSE database is the most reliable database.

UK HSE database (HSE, 1989) omitted the specimens with chord diameters less than 125 mm since the scale effects associated with both the size of specimen and the weld can be large. It also excluded the test data where insufficient information were provided.

The database summarizes the test results from a total of 16 tests. Some 70 tests results have been excluded due to the size of specimen. The 16 available test data are for balanced axially loaded YT joints. The test results relates to the compression brace. However, there is no information available to confirm which brace (45^0 or 90^0) was loaded in compression.

The API RP 2A doesn't recommend any design equations for the through brace capacity. It only provides the guidance on the capacity of the overlapping brace based on the axial capacity of overlapping brace/chord intersections. Therefore, the test data is compared with the API RP 2A design equations for simple T, Y, and non-overlapping K joints.

The API RP 2A design equations for non-overlapping K joints without the safety factor 1.7 is:

$$P_u = \frac{F_y T^2}{\sin\theta}(3.4 + 19\beta)Q_g Q_f \tag{9.1}$$

As the gap reduces for a simple K joint and becomes negative for overlapping joints, the strength of the joint increases. The term Q_g is used to describe the gap effects. For negatively gapped overlapping joints, it is used to describe the ratio of the strength of an overlapping joint to a simple Y or T joint.

All available test data are plotted as a multiple of the simple joint strength in Figure 9.2. The figure, which can be considered as a plot of the effective Q_g parameter, shows that the increase in strength as the gap reduces for overlapping joints. A bias factor of 3.56 and COV of 31.2% can be estimated based on the available data.

OVERLAPPING BRACE MEMBER. The API RP 2A design equations for overlapping joints are generally applied to determine the capacity of the overlapping brace member, or more specific, the axial capacity of overlapping brace/chord intersections. It is developed based on a "crude ultimate strength analysis in which the punching shear capacity for that portion of the brace reaching the main member, and the membrane shear capacity of the common weld between braces, are assumed to act simultaneously'. However, no reliable data are available to investigate the capacity of overlapping joints with failures associated with the overlapping braces. Therefore, no data is available to analysis the uncertainty of the API RP 2A design equations for the axial capacity of overlapping brace/chord intersections.

9.2   GROUTED JOINT

The connection to the seabed of traditional jacket steel structures is achieved by means of tubular steel piles which are passed through each main leg or skirt pile sleeve of the structure and either driven into or grouted into a pre-drilled hole in the seabed. Although piles passing through the main legs may be connected to the structure by welding at deck level, in many structures the annulus between each pile and leg or skirt pile sleeve is filled with cement grout. In addition, the use of a cement grouted sleeve is one of the means to strengthen, repair the tubular joints.

The presence of a pile and grout annulus results in an increased static strength of tubular joints. In the following sections, a quantitative description of composite action of grouted joints under various load type is given. Grout length as well as joint flexibility are brief treated. The discussion is mainly based on the experimental tests conducted by Tebbett (1979).

AXIAL LOAD (TENSION AND COMPRESSION). In ungrouted joints, ovalisation of the chord is the dominant factor for causing stress concentration. However, for grouted joints, the relatively large ovalisation of the chord are constrained by the grout mass under axial loading. The load deflection curve of axially loaded grouted joints is shown in Figure 9.3.

IN PLANE BENDING. In case of in plane bending, the chord wall in the tensile zone is locally separated from the grout. Due to the fact that contact pressure occurs in the compression zone, the expectation is that the neutral line of the reacting forces will shift to the compression zone for brace bending (Figure 9.4).

OUT OF PLANE BENDING. Out of plane bending can be roughly distinguished in axial compression and axial tension. The grout may provide major improvement in stress peak behavior. Here also the neutral line shifts.

BEHAVIOR UNDER COMBINED LOADING. Joints subjected to fatigue loading in general have stress peaks that, apart from some local plastification, remain in the elastic region. In overviewing the combined load cases, it will be assumed that there is neither plastic deformation in the steel nor significant cracking effects in the grout.

For instance, in case of bending in plane the neutral line will shift towards the compression zone when the load is increased. The stresses in the tensile zone will increase non-proportionally with the load. So the composite joint will act as a geometric non-linear substructure, which means that different loads can not superimposed in case of combined loading. Above all there is the complication of load level. In fact the designer faces an almost infinite number of cases she/he has to investigate before maximum stresses can be determined. This is not a practical option, the number of calculations/experiments will be large which results in increasing computer costs. Also, a vastly growing amount of data has to be studied.

The conclusion is that calculation of separate load cases and/or several (discrete) load levels provides limited insight in the exact stress behavior where combined loading is concerned. More research will provide more data, but the designer's insight in composite joint behavior is still the most important tool.

GROUT LENGTH. Due to the fact that stress peaks are (compared to the member length) of very local nature, increased grout length will yield little improvement in static strength behavior. The different Qu for grouted Joints.

Brace Loading	ISO
Axial Tension (AXT)	$2.5\beta\gamma K_a$
In-Plane Bending (IPB)	$1.5\,\beta\gamma$
Out-of-Plane Bending (OPB)	$1.5\beta\gamma Q_b$

9.3 STIFFENED JOINTS

The design guidance for stiffened joints, however, is still inadequate. For example, according to U.E.G (1985), the local ring stress of ring-stiffened nodes can be determined using Roark's formulae (Young, 1989) which are based on an elastic "closed ring" approach, while the joint capacity can be derived using the ultimate (plastic) strength of the un-stiffened joints in combination with a contribution provided by the ring strength capacity.

X-JOINT. Figure 9.5 shows the configuration of axially loaded uniplanar X joints. The dimensions of the X-joints considered are summarized in Table 9.1. The brace to chord diameter ratio β (0.25, 0.49, and 0.74) and two chord diameter to chord wall thickness ratios 2γ have been analyzed (36.4 and 48.8). The chord diameter do is taken as 1854 mm. For all joints, the chord length parameter α has been set to 16.

The configuration of the T-shaped stiffeners is illustrated in Figure 9.6, while the dimensions are given in Table 9.2. The internal ring--stiffener is positioned in the center of the X-joint. Each X-joint has been analyzed for each of the four different dimensions of the T-shaped stiffener. For reference, the un-stiffened uniplanar X-joints have been analyzed as well.

The steel grade of all chord and brace members is S355 with f_y =355 N/mm^2 and f_u =510 N/mm^2. The true stress-strain curves have been modeled as step-wise linear relationships, including strain hardening.

The mean bias is 2.23 for the numerical results. Based on the bias factor of 1.4 between the numerical analysis and design equation for unstiffned X-joints, the bias is about 3.12. The analysis results are summarized in Table 9.3.

T-JOINTS. Similar numerical analysis can be found for stiffened T-joints. The mean bias can be derived as a factor of 2.89 (Vegte, G. J., van der, et al 1996).

9.4 JOINTS RE-ENFORCED BY CAN

Tubular joints sometimes are strengthened by providing a thicker chord section or can right at the intersection of the chord and brace. As discussed in Section 3.0, API RP 2A adopted the derating equation in AWS to analyze the effect of short can on the ultimate strength of the simple joint. It gives the capacity for a joint with chord member outer diameter, D, and can length, L_c, as

$$P = P(1) + \frac{L_c}{2.5D} [P(2) - P(1)] \qquad \text{for } L_c < 2.5D$$

$$P = P(2) \qquad \text{for } L_c \geq 2.5D \qquad (9.1)$$

in which P(1) is the nominal strength obtained using the chord thickness away from the joint, and P(2) is obtained using the thickness at the joint.

T-JOINT. Madros, M et al (1995) conducted the numerical simulation for the T joints re-enforced by the short can. The material property is assumed to be governed by rate independent incremental flow theory with isotropic strain hardening. An elastic modulus of 200,000 Mpa is used with a yield stress 355Mpa, and a step-wise linear relationship representing the straining hardening. Only compression load is assumed along the brace member, and the Riks non-linear load control method is used in the peak region.

The mean bias and COV are determined to be 1.085 and 5.7%. Figure 9.7-9.9 details the results.

X-JOINT. Vegte, G. J. van der al (1995) conducted the numerical simulation for the X-joints re-enforced by the short can. The material property is the same as the simulation for T-joints conducted by Madros, M et al (1995). Only compression load is assumed along the brace member.

The mean bias and COV are determined to be 1.175 and 7.4%. Figure 9.10-9.12 details the results.

9.5   CRACKED JOINTS

A significant number of data from static strength tests and finite element analyses of cracked tubular joints are available (Stacey, A., et al 1995). In addition, several researches are currently underway.

The review of the available data indicated that, depending on the defect size, the presence of a defect in a tubular joint can have a significant influence on the static strength capacity. Predictions based on parametric static strength equations for intact joints can overestimate the capacity of a cracked joint.

Procedures for the prediction of the capacity of cracked tubular joints are currently being developed and recent results have been used to develop a fracture mechanics assessment procedure for offshore structures in the forthcoming revision to BS PD 6493. The procedure is generally based on the use of static strength equations for intact tubular joints in conjunction with correction factors, which allow for the presence of defect, and the sue of the Failure Assessment Diagram (FAD) approach.

The description of the FAD can be found in the references (BSI, 1991, Xu, 1997). In general, three level assessment are given in order of increasing complexity and decreasing conservatism.
1. Level 1 - a preliminary screening procedure,
2. Level 2 - the usual assessment procedure for structural application and that generally used for offshore structures. The level 2 method yields realistic predictions for situations where ductile tearing is limited.
3. Level 3 - this procedure is appropriate to ductile materials which exhibit stable tearing.

The fracture assessment procedure for offshore structures is generally based on the use of the Level 2 failure assessment diagram for low work hardening materials. However, special issues of tubular joints should be considered in applying the level 2 assessment.

LOCAL AND GLOBAL COLLAPSE. The evaluation of cracked tubular joints requires consideration to be given to local and global collapse. Local collapse corresponds to failure of the ligament and is therefore dependent on local yielding of the region adjacent to the crack front. Global collapse takes place when the deformations become unbounded and the whole structure becomes a failure mechanism.

The use of local collapse load is generally conservative. The degree of conservatism depends on the geometry and toughness of the flawed structure. Note that a redundant structure plastic collapse does not occur at the formation of the first plastic hing: the amount of plastic strain which can occur at the first hing is controlled by the elastic stiffness of the sounding structure.

Global collapse solutions are likely to apply in the case of through-thickness cracks. Available solutions are usually based on a plate or a tubular joint model. A plate model is appropriate for cracks on the brace side. Cracks on the chord side may be assessed using a tubular joint model.

COMBINED LOADING. Plastic collapse load solutions for a range of cracked geometries under pure axial and pure bending loading are presented (Gibstein, et al 1986). However, the through-thickness stress distribution is normally represented by a combined tension and bending load and consequently there is a need to predict collapse loads for the combined cases.

A lower bound estimate of the collapse load for a cracked tubular joint under combined loading, based on the equation for uncracked joints, is:

$$S_r = \left|\frac{P_a}{P_c}\right| + \left(\frac{M_{ai}}{M_{ci}}\right)^2 + \left|\frac{M_{ao}}{M_{co}}\right| \tag{9.2}$$

where, P_c, M_{ci} and M_{co} are adjusted to take account of the crack. The collapse load P_c is the load to raise the net area to an average stress equal to the yield strength. The S_r is combined with the fracture parameter K_r in the BSI level 2 assessment of cracked joints.

PLASTIC COLLAPSE SOLUTIONS. Plastic collapse solutions have been derived for tubular joints based on the application of a correction factor to the lower bound ultimate strength for the geometry concerned using the API RP 2A equations for intact joints and the specified minimum yield strength. The ultimate strengths for axial, in-plane and out-of-plane bending loads should be calculated separately. The analytical and experimental results indicate that a safe prediction of the collapse load of cracked joints can be made by multiplying the capacity of the intact joint by an area reduction factor F_{AR}.

F_{AR} is the reduction factor to allow for the loss of load-bearing cross-sectional area due to the presence of the flaw and is given by:

$$F_{AR} = \left(1 - \frac{\text{crack area}}{\text{weld length} \cdot T}\right) \cdot \left(\frac{1}{Q_\beta}\right)^{mq} \tag{9.3}$$

Q_β allows for the increased strength observed at β values above 0.6. Q_β is known as the geometrical modifier, usually used in design codes to account for the increased capacity of uncracked tubular joints at high β :

$$Q_\beta = 1 \qquad\qquad \text{for } \beta \leq 0.6$$

$$Q_\beta = \frac{0.3}{\beta(1 - 0.833\beta)} \qquad \text{for } \beta > 0.6 \tag{9.4}$$

m_q is the power allocated to Q_β and depends on the approach used to estimate the capacity of the uncracked joint:

- For tubular joints containing part-through thickness flaw, $m_q = 0$
- For tubular joints containing through-thickness flaws, validated correction factors giving lower bound estimates of the collapse load are at present limited to joints with ratios β less than 0.8 and the following configurations:

1. K-joints with a through-thickness crack at the crown subjected to balanced axial loading,
2. Axially loaded T and DT joints with a through-thickness crack at the saddle.

For K joints subjected to balanced axial loads, the revised BS PD 6493 procedure recommends the use of the API RP 2A compression design strength (omitting the safety factor of 1.7) with $m_q = 0$. For T and DT joints, the revised BS PD 6493 procedure recommends the use of the API RP 2A tension design strength with $m_q = 0$.

If the conservative assumptions lead to the global collapse values of S_r being lower than the local collapse value of S_r, the procedure allows the use of the local collapse value.

UNCERTAINTY ANALYSIS. The collapse load data determined by the experimental and numerical analysis were collected and compared with the API RP 2A design equations for intact joints. Table 9.4 summarizes the experimental database.

In the numerical analysis, the static strength of cracked joints was evaluated based on the load-displacement and moment-rotation curves generated in the finite element analysis of the cracked joints. Examples of non-dimensional moment-rotation and load-displacement curves for cracked joints of a β equals 0.95 K joint under axial and OPB loading are presented in Figures 9.13 and 9.14. Failure was generally signaled by the attainment of a plateau load which was taken as the maximum load/moment achieved. It was assumed that failure occurred at this stage as it was considered that the very high strains involved would be sufficient to cause ductile tearing failure.

The experimental and numerical analyses were analyzed further using the static strength equation of API RP 2A modified by the area correction factor in accordance with the revised BSI PD 6493. The results are presented in Figure 9.15 with the mean bias of 1.73 and COV of 15.4%. The data were also analyzed using the static strength equation of API RP 2A for intact joints. The results are presented in Figure 9.16.

9.6   SUMMARY AND CONCLUSIONS

This section summarizes the uncertainty analysis of complex joints including the overlapping joints, stiffened joints, joints re-enforced by the can, and the

cracked joints. Due to the limited data, the uncertainty is larger than that of simple joints, and multiplanar joints.

Based on the uncertainty analysis of complex joints, clearly there is a need for systematic experimental/numerical studies including some benchmark tests of the implied uncertainty of current design codes and analysis methods used to determine the strength of complex tubular joints.
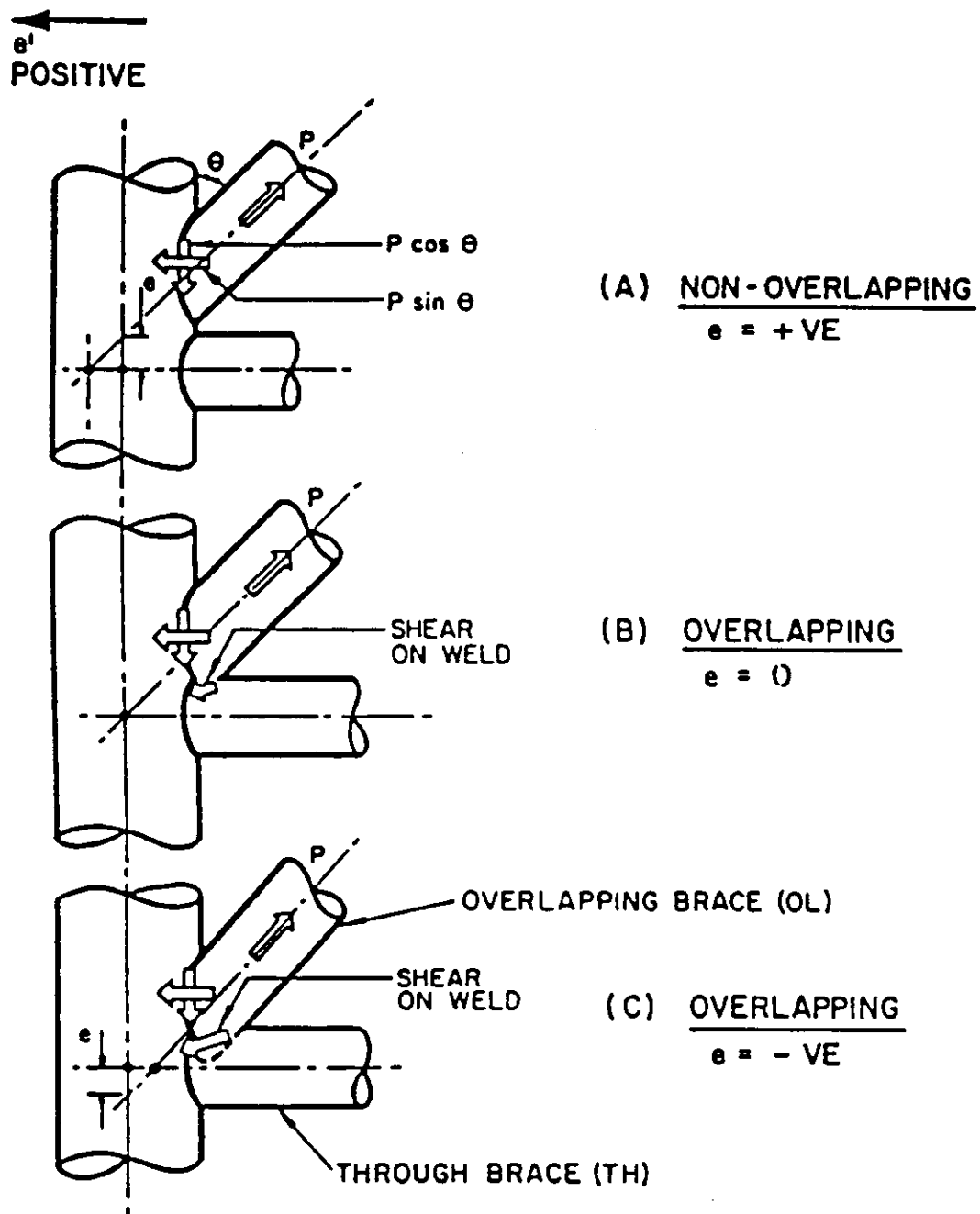
Figure 9.1 Overlapping Joint
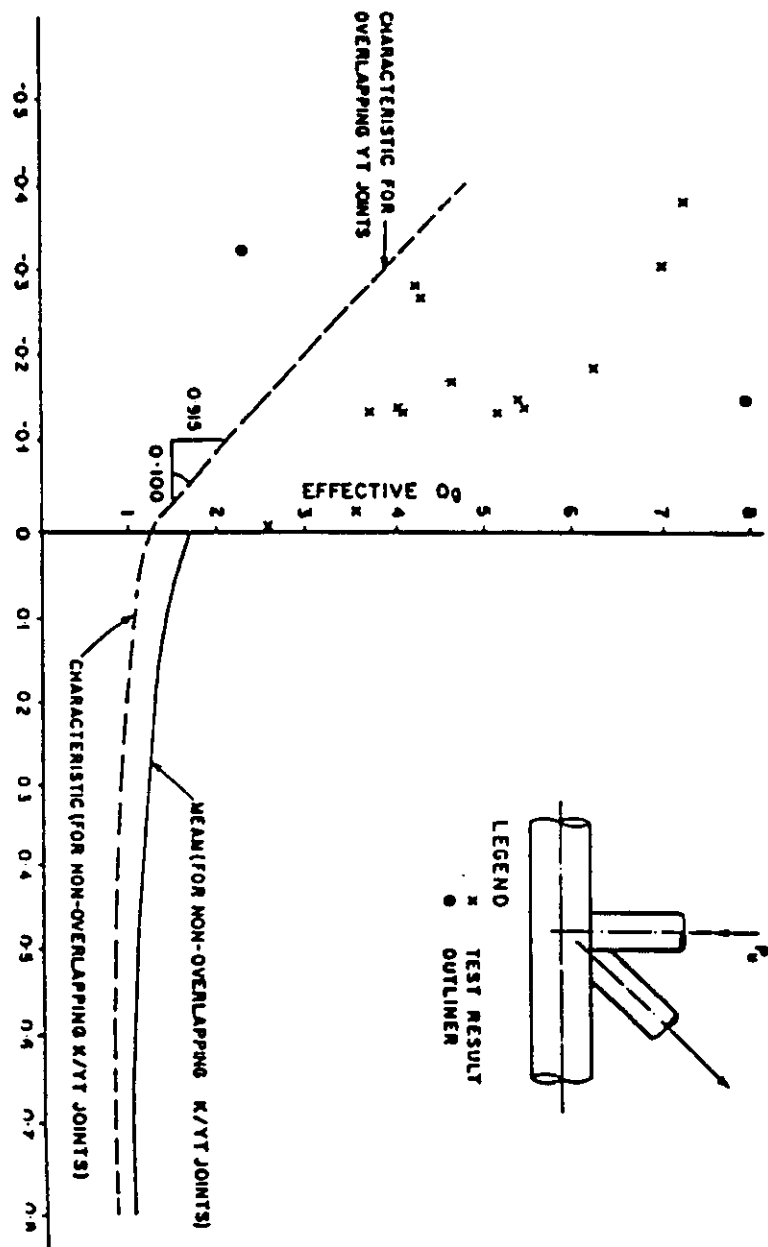
Figure 9.2 Uniplanar Overlapping YT Joints - Effect of Gap Parameter
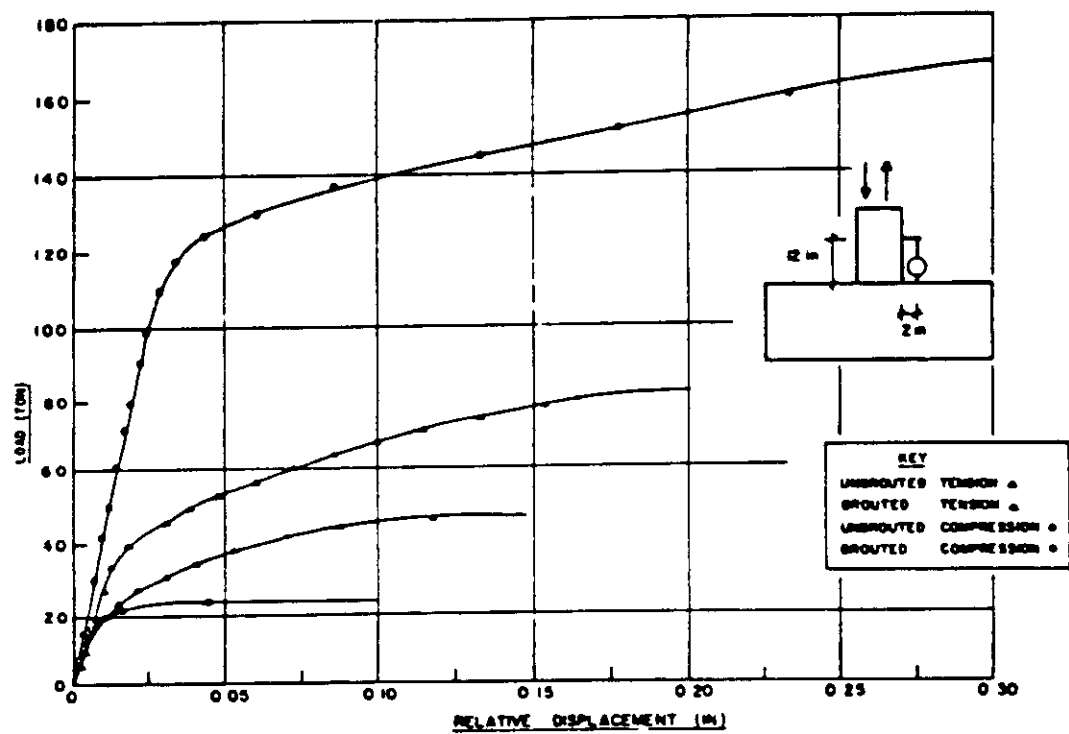
Figure 9.3 Behavior of Grouted Joint Under Axial Load
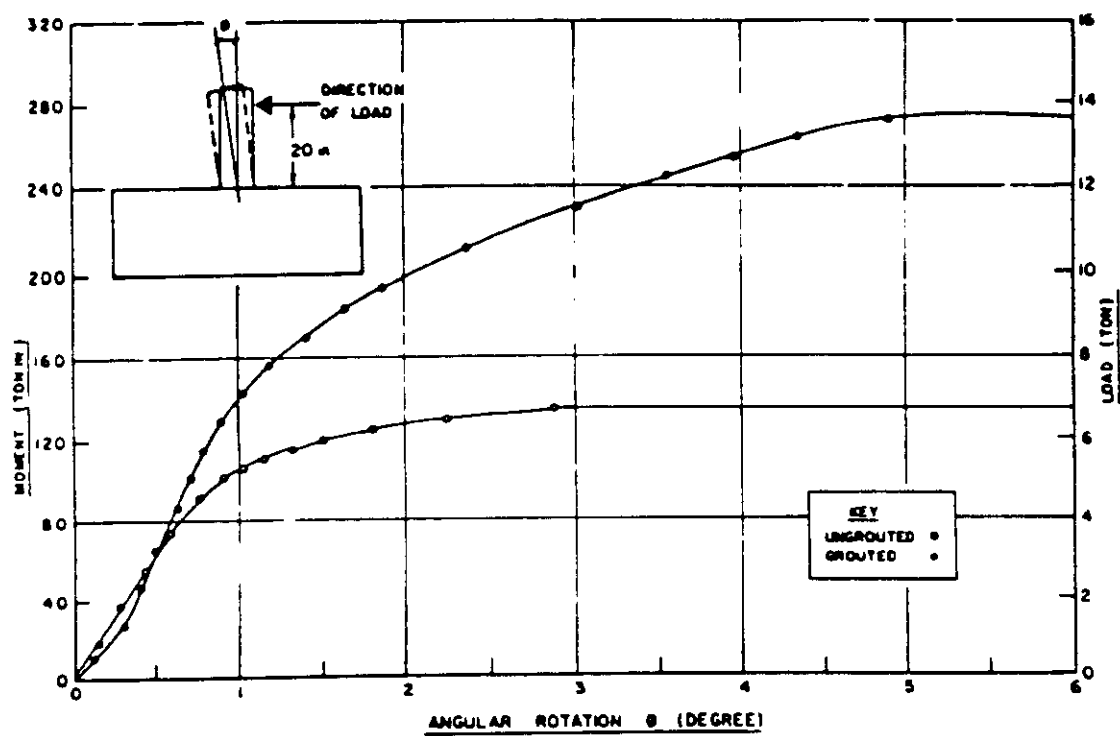
Figure 9.4 Behavior of Grouted Joint Under In Plane Moment
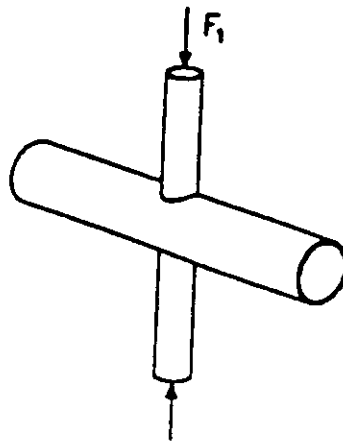
Figure 9.5 Configuration of Axially Loaded Stiffened X Joints
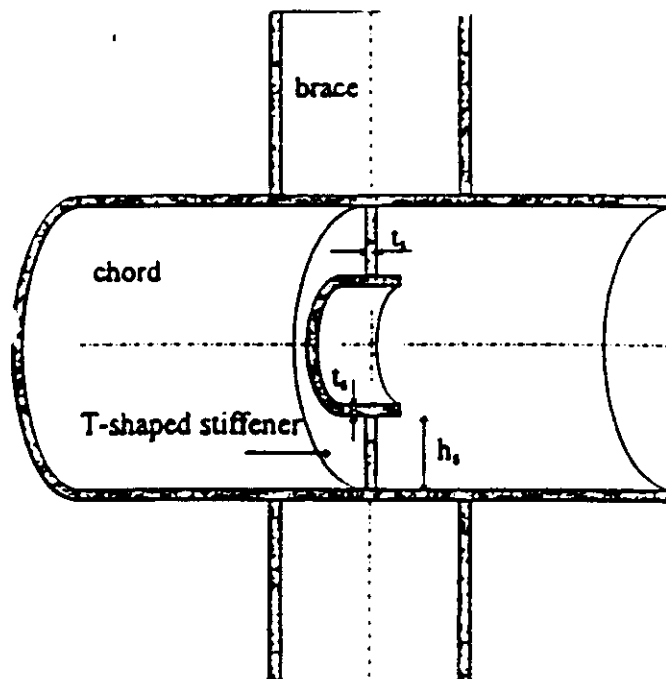
Figure 9.6 The Configuration of the T-shape Stiffeners
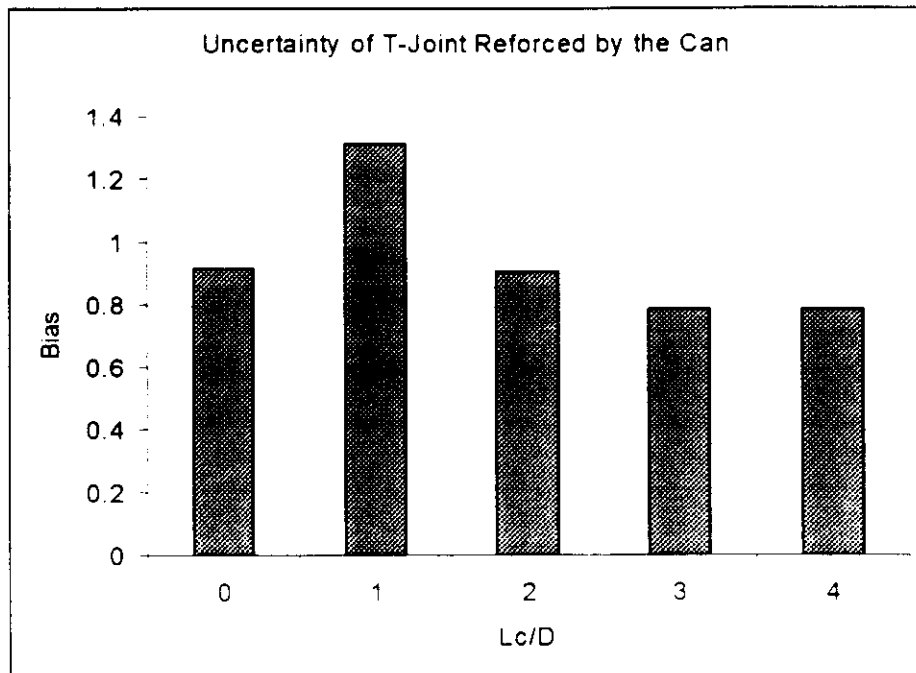
Figure 9.7 Uncertainty of T-joints Re-enforced by the Can (β=0.48, D/T_e=25.4,
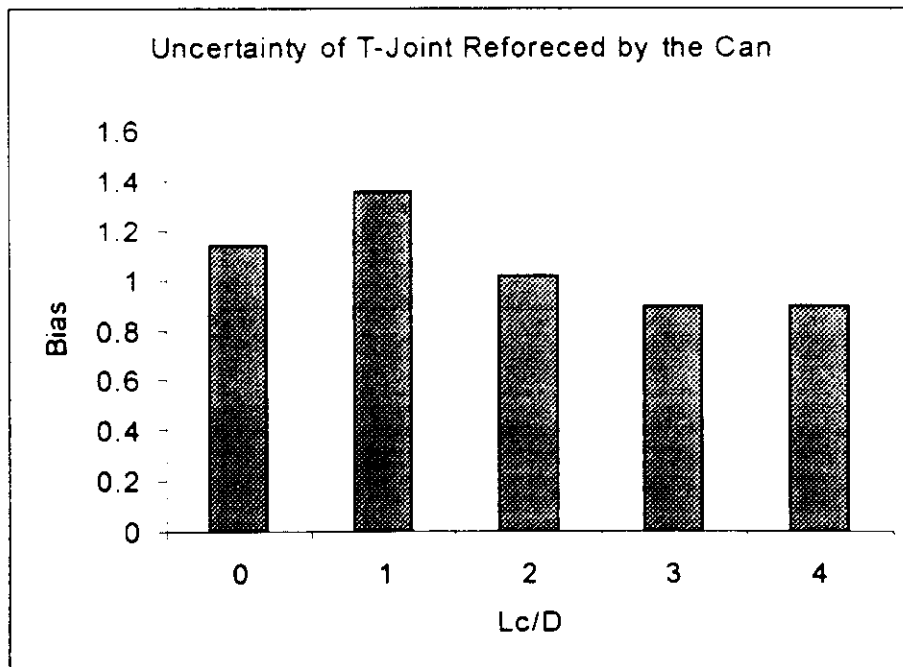
T_e/T=2.0)

Figure 9.8 Uncertainty of T-joints Re-enforced by the Can (β=0.25, D/T_e=25.4,

T_e/T=2.0)

Figure 9.9 Uncertainty of T-joints Re-enforced by the Can ($\beta=0.73$, $D/T_e=25.4$,

$T_e/T=2.0$)
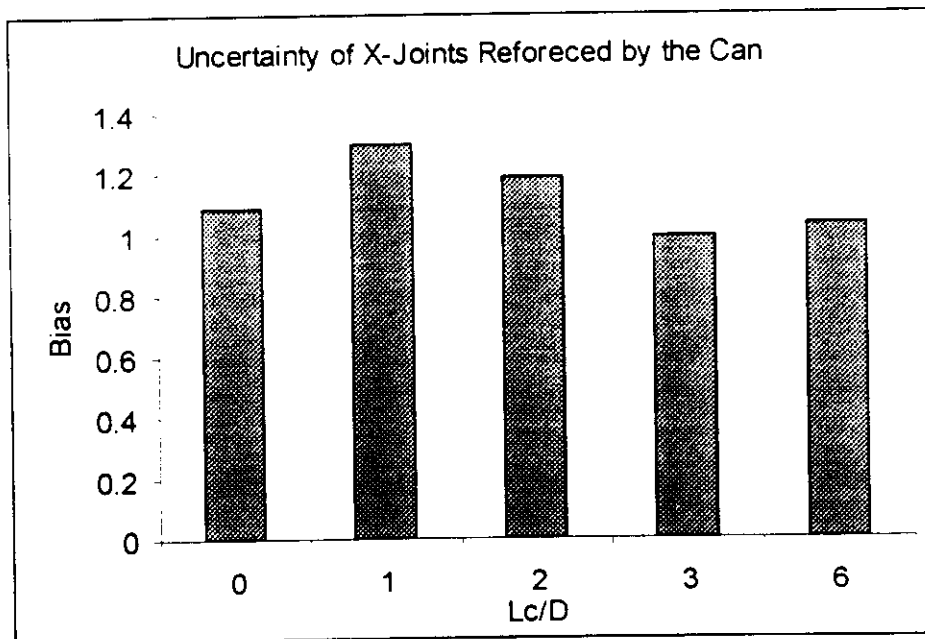
Figure 9.10 Uncertainty of T-joints Re-enforced by the Can ($\beta=0.25$, $D/T_e=25.4$,

$T_e/T=2.0$)
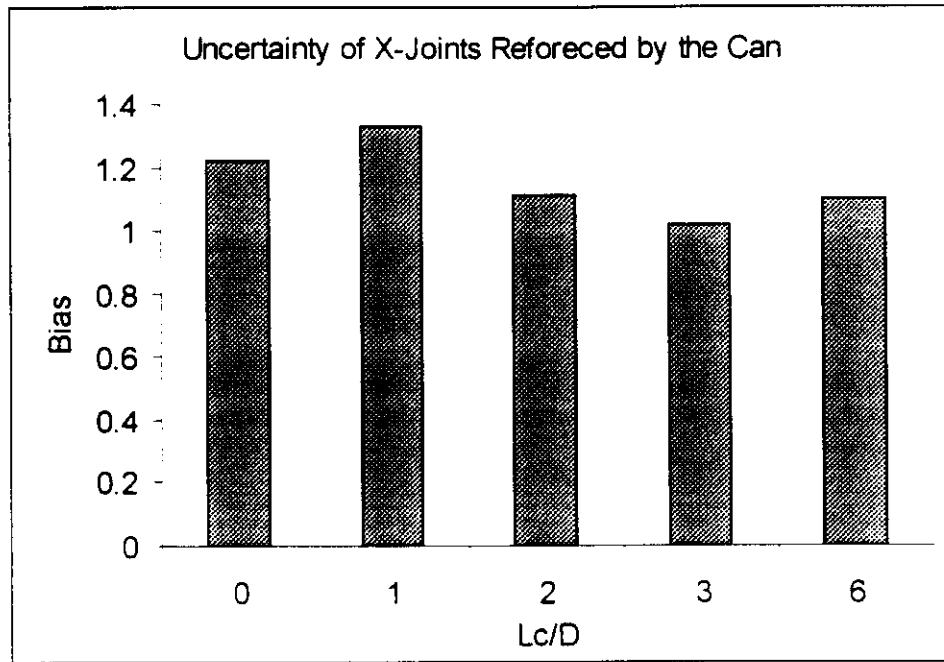
Figure 9.11 Uncertainty of T-joints Re-enforced by the Can (β=0.48, D/T_e=25.4,
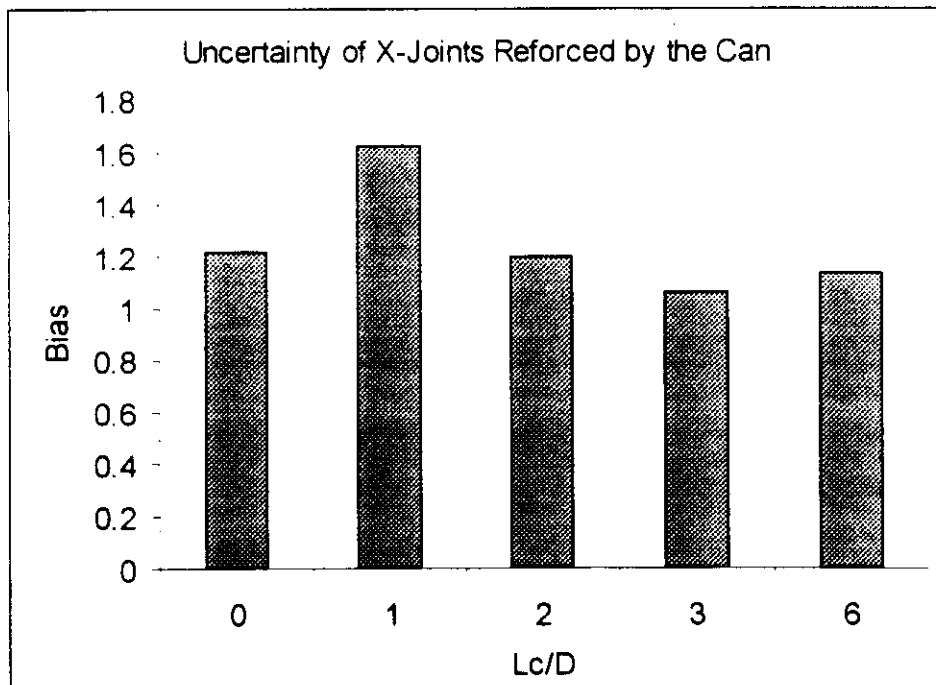
T_e/T=2.0)

Figure 9.12 Uncertainty of T-joints Re-enforced by the Can (β=0.73, D/T_e=25.4,

T_e/T=2.0)
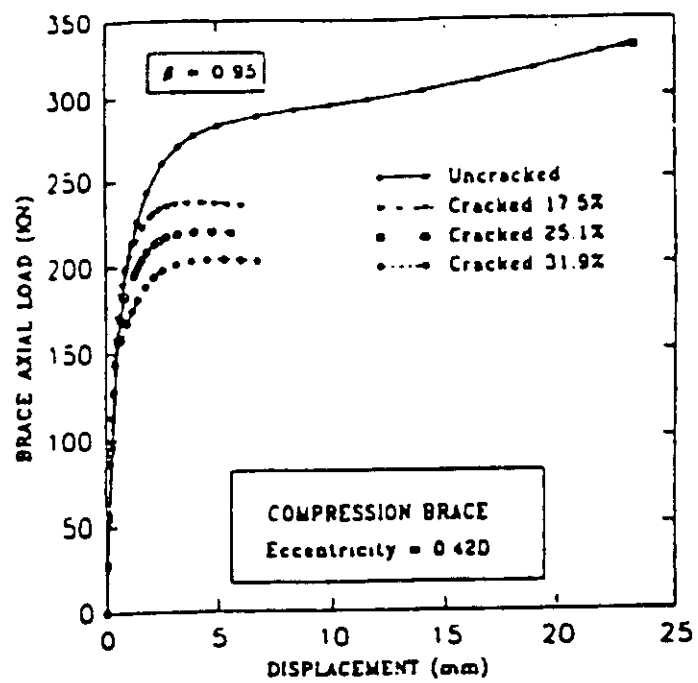
Figure 9.13 Load-Displacement Curves for Intact and Cracked K-Joints with Gap under Axial Loading

9.17
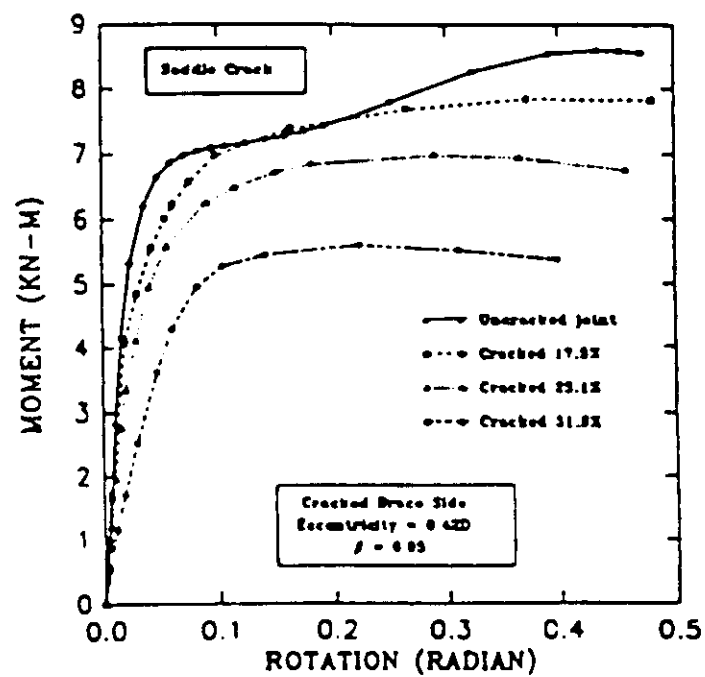
Figure 9.14 Moment-Rotation Curves for Intact and Cracked K Joints with Gap under Out-of-Plane Bending
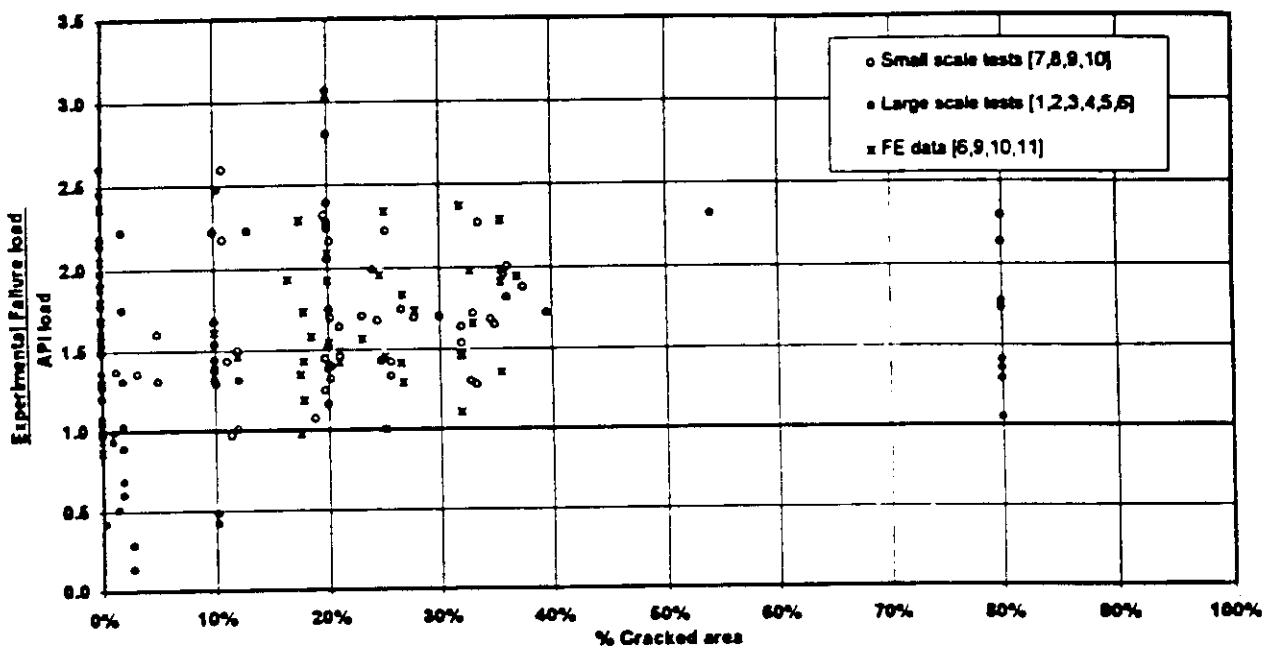
Figure 9.15 Normalized Ultimate Static Strength Capacity using API RP 2A Equations
with Area Reduction Factor
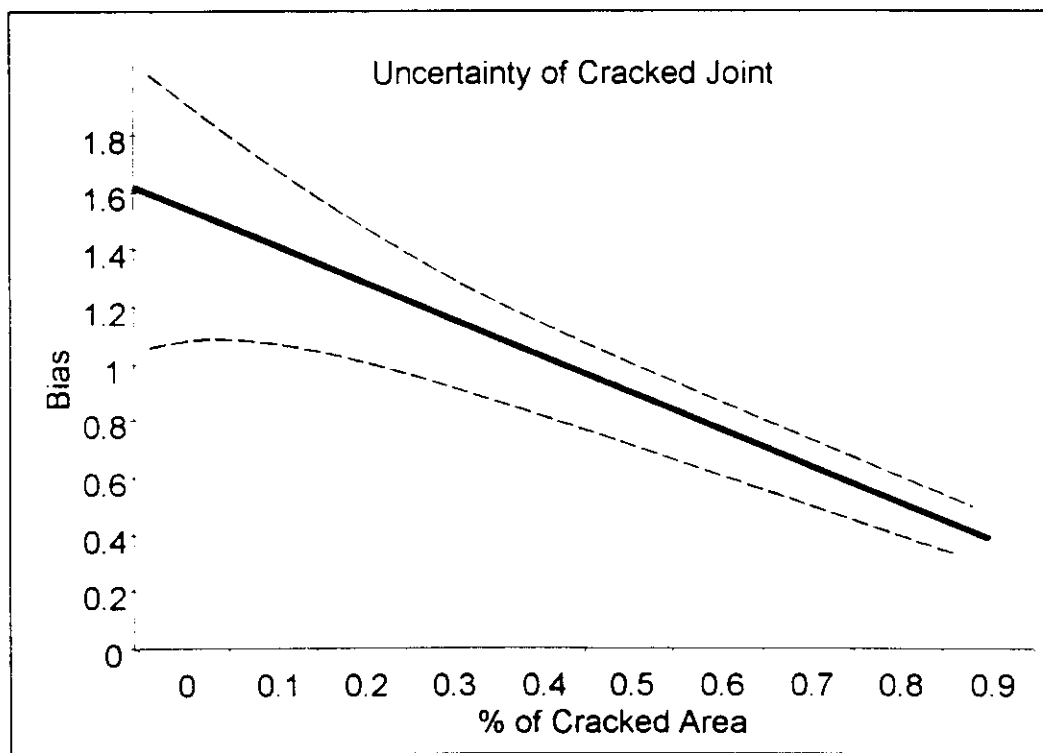
Figure 9.16 Uncertainty of Cracked Simple Joint Based on API RP 2A Intact Equations

Table 9.1 Dimensions of Unplanar X - Joints

	$2\gamma=36.4$ $d_o \times t_o = 1854 \times 51$ mm	$2\gamma=48.8$ $d_o \times t_o = 1854 \times 38$ mm
$\beta=0.25$ $(d_1=457$ mm$)$	-	X_3 $(t_1=32$mm$)$
$\beta=0.49$ $(d_1=914$ mm$)$	X_1 $(t_1=44$mm$)$	X_4 $(t_1=38$mm$)$
$\beta=0.74$ $(d_1=1370$ mm$)$	X_2 $(t_1=51$mm$)$	X_5 $(t_1=38$mm$)$

Table 9.2 Dimensions of the T-shaped Ring-Stiffeners

	$h_s=5t_o$	$h_s=10t_o$
$t_s=0.5to$	$h_s/t_s=10.0$	-
$t_s=0.76to$	$h_s/t_s=6.55$	-
$t_s=to$	$h_s/t_s=5.0$	$h_s/t_s=10.0$

Table 9.3 Numerical Results for the X-joints with the T-shaped ring-stiffened X-joints

	Joint	X_1	X_2	X_3	X_4	X_5
Unstiffened Joint	$\dfrac{F_{1,u}}{f_{y,0}t_0^2}$	12.13	16.74	7.46	12.49	17.14
	Bias*	1.0	1.0	1.0	1.0	1.0
$h_s = 5t_0$ $t_s = 0.5t_0$	$\dfrac{F_{1,u}}{f_{y,0}t_0^2}$	18.06	24.87	11.88	17.76	24.64
	Bias*	1.49	1.49	1.59	1.42	1.44
$h_s = 5t_0$ $t_s = 0.5t_0$	$\dfrac{F_{1,u}}{f_{y,0}t_0^2}$	20.92	28.73	14.18	20.60	28.71
	Bias*	1.72	1.72	1.90	1.65	1.68
$h_s = 5t_0$ $t_s = 0.5t_0$	$\dfrac{F_{1,u}}{f_{y,0}t_0^2}$	24.09	33.00	16.24	23.20	32.29
	Bias*	1.99	1.97	2.18	1.86	1.89
$h_s = 5t_0$ $t_s = 0.5t_0$	$\dfrac{F_{1,u}}{f_{y,0}t_0^2}$	34.25	46.63	24.30	34.90	46.24
	Bias*	2.82	2.77	3.26	2.79	2.70

Bias* = ultimate strength of each X-joint divided by the ultimate strength of corresponding un-stiffened X-joint.

Data	Scale	Joint	No. of Test	Loading	Comments
Gibstein	Large	T	7	Axial Tension	Fatigue tests followed by static tests on cracked joint
		Y	1		
Gibstein	Large	T	4	Axial Tension	Fracture test on brittle material
Machida	Large	T	2	Axial tension	Fracture test at low temperature -130° C
Van den Brink	Large	T	2	Axial tension	Fracture test at low temperature 0° C
Moe et al	Large	T	2	Axial Compression Axial Tension	Fracture tests on grind repaired joints
Skallerud	Large	T	2	Axial tension	Fracture tests at low temperature -10° C Finite Element Analysis
		T	2	OPB	
Kurobane	Small	K	5	Balanced axial	Fatigue tests on pre-cracked joints Finite element Analysis
Burdekin	Small	DT	9	Axial tension	Fracture tests on pre-cracked joints Finite Element Analysis
Cheatani	Small	K	9	Balanced axial	
Hyde	Small	T	15	Axial tension	Static tests on pre-cracked tin-lead alloy models
		T	1	Axial compression	
		T	13	OPB	
		Y	2	Axial tension	
		Y	2	Axial compression	
		Y	2	OPB	
		YT	5	Balanced axial	
Total			87		

Table 9.4 Database for Cracked Joints

10.0 SUMMARY AND CONCLUSIONS

Tubular joints are integral components of offshore structures and as such, many codes address their design. The ultimate capacity predicted by the codes often differ widely due to the adoption of different philosophies during code development and to differences in the underlying database used during design equation formulation and code calibrations.

In the development of reliability based screening methodology in use for platform reassessment and requalification, it is important to recognize these differences to develop the best estimates of joint strength (bias and COV).

This report summarizes this background. Based on the most extensive screened database, the present API RP 2A codes has been examined, and the uncertainty models are developed for the design equations of the API RP 2A. Other issues, such as multiplanar joints, chord length effects, can length and material yield effects are also discussed.

On the basis of this project, significant increase in the reliability of joint strength formulations can be achieved leading to more rational procedure in the risk based design and requalification criteria for offshore platforms where joints constitute the weak points.

Future research is recommended based on the current results:
- Interaction between the tubular joint capacity and the ultimate capacity of offshore structural systems,
- Effects of the tubular joint uncertainty on the risk of the offshore structural systems,
- Uncertainty models of the complex tubular joints, and
- Reliability based tubular joint design.

11.0 REFERENCES

Al-Laham, S., and Burdekin, F. M., (1995) "The Ultimate Strength of Cracked K-Joints", Final Report to the Health and Safety Executive

API RP 2A - Recommended Practice for Planning, Designing and Constructing Fixed Offshore Platforms, 1993

API RP 2T - Recommended Practice for Planning, Designing, and Constructing Tension Leg Platforms, First Edition, 1997

AWS - AWS Structural Welding Code - Steel, AWS D1.1-96, 1996

Baker, M. J., (1973) "Variability in the Strength of Structural Steels, A Study on Structural Safety", Part 1, CIRIA Technical Note 44.

Bolt, H. M., Billington, C. J., and Ward, J. K., (1994) "Results from Large Scale Ultimate Load Tests on Tubular Jacket Frame Structures", Proceedings of Offshore Technology Conference, Houston, TX

Bolt, H. M., (1995) "Results from Large Scale Ultimate STrength Tests of K-Braced Jacket Frame Structures", Proceedings of Offshore Technology Conference, Houston, TX

Bolt, H. M., Seyed-Kebari, H., and Ward, J. K., (1992) "The Influence of Chord Length and Boundary Conditions on K Joint Capacity", Proceedings of the International Conference on Offshore and Polar Engineering, an Fransico, CA

Boone, T. J., and Yura, J. A., and Hoadley, P. W., (1983) "Chord Stress Effects on the Ultimate Strength of Tubular Joints", Phase 1 Report to API

British Institute of Standards (BSI 6493) - Guidance on Methods for Assessing the Acceptability of Flaws in Fusion Welded Structures, 1991

British Institute of Standards (BSI 7608) - Code for Practice for Fatigue Design and Assessment of Steel Structures, 1993

Buitrago, J., et al (1993) "Local Joint Flexibility of Tubular Joints", Proceedings of the 12th International Conference on Offshore Mechancis and Arctic Engineering, Glassgow, United Kingdom

Burdekin, F. M., et al (1987) "Ultimate Failure of Tubular Connections", Final Report, Project DA 709 (Phase 1), Dept. of Civil and Structural Engineering, UMIST

Cheatani, M. J., (1991) "Ultimate Failure of Tubular Connections", Final Report, Project DA709,(Phase II), Dept. of Civil and Structural Engineering, UMIST

Efthymiou, M., "Development of SCF Formulae and Generalized Influence Functions for Use in Fatigue Analysis", Recent Developments in Tubular Joint Technology, London, 1988

Gibstein, M. B., (1981) "Fatigue Strength of Welded Tubular Joints Tested at DNV Laboratories", International Conference on Steel in Marine Structures

Gibstein, M. B., et al (1986) "Brittle Fracture Risks in Tubular Joints", Proceedings of 5th International Conference on Offshore Mechanics and Arctic Engineering

Hoadley, P. W., Clarkson, U., and Yura, J. A. (1985), "Ultimate Strength of Tubular Joints subjected to Combined Loads", Proceedings of the 17th Offshore Techlogy Conference, Houston, TX

ISO TC67/SC7/WG3/P3- Technical Core Group Joints Draft Code Provisions Revision 3, Section E Static Strength of Connections, 1996

Jubran, J. S., and Cofer, W. F., (1992) "Interaction Equations for Tubular T and Y Joints: A NUmerical Approach", Proceedings of the 11th International Conference on Offshore Mechancis and Arctic Engineering

Kurobane, Y. et al (1971) "Low Cycle Fatigue Research on Tubular K-Joints", IIW Doc XV-291-70, International Institute of Welding, London

Kurobane, Y., Makino, Y., and Ochi, K., (1984) "Ultimate Resistance of Unstiffened Tubular Joints", Journal of Structural Engineering, ASCE

Lalani, M., (1992) "Developments in Tubular Joint Technology for Offshore Structures", Proceedings of the International Conference on Offshore and Polar Engineering, San Fransico, CA

Lalani, M., and Bolt H., (1990) "Strength of Multiplanar Joints on Offshore Platforms", 3rd International Symposium on Tubular Structures, Lappeenranta, Finlind

Lee, M.S., Cheng, A. P., Sun, C. T., and Lai, R. Y., (1976) "Plastic Consideration on Punching Shear Strength of Tubular Joints", Proceedings of Offshore Technology Conference

Ma, Alan, Tahan, Naji, Nichols, Nigel, and Sharp, John, (1995) "Platform Assessment and Requalification Based on Historic Design Codes for Strength of Tubular Joints", Proceedings of the Offshore Mechanics and Arctic Engineering

Machinda, S. et al (1987) "Evaluation of Brittle Fracture Strength of Tubular Joints of Offshore Structures", Proceedings of 6th International Conference on Offshore Mechanics and Arctic Engineering

Madros, Z., Zettlemoyer, N., and Healy, B. E., (1995) "Effect of Chord Can on Strength of T Joints", Proceedings of the Offshore Technology Conference, Houston, TX

Makino Y., Kurobane Y., and Ochi K., (1984) "Ultimate Capacity of Tubular Double K-Joints", Proceedings of 2nd International Conference on WEIding of Tubular Structures, Boston, U. S. A.

Makino, Y., Kurobane, Y., Takagi, M., and Honi, A., (1993) "Diaphragm Stiffened Multiplanar Joints for Retractable Roofs", Proceedings of 4th International Conference Space Structures

Marshall, P. W., and Toprac, A. A., (1974) "Behavior for Tubular Joint Design", Welding Journal, Vol. 53

Marshall, P. W., (1978) "A Review of American Criteria for Tubular Structures - and Proposed Revision", IIW Doc. No. XV-405-77, Copenhagan

Marshall, P. W., (1984) "Discussion of 'Load Interaction in T-Joints of Steel Circular Hollow Sections' by Stamekovic, A., and Sparrow, K. D.," Journal of Structural Engineering, ASCE

Marshall, P. W., (1991) "Design of Welded Tubular Connections - Basis and Use of AWS Code Provisions", Elsevers Science Publishers, New York

Marshall P. W., - Design of Welded Tubular Connections, Elsevier Press, Amsterdam, 1992

Moe, E. T., et al (1987) "Static Strength Test on Grind Repaired Tubular Joints", Veritec, Report No. 87-3539

Pan, R. B., et al (1976) "Ultimate Strength of Tubular Joints", Proceedings of the Offshore Technology Conference, Houston, TX

Paul J. C., (1992) "The Ultimate Behavior of Multiplanar TT- and KK- joints made of Circular Hollow SEctions", Ph. D Dissertation, Kumamoto University, Japan

Paul, J. C., Van der Valk, C. A. C., Wardenier, J. (1989) "The Static Strength of Circular Multiplanar X-joints", The Third International Symposium on Tubular Structures, Lappenrata, Finland

Paul, J. C., Ueno, T., Makino, Y., and Kurobane, Y., (1991) "The Ultimate Behavior of Multiplanar Double K-joints", International Journal of Offshore and Polar Engineering

Paul, J. C., Makino, Y., and Kurobane, Y., (1991) "Ultimate Capacity of Tubular Double T-joints under Axial Brace Loading", Journal of Construction Steel Research

Paul, J. C., Makino, Y., and Kurobane, Y., (1993) "New Ultimate Capacity Formulae for Multiplanar Joints", Proceedings of 5th International Symposium on Tubular Structures, Nottingham, United Kingdom

Rodabaugh, E. C., (1980) "Review of Data Relevant to Design of Tubular Joints for Use in Fixed Offshore Platforms", WRC Bulletin No. 256

Sakllerud, B. et al (1984) "Ultimate Capacity of Cracked Tubular Joints : Comparision Between Numerical Simulation and Experiments", Proceedings of the 7th International Behavior of Offshore Structures

Sawada, Y., et al (1979) "Static and Fatigue Tests on T-Joints Stiffened by an Internal Ring", Proceedings of the Offshore Technology Conference, Houston, TX

Scola S., REdwood R. G., and Mitri H. S., (1990) "Behavior of AXially LOaded Tubular V-JOints", JOurnal of Constructional Steel REsearch

Sparrow, K. D., and Stamenkovie, A., (1981) "Experimental Determination of the Ultimate Strength of T-Joints in Circular Hollow Steel Sections Subject to Axial Load and Moment", Proceedings of the International Conference on Joints in Structural Steelwork, Teeside Polytechnic

Stamekovic, A. and Sparrow, K. D., (1983) "Load Interaction in T-Joints of Steel Circular Hollow Sections", Journal of Strcutural Engineering, ASCE

Stacey, A. et al (1996a) "Static Strength Assessment of Cracked Tubular Joints", Proceedings of 15th International Conference on Offshore Mechanics and Arctic Engineering, Florence, Italy

Stacey, A. et al (1996b) "The Influence of Cracks on the Static Strength of Tubular Joints", Proceedings of 15th International Conference on Offshore Mechanics and Arctic Engineering, Florence, Italy

Stol, H. G. A., Puthli, R. S., and Bijlaard, F. S. K., (1985) "Experimental Research on Tubular T joints under Proportionally Applied Combined Static Loading", Behavior of Offshore Structures, Proceedings of 4th International Conference, Delft, Netherlands

Tebbett, I. E., et al (1979) "The Punching Shear Strength of Tubular Joints Reinforced with Grouted Pile", Proceedings of Offshore Technology Conference, Houston, TX

Underwater Engineering Group (1985) "Design of Tubular Joints for Offshore Structures", UEG Publication, UR 33

UK DEn (1989), "Background to New Formulae for the Ultimate Limited State of Tubular Joints", OTH Report 89-308, London, United Kingdom

UK DEn (1989), "Static Strength of Large Scale Tubular Joints", OTH Report 89-297, London, United Kingdom

UK DEn (1989), "Background to New Formulae for the Ultimate Limited State of Tubular Joints", OTH Report 89-297, London, United Kingdom

UK DEn (1989), "Draft Guidance Notes on Static Strength of Tubular Joints - Commentary and Assessment of Comments from Industry", OTH Report 89-297, London, United Kingdom

UK DEn - Offshore Installation: Guidance on Design, Construction, and Certification, Fourth Edition, 1990

Valk, C. A. C. van der (1988) Factors controlling the Static Strength of Tubular T-joints", Proceedings of the International Conference on Behavior of Offshore Structures (BOSS, 88), TRondheim, Norway

Van der Brink, et al (1987) "Assessment of Fracture Toughness Properties of Material in Welded Tubular Joints", International Conference on Steel in Marine Structures

van der Vegte, G. J., de Koning, C. H. M., Puthli, R. S., Wardenier, J., (1991) " Numerical Simulation of Experiments on Multiplanar Tubular Steel X-Joints", International Journal of Offshore and Polar Engineering

van der Vegte, G. J., and Wardenier, J., (1996) "The Influence of the Can Length on the Static Strength of Multiplanar XX-Joints", International Journal of Offshore and Polar Engineering

Vegte G. J., van der, Koning C. H. M., Puthli R. S., and Wardenier J., (1991) "The Static Strength and Stiffness of Multiplanar Steel X Joints", International Journal of Offshore and POlar Engineering

Vegte, GJ van der, Puthli, RS and Wardenier, J., (1992) "The Static Strength of Uniplanar Tubular Steel X-joints REinforced by a Can", International Journal of Offshore and Polar Engineering

Ward, J. K., Billington, C. J., and Smith, J. K., (1992) "Strength Assessment of a Multiplanar Joints in a North Sea Jacket Structure", Proceedings of the International Conference on Offshore and Polar Engineering, an Fransico, CA

Wilmshurst S. R., and Lee M. M. K., (1992) Ultimate Capacity of Axially Loaded Multiplanar Double K-joints in Circular Hollow Sections", Proceedings of 5th International Symposium on Tubular Structures, Nottingham, United Kington

Wilmshurst, S. R., and Lee, M. M. K., (1994) "The Static Strength of Multiplanar Joints: A Design Formulation", Proceedings of the 4th International Offshore and Polar Engineering Conference, Osaka, Japan

Zettlemoyer, N. (1988) "Developments in Ultimate Strength Technology for Simple Tubular Joints", Proceedings of Conference on Recent Developments in Tubular Joint Technology. Surrey, United Kingdom

Zettlemoyer, N., (1996) "ISO Harmonization of Offshore Guidance on Strength of Tubular Joints", Proceedings of the sixth International Conference on Offshore and Polar Engineering, Los Angeles, CA

APPENDIX A

TABLE 1

DATA SUMMARY: T, Y, AND DT JOINTS IN COMPRESSION

Test	D mm	d mm	T mm	F_y M Pa	γ	β	$\dfrac{P_T \sin\theta}{T^2 F_y}$	$\dfrac{Col(8)}{API\text{-}73}$	$\dfrac{Col(8)}{API\text{-}77}$	$\dfrac{Col(8)}{Eq.\ 2\ or\ 3}$
(1)	(2)	(3)	(4)	(5)	(6)	(7)	(8)	(9)	(10)	(11)
T-JOINTS										
Kanatani (Ref. 9)										
CE 3	139.8	101.6	6.5	323	10.8	0.727	17.26	0.884	0.884	1.003
CF 4	139.8	101.6	6.5	323	10.8	0.727	18.70	0.957	0.957	1.086
JISC (Ref. 20)										
CB-40-.2	164.5	42.7	4.7	440	17.5	0.258	8.65	1.121	1.121	1.037
CB-40-.4	164.5	76.3	4.7	440	17.5	0.462	11.97	0.870	0.870	0.980
CB-70-.2	319.5	60.5	4.5	410	35.5	0.190	7.05	1.017	1.017	1.008
CB-70-.4	319.5	139.8	4.5	410	35.5	0.440	12.23	0.761	0.761	1.043
CB-100-.2	455.7	89.1	4.9	390	46.5	0.195	6.67	0.856	0.856	0.936
CB-100-.4	455.7	165.2	4.9	390	46.5	0.362	10.41	0.721	0.721	1.011
Y-JOINTS										
JISC, θ = 45° (Ref. 20)										
CB'-40-.4	164.5	76.3	4.7	430	17.5	0.464	13.82	0.832	0.832	1.131
CB'-70-.4	319.5	139.8	4.4	410	35.5	0.440	15.56	0.802	0.802	1.327
CB'-100-.4	455.7	165.2	4.9	390	46.5	0.362	11.56	0.663	0.663	1.122
DT-JOINTS										
JISC (Ref. 20)										
CS-40-.2	165.2	42.7	4.7	480	17.5	0.260	6.84	0.894	0.894	1.013
CS-40-.4	165.2	76.3	4.7	480	17.5	0.460	9.61	0.701	0.949	1.022
CS-40-.6	165.2	114.3	4.7	480	17.5	0.690	12.93	0.617	0.881	1.020
CS-40-1.0	165.2	165.2	4.7	480	17.5	1.000	30.49	0.572	0.817	1.033
CS-70-.2	318.5	60.5	4.4	420	36.2	0.190	6.01	0.858	0.858	1.023
CS-70-.4	318.5	139.8	4.4	420	36.2	0.435	10.01	0.618	0.820	1.099
CS-70-.6	318.5	165.2	4.5	410	35.4	0.520	11.29	0.594	0.833	1.113
CS-70-1.0	318.5	318.5	4.5	410	35.4	1.000	37.04	0.563	0.804	1.255
*CS-100-.2	457.2	89.1	4.8	390	47.6	0.195	5.54	0.709	0.709	0.933
CS-100-.4	457.2	165.2	4.8	390	47.6	0.361	8.90	0.616	0.740	1.100
Kanatani (Ref. 9)										
CG-1	139.8	139.8	6.5	323	10.3	1.000	32.37	0.712	1.017	1.097
CG-2	139.8	114.3	6.5	323	10.3	0.818	17.99	0.755	1.079	1.113
CG-3	139.8	101.6	6.5	323	10.3	0.727	14.46	0.752	1.039	1.075
CG-4	139.8	76.3	6.5	323	10.3	0.546	11.37	0.823	1.167	1.083
CG-5	139.8	48.6	6.5	323	10.3	0.348	8.42	0.956	1.126	1.063
Gibstein (Ref. 7)										
1	190.1	48.3	4.69	310	20.3	0.254	6.94	0.881	0.881	1.036
2	193.7	48.3	6.50	330	14.9	0.250	6.81	0.964	0.964	1.024
3	193.7	48.3	9.39	280	11.0	0.250	6.97	1.081	1.081	1.048
4	188.9	101.6	4.65	310	20.3	0.538	11.28	0.676	0.955	1.085
5	193.7	101.6	6.50	330	14.9	0.520	10.78	0.734	1.030	1.061
6	193.7	101.6	9.30	280	10.4	0.520	11.37	0.861	1.210	1.119
7	190.0	159.0	4.56	310	20.8	0.837	19.20	0.620	0.885	1.164
8	193.7	159.0	6.50	333	14.9	0.820	16.00	0.598	0.854	0.985
9	193.7	159.0	9.35	280	10.4	0.820	18.23	0.759	1.084	1.122
Sammet (Ref. 17)										
A2-3	159	83	5	340	15.9	0.522	10.97	0.729	1.025	1.077
A2-4	159	83	5	340	15.9	0.522	10.63	0.707	0.992	1.044

*Deformation controlled

TABLE 2

DATA SUMMARY: T, Y, AND DT JOINTS IN TENSION

Test	D mm	d mm	T mm	F_y MPa	γ	β	$\dfrac{P_T \sin\theta}{T^2 F_y}$	$\dfrac{Col(8)}{API-73}$	$\dfrac{Col(8)}{API-77}$	$\dfrac{Col(8)}{Eq.\ 2}$
(1)	(2)	(3)	(4)	(5)	(6)	(7)	(8)	(9)	(10)	(11)
T-JOINTS										
Toprac (Ref. 21)										
T1	323.9	73.0	12.7	283	12.3	0.218	6.82	1.173	0.838	0.904
T2	323.9	73.0	6.4	283	25.5	0.214	17.56	2.471	1.765	2.352
T3	406.4	88.9	6.4	283	31.5	0.209	15.61	2.111	1.508	2.118
T4	323.9	141.3	6.4	283	25.5	0.425	14.83	1.051	0.751	1.292
T5	219.1	141.3	6.4	283	16.8	0.643	24.20	1.278	0.917	1.550
T6	323.9	141.3	6.4	283	25.5	0.425	16.78	1.189	0.849	1.462
T7	323.9	141.3	6.4	283	25.5	0.425	15.22	1.078	0.770	1.326
Brown & Root (Ref. 5)										
1	219.1	141.3	7.1	324	15.5	0.645	39.4	2.124	1.526	2.517
2	219.1	141.3	7.1	324	15.5	0.645	39.1	2.108	1.514	2.497
3	219.1	141.3	7.1	324	15.5	0.645	33.6	1.811	1.301	2.146
Beale (Ref. 2)										
1	323.9	60.3	6.4	290	25.5	0.173	5.71	0.994	0.710	0.854
2	323.9	101.6	6.4	290	25.5	0.302	9.14	0.991	0.651	1.002
3	323.9	273.1	6.4	290	25.5	0.840	19.05	0.573	0.488	0.984
Y-JOINTS										
Beale, $\theta = 45°$ (Ref. 2)										
5	323.9	60.3	6.4	290	25.5	0.173	5.93	0.855	0.890	0.887
6	323.9	101.6	6.4	290	25.5	0.302	8.08	0.668	0.695	0.884
7	323.9	273.1	6.4	290	25.5	0.840	16.16	0.403	0.420	0.835
DT-JOINTS										
Gibstein (Ref. 7)										
10	193.7	48.3	6.67	333	14.5	0.249	9.25	1.325	1.325	1.138
11	193.7	101.6	6.59	333	14.7	0.525	13.55	0.917	0.917	1.013
12	193.7	159	6.65	333	14.6	0.821	19.95	0.748	0.748	1.050

TABLE 3

DATA SUMMARY: AXIALLY LOADED K JOINTS

Test (1)	D mm (2)	d mm (3)	T mm (4)	F_y MPa (5)	γ (6)	β (7)	g/d (8)	$\dfrac{P_T \sin\theta}{T^2 F_y}$ (9)	Col(9) API-73 (10)	Col(9) API-77 (11)	Col(9) Eq. 4 (12)
Bouwkamp, $\theta_c = 90°$, $\theta_t = 45°$ (Ref. 3, 4)											
1	323.9	168.3	6.4	290	25.0	0.520	0.236	36.90	2.150	2.039	1.725
II-3	168.3	60.3	5.6	395	14.6	0.358	0.186	20.60	2.049	1.756	1.223
II-6	219.1	88.9	5.6	395	19.2	0.406	0.024	20.60	1.664	1.299	1.041
II-9	273.1	88.9	4.8	425	28.1	0.326	0.324	14.58	1.308	1.201	0.986
I-10	168.3	60.3	7.1	290	11.3	0.358	0.186	18.22	1.957	1.677	1.082
EPRC, $\theta_c = 45°$, $\theta_t = 45°$ (Ref. 6)											
7	508.0	219.0	12.7	494	20.0	0.431	0.905	16.70	1.040	1.040	1.339
8	508.0	219.0	12.7	494	20.0	0.431	0.905	16.70	1.040	1.040	1.339
9	508.0	324.0	12.7	494	20.0	0.638	0.154	25.92	1.086	0.988	0.996
10	508.0	324.0	12.7	494	20.0	0.638	0.154	27.31	1.145	1.041	1.049
11	508.0	324.0	12.7	276	20.0	0.638	0.154	34.79	1.458	1.326	1.337
12	508.0	324.0	12.7	276	20.0	0.638	0.154	33.54	1.406	1.279	1.289
JISC, $\theta_c = 90°$, $\theta_t = 45°$ (Ref. 20)											
CK-40-.2	165.5	42.7	4.6	484	17.8	0.258	0.730	9.34	1.214	1.214	0.925
CK-70-.2	318.4	60.5	4.4	412	36.2	0.190	1.425	10.82	1.544	1.544	1.544
CK-100-.2	456.9	89.1	4.9	402	46.5	0.195	1.357	9.14	1.178	1.178	1.286
CK-100-.4	458.9	165.2	4.9	402	46.8	0.360	0.182	24.38	1.700	1.454	1.439
JISC, $\theta_c = 45°$, $\theta_t = 45°$ (Ref. 20)											
TK-40-.2	165.5	42.7	4.7	490	17.6	0.258	2.460	9.28	1.003	1.003	1.118
TK-40-.4	165.9	76.3	4.7	490	17.6	0.460	0.760	15.68	0.951	0.951	1.084
TK-40-.6	165.2	114.3	4.7	490	17.6	0.692	0.031	31.05	1.223	0.995	1.057
TK-70-.2	318.4	60.5	4.5	422	35.4	0.190	3.849	8.93	1.063	1.063	1.274
*TK-70-.4	321.4	139.8	4.5	422	35.7	0.435	0.855	16.24	0.842	0.842	1.247
TK-70-.6	317.7	165.2	4.5	422	35.3	0.520	0.509	21.11	0.919	0.919	1.141
*TK-100-.2	456.9	89.1	5.0	451	45.7	0.195	3.714	7.38	0.793	0.793	1.039
*TK-100-.4	458.9	165.2	5.0	432	45.1	0.360	1.364	13.44	0.785	0.785	1.313
Nakajima, $\theta_c = 45°$, $\theta_t = 90°$ (Ref. 13)											
1	165.2	76.3	1.6	348	51.6	0.461	0.131	38.20	1.673	1.419	1.853
2	165.2	76.3	2.3	288	35.9	0.461	0.131	28.05	1.370	1.162	1.361
3	165.2	60.5	2.3	338	35.9	0.366	0.165	23.52	1.447	1.227	1.362
4	165.2	48.6	2.3	340	35.9	0.294	0.205	23.00	1.762	1.494	1.565
5	165.2	76.3	2.3	294	35.9	0.461	0.131	35.56	1.737	1.473	1.725
6	165.2	76.3	3.2	314	24.8	0.461	0.131	30.04	1.639	1.390	1.457
7	165.2	76.3	4.5	348	18.4	0.461	0.131	28.33	1.691	1.434	1.374
8	165.2	76.3	6.0	278	13.8	0.461	0.131	24.78	1.612	1.367	1.202
9	165.2	76.3	6.0	282	13.8	0.461	0.131	22.17	1.443	1.223	1.076
10	165.2	76.3	1.6	358	51.6	0.461	0.131	42.92	2.270	1.925	2.062
11	165.2	76.3	2.3	339	35.9	0.461	0.131	41.80	2.470	2.095	2.033
12	165.2	60.5	2.3	342	35.9	0.366	0.165	31.31	2.325	1.972	1.813
13	165.2	48.6	2.3	270	35.9	0.294	0.205	32.72	3.025	2.565	2.226
14	165.2	76.3	2.3	285	35.9	0.461	0.131	35.34	2.084	1.767	1.715
15	165.2	76.3	3.2	263	25.8	0.461	0.131	39.97	2.602	2.207	1.939
16	165.2	76.3	6.0	360	13.8	0.461	0.131	20.81	1.635	1.386	1.010
17	165.2	76.3	6.0	292	13.8	0.461	0.131	22.56	1.772	1.503	1.095
Yura, $\theta_c = 90°$, $\theta_t = 30°$ (Ref. 25)											
*C1-1	507.2	326.4	11.1	352	22.8	0.643	.117	28.03	1.364	1.181	1.052
*C1-2	507.2	326.4	11.1	352	22.8	0.643	.117	29.67	1.437	1.250	1.113
Zimmermann, $\theta_c = 60°$, $\theta_t = 60°$ (Ref. 26)											
1	419.0	168.3	10.0	340	21.0	0.402	0.284	15.32	1.129	1.054	0.882
2	419.0	168.3	10.0	340	21.0	0.402	0.284	15.42	1.136	1.061	0.888
3	419.0	168.3	10.0	340	21.0	0.402	0.284	15.02	1.107	1.033	0.865
4	419.0	168.3	10.0	239	21.0	0.402	0.284	17.28	1.273	1.189	0.995
Beale - TK Joint, $\theta_c = 45°$, $\theta_t = 90°$, $\theta_c = 45°$ (Ref. 2)											
8	323.9	60.3	6.5	290	15.4	0.173	1.225	9.15+	1.853	1.853	1.368
9	323.9	101.6	6.5	290	15.4	0.302	0.237	13.91+	1.614	1.395	0.945

* Deformation controlled
+ Load in tension branch

TABLE 4
DATA SUMMARY: IN-PLANE BENDING

Test	D mm	d mm	T mm	F_y MPa	γ	β	$\dfrac{M_s \sin\theta}{dT^2F_y}$	$\dfrac{M_c \sin\theta}{dT^2F_y}$	$\dfrac{\text{Col}(8)}{\text{API-73}}$	$\dfrac{\text{Col}(8)}{\text{API-77}}$	$\dfrac{\text{Col}(8)}{\text{Eq. 5}}$
(1)	(2)	(3)	(4)	(5)	(6)	(7)	(8)	(9)	(10)	(11)	(12)
T-JOINTS											
Gibstein (Ref. 8)											
4	219.1	71.6	6.3	314	17.4	0.327	9.24	9.64	3.818	1.909	1.201
6	298.5	101.6	7.2	294	20.7	0.340	9.24	9.79	3.485	1.743	1.171
7	219.1	101.6	5.5	305	19.9	0.464	12.45	12.99	3.482	1.741	1.274
8	219.1	101.6	8.4	367	13.0	0.464	9.81	10.24	3.118	1.559	1.004
9	219.1	101.6	10.0	368	11.0	0.464	9.34	9.75	3.121	1.560	0.956
11	219.1	139.7	6.0	314	18.3	0.638	16.34	17.06	3.396	1.698	1.316
12	219.1	139.7	8.8	422	12.4	0.638	12.90	13.46	3.013	1.507	1.039
14	298.5	193.7	7.3	296	20.4	0.649	17.48	18.53	3.448	1.724	1.408
17	219.1	177.8	5.9	314	18.6	0.812	20.85	21.77	2.978	1.489	1.384
18	219.1	177.8	8.6	422	12.7	0.812	17.68	18.46	2.832	1.416	1.174
JISC (Ref. 20)											
B-70-0.2	318.5	60.5	4.4	441	36.2	0.190	6.45	8.02	3.682	1.841	1.150
B-70-0.4	318.5	139.8	4.4	441	36.2	0.439	12.48	14.81	3.083	1.542	1.329
B-100-0.2	457.2	89.1	4.8	402	47.6	0.195	7.37	9.52	3.776	1.888	1.297
B-100-0.4	457.2	165.2	4.8	402	47.6	0.361	11.79	14.53	3.263	1.631	1.437
K-JOINTS											
Yura (Ref. 25)											
A2-X-90°	507.2	326.4	11.4	350	22.2	0.644	18.34	22.16	3.559	1.583	1.466
A2-X-30°	507.2	455.9	11.4	350	22.2	0.899	16.73	20.92	1.353	1.198	1.021

TABLE 5
DATA SUMMARY: OUT-OF-PLANE BENDING

Test	D mm	d mm	T mm	F_y MPa	γ	β	$\dfrac{M_s \sin\theta}{dT^2F_y}$	$\dfrac{M_c \sin\theta}{dT^2F_y}$	$\dfrac{\text{Col}(8)}{\text{API-73}}$	$\dfrac{\text{Col}(8)}{\text{API-77}}$	$\dfrac{\text{Col}(8)}{\text{Eq. 6}}$
(1)	(2)	(3)	(4)	(5)	(6)	(7)	(8)	(9)	(10)	(11)	(12)
T JOINTS											
JISC (Ref. 20)											
*BL-40-0.5	165.2	76.3	4.5	471	18.4	0.462	5.46	6.08	1.570	1.570	1.029
*BL-70-0.2	318.5	60.5	4.4	441	36.2	0.190	4.10	5.10	2.340	2.340	1.084
*BL-70-0.4	318.5	139.8	4.4	441	36.2	0.439	5.53	6.56	1.366	1.366	1.068
*BL-100-0.2	457.2	89.1	4.8	402	47.6	0.195	4.12	5.32	2.111	2.111	1.081
BL-100-0.4	457.2	165.2	4.8	402	47.6	0.361	4.36	5.37	1.207	1.207	0.920
Yura (Ref. 25)											
*G1	507.2	171.5	11.1	352	22.8	0.338	4.39	5.31	1.618	1.618	0.952
*G2	507.2	171.5	11.1	352	22.8	0.338	4.83	5.84	1.780	1.780	1.047
*H1	507.2	326.4	11.1	352	22.8	0.644	7.29	8.81	1.403	1.403	1.147
*H2	507.2	326.4	11.1	352	22.8	0.644	7.86	9.50	1.513	1.513	1.236
*I1	507.2	455.9	11.1	352	22.8	0.899	13.40	14.79	1.398	1.398	1.300
*I2	507.2	455.9	11.1	352	22.8	0.899	13.45	14.86	1.403	1.403	1.305
Y JOINTS											
Yura, θ = 30° (Ref. 25)											
*E1	507.2	455.9	11.1	352	22.8	0.899	14.96	18.70	1.200	1.595	1.452
*E2	507.2	455.9	11.1	352	22.8	0.899	14.90	18.62	1.195	1.588	1.446
K JOINTS											
Yura (Ref. 25)											
*C2-1, 90°	507.2	326.4	11.1	352	22.8	0.644	5.83	7.04	1.122	1.122	0.917
30°	507.2	455.9	11.1	352	22.8	0.899	12.31	15.39	0.987	1.312	1.195
*C2-2, 90°	507.2	326.4	11.1	352	22.8	0.644	8.32	10.06	1.602	1.602	1.309
30°	507.2	455.9	11.1	352	22.8	0.899	14.67	18.33	1.177	1.564	1.424

*Deformation controlled

TABLE A.1 DATABASE FOR T AND Y JOINTS IN COMPRESSION – Continued

Specimen	Type	D (mm)	d (mm)	T (mm)	L (mm)	F_y (N/mm²)	θ_c	θ_t	$\alpha=\frac{2L}{D}$	$\zeta=g/D$	$\gamma=\frac{D}{2T}$	$\beta=\frac{d}{D}$	(1)	(2)	$\frac{(1)}{(2)}$	(3)	$\frac{(1)}{(3)}$
(17)																	
C-A1	T	139.8	139.8	6.5	400	329			5.7		10.8	1.000	32.23	35.51	0.91	34.81	0.93
C-A2		139.8	114.3	6.5	400	329			5.7		10.8	0.818	24.54	23.51	1.04	23.24	1.06
C-A3		139.8	101.6	6.5	400	329			5.7		10.8	0.727	21.16	20.10	1.05	19.97	1.06
C-A4		139.8	76.3	6.5	400	329			5.7		10.8	0.546	14.97	15.20	0.98	15.25	0.98
C-A5		139.8	48.6	6.5	400	329			5.7		10.8	0.348	9.57	10.27	0.93	10.57	0.91
C-B1		139.8	139.8	6.5	400	329			5.7		10.8	1.000	38.40	35.51	1.08	34.81	1.10
C-B2		139.8	101.6	6.5	400	350			5.7		10.8	0.727	22.31	17.64	1.11	19.97	1.12
C-B3		135.8	85.1	6.5	400	350			5.7		10.8	0.637	18.93	10.27	1.08	17.44	1.08
C-B4		139.8	48.6	6.5	400	350			5.7		10.8	0.348	8.31	9.20	1.01	10.57	0.98
C-B5		139.8	42.7	6.5	400	390			5.7		10.8	0.305	7.10	7.66	0.90	9.58	0.87
C-B6		139.8	34.0	6.5	400	390			5.7		10.8	0.243			0.93	8.11	0.86
C-31		139.8	139.8	4.5	400	400			5.7		15.5	1.000	44.67	35.51	1.26	34.81	1.28
C-02		139.8	114.3	4.5	400	409			5.7		15.5	0.818	31.15	23.51	1.32	23.24	1.34
C-03		139.8	101.6	4.5	400	409			5.7		15.5	0.727	27.17	20.10	1.35	19.97	1.36
C-04		139.8	76.3	4.5	400	409			5.7		15.5	0.546	19.68	15.20	1.29	15.25	1.29
C-05		139.8	48.6	4.5	400	409			5.7		15.5	0.348	12.58	10.27	1.22	10.57	1.19
C-FA		139.8	101.6	6.5	600	323			5.7		10.8	0.727	17.26	20.10	0.86	19.97	0.86
C-FA		139.8	101.6	6.5	600	323			8.6		10.8	0.727	18.70	20.10	0.93	19.97	0.94
B-0		139.8	76.3	6.4	400	307			8.6		10.9	0.546	17.10	15.20	1.12	15.25	1.12
B-E		139.8	60.5	6.4	400	307			5.7		10.9	0.433	13.44	12.39	1.08	12.58	1.07
(21)																	
C3-40-.2	T	164.5	42.7	4.7	826	440	90		10.0		17.5	0.258	8.65	8.03	1.08	8.50	1.02
C3-40-.4		164.5	76.3	4.7	826	440			10.0		17.5	0.462	11.97	13.11	0.92	13.32	0.90
C3-70-.2		319.5	60.5	4.5	1593	410			10.0		35.5	0.190	7.05	6.34	1.11	6.84	1.03
C3-70-.4		319.5	139.8	4.5	1593	410			10.0		35.5	0.440	12.23	12.56	0.97	12.70	0.96
C3-100-.2		455.7	89.1	4.9	2286	390			10.0		46.5	0.195	6.67	6.47	1.03	6.98	0.96
C3-100-.4		455.7	165.2	4.9	2286	390			10.0		46.5	0.362	10.41	10.62	0.98	10.93	0.95
(22)																	
A 13	T	508.0	168.0	7.9	2032	324	90		8.0		32.0	0.331	12.68	9.85	1.29	10.18	1.25
A 15		508.0	168.0	7.9	2032	324			8.0		32.0	0.331	11.75	9.85	1.19	10.18	1.16
W 3		508.0	194.0	12.7	2032	326			8.0		20.0	0.381	12.72	11.10	1.15	11.38	1.12
W 5		508.0	194.0	12.7	2032	326			8.0		20.0	0.381	12.72	11.10	1.15	11.38	1.12
(23)																	
SH-A	T	641.1	256.2	16.0	3000	393	90		9.4		20.0	0.399	10.94	11.54	0.95	11.80	0.93
SH-B		642.5	384.0	16.2	3000	392			9.3		19.8	0.598	15.30	16.50	0.93	16.48	0.93
SH-C		642.3	512.5	16.0	3000	392			9.3		20.1	0.798	21.36	22.76	0.94	22.45	0.95
SR-A		641.8	255.5	16.0	3000	366			9.3		20.0	0.398	10.31	11.52	0.90	11.77	0.88
SH-A		643.4	255.8	16.0	3000	728			9.3		20.1	0.398	10.88	11.52	0.94	11.75	0.93
T-0		1400.0	800.0	26.0	7000	280			10.0		26.9	0.571	17.40	15.82	1.10	15.86	1.10
T-R		1400.0	800.0	36.0	7000	254			10.0		19.4	0.571	15.16	15.82	0.96	15.86	0.96

Specimen	Type	D (mm)	d (mm)	T (mm)	L (mm)	F_y (N/mm²)	θ_c	θ_t	$\alpha=\frac{2L}{D}$	$c=\frac{g}{D}$	$\gamma=\frac{D}{2T}$	$\beta=\frac{d}{D}$	(1)	(2)	$\frac{(1)}{(2)}$	(3)	$\frac{(1)}{(3)}$
J CBI-40-.4		164.5	76.3	4.7	826	430			10.0		17.5	0.464	13.82	15.88	0.87	16.08	0.86
I CBI-70-.4	Y	319.4	139.8	4.4	1593	410	45	-	10.0	-	35.5	0.440	15.56	15.16	1.03	15.33	1.02
S CBI-100-.4		455.9	165.2	4.9	2286	390			10.0		46.5	0.362	11.56	12.82	0.90	13.18	0.88
C (21)																	
S																	
A																	
W R-0-1	T	711.2	318.2	9.9	-	389	90	-	-	-	35.9	0.448	10.27	12.76	0.81	12.93	0.80
A R-0-2		711.2	318.2	10.4	-	363	90	-	-	-	34.2	0.448	10.27	12.76	0.81	12.93	0.80
A																	
D																	
A (24)																	

(1) = Measured non-dimensional strength $P_u \sin\theta / F_y T^2$

(2) = Preliminary Predicted non-dimensional strength $(1.61 + 24.89\beta)\ \dfrac{\gamma^{0.5}}{\beta}\ K_a$

(3) = Final Predicted non-dimensional strength $(2.37 + 23.60\beta)\ \dfrac{\gamma^{0.5}}{\beta}\ K_a$

TABLE A.1   DATABASE FOR T AND Y JOINTS IN COMPRESSION

Specimen	Type	D (mm)	d (mm)	t (mm)	F_y (N/mm²)	θ'_a	θ'_t	$\zeta = g/D$	$\gamma = \frac{D}{2T}$	$\beta = \frac{d}{D}$	(1)	(2)	$\frac{(1)}{(2)}$
CB-40-0.2		165.2	43.7	4.7	400				17.5	0.258	6.04	6.96	0.98
-48-0.4		165.2	76.3	4.7	400				17.5	0.462	9.61	10.11	0.95
-40-0.6		165.2	114.3	4.7	400				17.5	0.692	12.93	14.00	0.92
-40-1.0	DT	165.2	165.2	4.7	400	90			17.5	1.000	36.49	33.17	0.92
-70-0.2		318.5	60.5	4.4	420				36.2	0.190	6.01	5.91	1.02
-70-0.4		318.5	139.8	4.4	420				36.2	0.439	10.01	9.76	1.03
-70-0.6		318.5	165.2	4.5	410				35.4	0.519	11.29	11.00	1.03
-70-1.0		318.5	318.2	4.5	410				35.4	1.000	37.04	33.37	1.12
-100-0.2		457.2	89.1	4.8	390				47.6	0.195	5.54	5.99	0.92
-100-0.4		457.2	165.2	4.8	390				47.6	0.361	8.90	8.55	1.04
CC-1		139.8	139.8	6.5	323				10.3	1.000	32.37	33.17	0.98
CC-2		139.8	114.3	6.5	323				10.3	0.818	17.99	17.97	1.00
CC-3	DT	139.8	101.6	6.5	323	90			10.3	0.727	14.46	14.87	0.97
CC-4		139.8	76.3	6.5	323				10.3	0.546	11.37	11.41	1.00
CC-5		139.8	48.6	6.5	323				10.3	0.348	8.42	8.55	1.01
1		190.1	48.3	4.68	310				20.3	0.254	6.94	6.90	1.01
2		193.7	48.3	6.50	330				14.9	0.250	6.81	6.64	1.02
3		193.7	48.3	9.39	280				11.0	0.250	6.97	6.64	1.00
4		188.9	101.6	4.63	310				20.1	0.538	11.28	11.29	0.98
5	DT	193.7	101.6	6.5	330	90			14.9	0.528	10.78	11.01	1.03
6		193.7	101.6	9.30	280				10.4	0.528	11.37	11.01	1.03
7		190.8	159.0	4.56	310				20.8	0.837	19.28	18.83	1.02
8		193.7	159.0	6.50	331				14.9	0.820	16.00	18.06	0.89
9		193.7	159.0	9.35	280				10.4	0.820	18.23	18.06	1.01
A3.3		159.0	83.0	5.0	340	90			15.9	0.522	10.97	11.04	0.99
A3.4	DT	159.0	83.0	5.0	340				15.9	0.522	10.63	11.04	0.96
A1		407.7	274.3	8.1	321	90		-	25.2	0.673	16.64	13.57	1.23
A21	DT	407.8	407.0	8.0	336	90		-	25.4	1.000	35.72	33.17	1.08
A41		407.0	142.1	8.0	336	90		-	25.4	0.350	9.56	8.38	1.14

(1) = Measured non-dimensional strength $\dfrac{P_u}{F_y T^2}$ (2) = Predicted non-dimensional strength $(2.976 + 15.450\beta)\, Q'\beta$

TABLE A.2   DATABASE FOR DT JOINTS IN COMPRESSION

TABLE A.3 DATA... FOR K AND YT JOINTS IN COMPRESSION – Continued

Specimen	Type	D (mm)	d (mm)	T (mm)	f_y (N/mm²)	θ_c	θ_t	$\zeta = g/D$	$\gamma = \dfrac{D}{2T}$	$\beta = \dfrac{d}{D}$	(1)	(2)	(1)/(2)	(3)	(1)/(3)
BOUNK-APP (29) 11-3	YT	168.3	60.3	5.6	395	90	45	0.067	15.0	0.358	20.60	15.34	1.34	15.66	1.32
11-6		219.1	88.9	4.8	395	90	45	0.010	39.1	0.406	20.60	18.58	1.11	18.92	1.09
11-9		273.1	88.9	4.8	425	90	45	0.106	28.1	0.326	14.58	13.64	1.07	13.97	1.04
1.10		168.3	60.3	7.1	290	90	45	0.067	11.3	0.358	18.22	15.33	1.19	15.66	1.16
E 7	K	508.0	219	12.7	494	90	45	0.188	20.0	0.258	16.70	17.29	0.97	17.14	0.98
P 8		508.0	219	12.7	412	90	45	0.271	20.0	0.190	16.70	17.29	0.97	17.14	0.98
R 9		508.0	324	12.7	402	90	45	0.265	20.0	0.193	25.92	29.89	0.87	29.50	0.88
C 10		508.0	324	12.7	494	90	45	0.098	20.0	0.638	25.92	29.89	0.87	29.50	0.88
11		508.0	324	12.7	276	45	45	0.098	20.0	0.638	27.31	29.89	0.91	29.50	0.93
12		508.0	324	12.7	276	45	45	0.098	20.0	0.638	34.79	29.89	1.16	29.50	1.18
C (30) CX-4G-.2	K	458.9	165.2	5.0	432	45	45	0.491	46.8	0.360	24.38	15.43	1.58	15.74	1.55
CX-70-.2		456.9	165.2	5.0	451	45	45	0.724*	43.7	0.520	34.79	21.95	0.96	21.67	0.93
CX-100-.2		317.7	89.1	4.5	422	45	45	0.265	35.3	0.435	21.11	17.62	0.92	17.45	0.93
CX-100-.4		321.4	139.8	4.5	422	45	45	0.372	35.7	0.439	23.00	7.63	1.17	8.27	1.08
J S (21) TK-40-.2	YT	318.4	60.5	4.5	422	45	45	0.731*	35.4	0.190	31.05	35.57	0.87	35.21	0.88
TK-40-.4		165.9	114.3	4.7	490	45	45	0.022	17.6	0.692	31.05	35.57	0.87	35.21	0.88
TK-40-.6		165.5	76.3	4.7	490	45	45	0.350	38.2	0.460	15.68	18.72	0.84	18.52	0.85
TK-70-.2		165.5	42.7	4.7	490	45	45	0.639*	17.6	0.258	9.28	9.91	0.94	10.21	0.91
K TK-40-.2	K	165.2	42.7	4.7	340	45	45	0.060	36.9	0.294	24.24	N/A	N/A	N/A	N/A
TK-40-.4		165.9	76.3	2.3	294	45	45	0.060	35.6	0.462	34.95	N/A	N/A	N/A	N/A
TK-40-.6		165.2	76.3	2.2	314	45	45	0.060	16.1	0.462	30.23	N/A	N/A	N/A	N/A
TK-70-.2		165.2	76.3	3.2	348	45	45	0.060	13.1	0.462	23.00	N/A	N/A	N/A	N/A
TK-70-.4		165.2	76.3	5.1	278	45	90	0.060	13.6	0.462	22.53	N/A	N/A	N/A	N/A
TK-70-.6		165.2	76.3	6.1	282	45	90	0.060	13.6	0.462	21.32	N/A	N/A	N/A	N/A
TK-100-.2		165.2	76.3	1.6	358	45	90	0.060	90.7	0.462	41.33	N/A	N/A	N/A	N/A
TK-100-.4		165.2	76.3	2.2	339	45	45	0.060	37.5	0.462	45.68	N/A	N/A	N/A	N/A
A (31) L-1.6-.1	YT	165.2	76.3	2.4	342	45	45	0.060	34.9	0.366	29.48	N/A	N/A	N/A	N/A
L-2.3-1		165.2	48.6	2.3	270	45	45	0.060	35.8	0.294	32.16	N/A	N/A	N/A	N/A
L-2.3-2		165.2	60.5	2.3	285	45	45	0.060	26.0	0.462	35.03	N/A	N/A	N/A	N/A
L-2.3-3		165.2	76.3	2.2	263	45	45	0.060	36.9	0.462	24.24	N/A	N/A	N/A	N/A
L-3.2-1		165.2	76.3	3.2	360	45	45	0.060	13.5	0.462	19.88	N/A	N/A	N/A	N/A
L-4.5		165.2	76.3	6.1	292	45	45	0.060	13.4	0.462	21.26	N/A	N/A	N/A	N/A

Specimen	Type	D (mm)	d (mm)	T (mm)	F_y (N/mm²)	θ_c	θ_t	$\zeta = g/D$	$\gamma = \frac{D}{2T}$	$\beta = \frac{d}{D}$	(1)	(2)	$\frac{(1)}{(2)}$	(3)	$\frac{(1)}{(3)}$
Y U R A (4) C1-1	YT	507.2	326.4	11.1	352	90	30	0.074	22.8	0.643	28.03	25.53	1.10	25.26	1.11
C1-2	YT	507.2	326.4	11.1	352	90	30	0.074	22.8	0.643	29.67	25.53	1.16	25.26	1.18
ZIMMER-MAN (32) 1	K	419.0	168.3	10.0	340	60	60	0.114	21.0	0.402	15.32	17.43	0.88	17.60	0.87
2		419.0	168.3	10.0	340	60	60	0.114	21.0	0.402	15.42	17.43	0.88	17.60	0.88
3		419.0	168.3	10.0	340	60	60	0.114	21.0	0.402	15.02	17.43	0.86	17.60	0.85
4		419.0	168.3	10.0	239	60	60	0.114	21.0	0.402	17.28	17.43	0.99	17.60	0.98
K O N - N G (33) 7	K	165.1	51.0	4.8	281	45	45	0.55	17.2	0.309	13.32	11.97	1.11	12.02	1.11
8		165.1	108.0	4.8	281	45	45	0.08	17.2	0.654	27.52	31.16	0.88	30.78	0.89
10		273.5	88.9	4.8	324	45	45	0.53	28.5	0.325	13.26	12.82	1.03	12.63	1.05
11		273.5	88.9	4.8	324	45	45	0.53	28.5	0.325	14.30	12.82	1.12	12.63	1.13
12		273.0	178.0	5.0	373	45	45	0.07	27.3	0.652	28.51	31.39	0.91	31.02	0.92
13		273.0	178.0	5.0	373	45	45	0.07	27.3	0.652	27.30	31.39	0.87	31.02	0.88
W L L (34) 1	K	457.0	406.0	9.5	342	60	60	0.12	24.0	0.888	53.23	40.32	1.32	39.30	1.36
2		457.0	406.0	9.5	342	60	60	0.12	24.0	0.888	54.42	40.32	1.35	39.30	1.39

(1) = Measured non-dimensional strength $P_u \sin\theta / F_y T^2$

(2) = Preliminary Predicted non-dimensional strength $(1.61 + 24.89\beta) \sqrt{\gamma} \beta K_a Q_g$ with $Q_g = 1.67 - 0.31 \zeta^{0.5}$ but not less than 1.0

(3) = Final Predicted non-dimensional strength $(2.37 + 23.60\beta) \sqrt{\gamma} \beta K_a Q_g$ with $Q_g = 1.57 - 0.86 \zeta^{0.5}$ but not less than 1.0

* = Large gap joints used in statistical analysis of T/Y joints

(4) = N/A refers to Nakajima data not used in statistical analysis

TABLE A.3 DATABASE FOR K AND YT JOINTS IN COMPRESSION

TABLE A.4 DATABASE FOR T AND Y JOINTS IN TENSION

$a = 5.0$

(1) = Measured non-dimensional strength $\dfrac{P_u \sin\theta}{F_y T^2}$

(2) = Predicted non-dimensional strength $(11.700 + 32.260\beta)\,K_a$

Specimen		Type	D (mm)	d (mm)	T (mm)	L (mm)	F_y (N/mm²)	θ_c	θ_t	$c = g/D$	$a = \dfrac{2L}{D}$	$\gamma = \dfrac{D}{2T}$	$\beta = \dfrac{d}{D}$	(1)	(2)	$\dfrac{(1)}{(2)}$
W	A11	T	500.0	160.0	12.7	2032	324	-	90	-	8.0	20.0	0.301	23.09	24.00	0.96
W	W1	T	500.0	194.0	12.7	2032	326	-	90	-	8.0	20.0	0.331	21.91	22.38	0.98
L(22)	B-D	T	139.8	76.3	6.4	400	306	-	90	-	5.7	10.9	0.545	24.20	21.20	1.02
	B-E		139.8	60.5	6.4	400	305				5.7	10.9	0.433	19.00	20.40	0.93
I(17)		T	164.0	42.7	4.7	826	450	-	90	-	10.0	17.5	0.258	21.24	20.02	1.12
			164.8	76.3	4.7	826	450				9.9	17.5	0.462	25.79	26.49	1.10
S			320.4	60.5	6.4	1593	423				9.9	35.6	0.189	26.20	17.00	1.48
J			320.4	139.0	6.5	1593	423				10.0	35.6	0.436	31.24	25.77	1.21
C			455.7	165.2	4.9	2286	400				10.0	46.5	0.363	41.76	23.00	1.62
	1-T-40-0.2		322.9	73.0	6.4	826	290	-	90	-	•	25.5	0.226	21.23	18.99	1.12
	-40-0.4		324.9	88.9	6.4	826	290				•	32.0	0.219	20.57	18.76	1.10
	-70-0.2		324.9	141.3	6.4	826	290				•	35.5	0.436	31.24	25.77	1.21
	-70-0.4		322.9	141.3	6.4	826	290				•	35.5	0.436	29.67	25.77	1.15
	-100-0.4		322.9	60.5	6.4	826	290				•	35.5	0.187	17.24	25.00	1.21
C(35)	T8		322.9	107.6	6.4	—	290	-	90	-	•	25.5	0.314	16.79	17.73	0.95
R	T9		322.9	107.6	6.4	—	290				•	25.5	0.187	21.33	21.03	0.98
B	5	Y	323.9	60.3	6.4	—	290	-	45	-	•	25.5	0.187	17.92	21.40	0.82
E(36)	6		323.9	101.6	6.4	—	290				•	25.5	0.314	21.55	26.35	0.82

Specimen	D (mm)	d (mm)	T (mm)	F_y (N/mm²)	θ°o	θ°t	ζ = g/D	γ = D/2T	β = d/D	(1)	(2)	(1)/(2)
B A M M E T (26)												
A2-3	159.0	83.0	5.0	340	-	90		15.9	0.522	19.00	21.01	0.90
A2-4	159.0	83.0	5.0	340				15.9	0.522	21.34	21.01	1.02
D n V (25)												
10	193.7	48.3	6.7	334	-	90		14.5	0.249	11.35	14.83	0.77
11	193.7	101.6	6.6	334				14.7	0.525	17.06	21.08	0.81
12	193.7	159.0	6.6	334				14.5	0.821	28.38	32.11	0.88
J M S C (21)												
1-TS-40-0.2	164.5	42.7	4.7	471				17.5	0.260	14.94	15.08	0.99
-40-0.4	165.6	76.3	4.6	471				18.0	0.461	22.00	19.63	1.12
-40-0.6	165.6	114.3	4.6	471		90		18.0	0.690	31.70	25.37	1.25
-40-1.0	165.6	165.2	4.6	471	-			18.0	1.000	78.11	57.29	1.37
-70-0.2	321.2	60.5	4.4	441				36.5	0.188	17.04	13.45	1.27
-70-0.4	321.2	139.8	4.4	441				36.5	0.435	21.26	19.04	1.12
-70-0.6	321.2	165.2	4.4	441				36.5	0.514	23.55	20.83	1.13
-100-0.2	455.7	89.1	4.9	402				46.5	0.200	16.73	13.72	1.22
-100-0.4	455.7	165.2	4.9	402				46.5	0.363	20.76	17.41	1.19
Y A M A S A K I (23)												
DT-M	1400.0	800.0	16.0	254	-	90	-	19.4	0.571	23.49	22.12	1.06
DT-M	1400.0	800.0	16.0	336				19.4	0.571	18.86	22.12	0.85

(1) = Measured non-dimensional strength $\dfrac{P_u}{F_y T^2}$

(2) = Predicted non-dimensional strength $(9.196 + 22.630 \beta)\, Q'_\beta$

TABLE A.5   DATABASE FOR DT JOINTS IN TENSION

Specimen	Type	D (mm)	d (mm)	T (mm)	P_y (N/mm²)	θ°	$\gamma = \frac{D}{2T}$	$\beta = \frac{d}{D}$	(1)	(2)	$\frac{(1)}{(2)}$
4	t	219.1	71.6	6.3	314		17.4	0.327	9.28	7.25	1.28
5		219.1	71.6	8.9	422		12.3	0.327	7.54	6.18	1.22
6		298.5	101.6	7.2	294		20.7	0.340	9.29	8.24	1.12
7		219.1	101.6	5.5	305		19.9	0.464	12.65	11.64	1.08
8		219.1	101.6	8.4	367		13.0	0.464	9.97	9.41	1.06
9		219.1	101.6	10.0	368	90	11.0	0.464	9.49	8.66	1.10
10		219.1	101.6	12.3	404		8.9	0.464	8.02	7.79	1.13
11		219.1	139.7	6.0	314		18.3	0.638	16.60	15.79	1.05
12		219.1	139.7	8.8	422		12.4	0.638	13.18	12.99	1.01
13		219.1	139.7	12.3	392		8.9	0.638	10.82	11.00	0.98
14		298.9	193.7	7.3	296		20.4	0.649	17.76	16.98	1.05
15		298.5	193.7	10.0	294		14.9	0.649	13.78	14.51	0.95
16		298.5	193.7	10.0	294		14.9	0.649	15.26	14.51	1.05
17		219.1	177.8	5.9	314		18.6	0.812	21.19	20.57	1.03
18		219.1	177.8	8.6	422		12.7	0.812	17.97	17.00	1.06
19		219.1	177.8	12.5	392		8.8	0.812	14.99	14.15	1.06
B-40-0.3	t	169.5	42.7	4.7	471		17.5	0.259	4.75	5.61	0.85
-40-0.5		166.5	76.3	4.5	471		18.5	0.458	8.63	11.10	0.78
-70-0.2		318.5	60.5	4.4	441	90	36.2	0.190	6.45	5.48	1.17
-70-0.4		318.5	139.8	4.4	441		36.2	0.439	12.48	14.80	0.84
-100-0.2		457.2	89.1	4.8	402		47.6	0.195	7.37	6.49	1.13
-100-0.4		457.2	165.2	4.8	402		47.6	0.361	11.29	13.59	0.87
V7	t	508.0	193.7	12.7	327		20.0	0.381	7.56	9.29	0.81
V9		508.0	193.7	12.7	327	90	20.0	0.381	7.74	9.29	0.83
A17		508.0	168.3	7.9	324		32.2	0.331	10.84	10.16	1.07
A19		508.0	168.3	7.9	324		32.2	0.331	10.55	10.16	1.04
BC1-90	t	220.0	220.0	7.1	284		15.5	1.000	23.15	23.28	0.99
BC2-90		219.7	219.7	8.2	181		13.4	1.000	23.67	21.74	1.09
4C1-90		114.6	114.6	5.9	224	90	9.7	1.000	17.28	18.50	0.93
BT1-90		220.0	220.0	7.1	284		15.5	1.000	27.78	23.28	1.19
BT2-90		219.7	219.7	7.6	312		14.5	1.000	28.71	22.62	1.27

(1) = Measured non-dimensional strength $\dfrac{M}{P_y T^2 d}$

(2) = Predicted non-dimensional strength $(6.202\beta - 0.266)\gamma^b$

TABLE A.6   DATABASE FOR T JOINTS UNDER IN PLANE MOMENT LOAD

Specimen	Type	D (mm)	d (mm)	T (mm)	F_y (N/mm²)	θ°	$\gamma = \dfrac{D}{2T}$	$\beta = \dfrac{d}{D}$	(1)	(2)	$\dfrac{(1)}{(2)}$
BL-40-.3	T	164.5	42.7	4.7	471	90	17.5	0.260	4.09	4.13	0.99
BL-40-.5		165.2	76.3	4.5	471	90	18.4	0.462	5.46	5.87	0.93
BL-70-.2		318.5	60.5	4.4	441	90	36.2	0.190	4.10	3.52	1.16
BL-70-.4		318.5	139.8	4.4	441	90	36.2	0.439	5.51	5.67	0.97
BL-100-.2		457.2	89.1	4.8	402	90	47.6	0.195	4.12	3.56	1.16
BL-100-.4		457.2	165.2	4.8	402	90	47.6	0.361	4.36	5.00	0.87
G1	T	507.2	171.5	11.1	352	90	22.8	0.338	4.39	4.80	0.91
G2		507.2	171.5	11.1	352	90	22.8	0.338	4.83	4.80	1.01
H1		507.2	326.4	11.1	352	90	22.8	0.644	7.29	7.45	0.97
H2		507.2	326.4	11.1	352	90	22.8	0.644	7.86	7.45	1.05
I1		507.2	455.9	11.1	352	90	22.8	0.899	13.40	12.82	1.05
I2		507.2	455.9	11.1	352	90	22.8	0.899	13.45	12.82	1.05
E1	Y	507.2	455.9	11.1	352	30	22.8	0.899	14.96	12.82	1.17
E2		507.2	455.9	11.1	352	30	22.8	0.899	14.90	12.82	1.16
C2-1-90	X	507.2	326.4	11.1	352	90	22.8	0.644	5.83	7.45	0.78
C2-1-30		507.2	455.9	11.1	352	30	22.8	0.899	12.31	12.82	0.96
C2-2-90		507.2	326.4	11.1	352	90	22.8	0.644	8.32	7.45	1.11
C2-2-30		507.2	455.9	11.1	352	30	22.8	0.899	14.67	12.82	1.14

(1) = Measured non-dimensional strength $\dfrac{M_u \sin\theta}{F_y T^2 d}$

(2) = Predicted non-dimensional strength $(1.879 + 8.642\beta)\, Q'_\beta$

TABLE A.7   DATABASE FOR T, Y and K JOINTS UNDER OUT-OF-PLANE MOMENT LOAD

Specimen	Type	D (mm)	d (mm)	T (mm)	F_y (N/mm²)	θ°	$\gamma = \dfrac{D}{2T}$	$\beta = \dfrac{d}{D}$	(1)	(2) or (3)	$\dfrac{(1)}{(2)}$	$\dfrac{(1)}{(3)}$	Load
B													
O I7	DT	407.7	274.3	8.1	321	90	25.2	0.673	20.65	19.62	1.05	-	IPB
O 08	DT	407.7	274.3	8.1	321	90	25.2	0.673	7.82	7.75	-	1.01	OPB
N													
E (27)													
T I24	DT	407.0	407.0	8.0	336	90	25.4	1.000	29.25	29.92	0.98	-	IPB
E 023	DT	407.0	407.0	8.0	336	90	25.4	1.000	14.25	14.10	-	1.01	OPB
X													
A													
S (28)													

(1) = Measured non-dimensional strength $\dfrac{M_1}{F_y T^2 d}$

(2) = IPB predicted non-dimensional strength $(6.202\beta - 0.266)\gamma^b$

(3) = OPB predicted non-dimensional strength $(1.879 + 8.642\beta) \sqrt{\gamma\beta}$

TABLE A.8   DATABASE FOR DT JOINTS UNDER IN-PLANE AND OUT-OF-PLANE MOMENT LOADS

APPENDIX B

Table structure (rotated 90°). Column headers, left to right:

| Specimen | Joint Type | Brace Load | D (mm) | d (mm) | T (mm) | F_y (N/mm²) | θ'_c | θ'_t | $\zeta = \frac{g}{D}$ | $\tau = \frac{D}{T}$ | $\rho = \frac{d}{D}$ | $P_u \sin\theta$ (kN) | u | Test Q_f | $\gamma\beta^2$ | Chord load |

TABLE B.1 DATABASE FOR CHORD STRESS EFFECTS - Continued

TABLE B.1 DATABASE FOR CHORD STRESS EFFECTS

Specimen	Joint Type	Brace Load	D (mm)	d (mm)	T (mm)	F_y (N/mm²)	θ'_a	θ'_t	$C = \beta$	$\tau = \frac{D}{T}$	$\beta = \frac{d}{D}$	$P_u \sin\theta$ (kN)	U	Test Q_f	γU^2	Chord load
L-1.6-2	YT	balanced axial load	165.2	76.3	1.6	331	45	90	0.46	51.0	0.462	20.3	-0.354	0.93	6.3	Axial compression
L-2.3-15			165.2	76.3	2.3	282	45	90	0.46	35.1	0.462	36.9	-0.417	0.83	6.7	Axial compression
L-3.2-2			165.2	76.3	3.2	283	45	90	0.46	25.8	0.462	82.8	-0.417	0.84	4.5	Axial compression
W-1.6-2			165.2	76.3	1.6	326	90	45	0.46	50.7	0.462	28.3	-0.361	0.82	6.6	Axial compression
W-2.3-5			165.2	76.3	2.3	284	90	45	0.46	35.8	0.462	48.5	-0.415	0.92	6.2	Axial compression
W-3.2-2			165.2	76.3	3.2	331	90	45	0.46	26.0	0.462	103.8	-0.354	0.75	3.3	Axial compression
A22	DT	Comp	407.7	274.3	8.1	331	90	-	-	25.2	0.673	103.3	-0.798	0.52	15.7	Compression
A95		Comp	407.7	274.3	8.1	331	90	-	-	25.2	0.673	237.3	-0.608	0.74	9.1	Compression
A46		Comp	407.7	274.3	8.1	331	90	-	-	25.2	0.673	305.1	-0.458	0.87	5.1	Comp/bend
IP12		IPB	407.7	274.3	8.1	331	90	-	-	25.2	0.673	72.8*	-0.608	0.63	5.1	Compression
IM11		IPB	407.7	274.3	8.1	331	90	-	-	25.2	0.673	87.6*	-0.458	0.81	5.1	Comp/bend
OP9		OPB	407.7	274.3	8.1	331	90	-	-	25.2	0.673	36.55*	-0.668	0.81	9.1	Compression
OM16		OPB	407.7	274.3	8.1	331	90	-	-	25.2	0.673	41.9*	-0.458	0.93	5.1	Comp/bend
A233	DT	Comp	407.0	407.8	8.0	336	90	-	-	25.4	1.000	778.4	-0.670	1.01	11.4	Compression
A46		Comp	407.0	142.1	8.0	336	90	-	-	25.4	0.350	130.0	-0.610	0.63	9.5	Compression
AM47		Comp	407.0	142.1	8.0	336	90	-	-	25.4	0.350	154.8	-0.470	0.75	3.6	Comp/bend
IP29		IPB	407.0	407.8	8.0	336	90	-	-	25.4	1.000	159.1*	-0.660	0.62	11.1	Compression
IM30		IPB	407.0	407.0	8.0	336	90	-	-	25.4	1.000	173.8*	-0.470	0.68	5.6	Comp/bend
OP27		OPB	407.0	407.8	8.0	336	90	-	-	25.4	1.000	126.3*	-0.660	1.01	11.1	Compression

(1) - * denotes brace load in kN (IPB/OPB in brace)

(2) - Chord compressive stresses denoted by negative sign

(3) $U = \sqrt{f_a^2 + f_{b1}^2 + f_{bo}^2}$

TABLE B.2   DT JOINTS – DATABASE FOR BRACE LOAD INTERACTION EFFECTS

Specimen	Joint Type	D (mm)	d (mm)	T (mm)	F_y (N/mm²)	θ°	γ	β	RESULTS COMP (kN)	RESULTS OFB (kNM)	RESULTS IPB (kNM)	(1)	(2)	(3)
A-1		407.7	274.3	8.1	321	90	25.2	0.673	350	–	–	1.00	1.67	1.00
O-8		407.7	274.3	8.1	321	90	25.2	0.673	–	45	–	1.00	1.70	1.00
I-7		407.7	274.3	8.1	321	90	25.2	0.673	–	–	119	1.00	1.77	1.00
AO-4		407.7	274.3	8.1	321	90	25.2	0.673	88	36	–	1.01	1.86	1.05
AO-13	DT	407.7	274.3	8.1	321	90	25.2	0.673	234	20	–	1.04	1.83	1.11
AI-20		407.7	274.3	8.1	321	90	25.2	0.673	112	–	100	1.01	2.83	1.03
AI-17		407.7	274.3	8.1	321	90	25.2	0.673	234	–	78	1.08	2.48	1.10
IO-15		407.7	274.3	8.1	321	90	25.2	0.673	24	43	39	1.03	2.22	1.13
IO-14		407.7	274.3	8.1	321	90	25.2	0.673	22	30	77	1.01	2.59	1.15
AIO-16		407.7	274.3	8.1	321	90	25.2	0.673	88	38	37	1.15	2.25	1.19
AIO-18		407.7	274.3	8.1	321	90	25.2	0.673	221	17	46	1.08	2.09	1.16
AIO-19		407.7	274.3	6.1	321	90	25.2	0.673	219	16	40	1.01	1.93	1.09

NOTES   (1) = Normalised by measured values of P_u and M_u using Equation 46

(2) = Normalised by predicted characteristic values of P_k and M_k using Equation 46

(3) = Normalised by measured values of P_u and M_u using Equation 47

Reference	Specimen	β	Y	Results			(1)	(2)	(3)	(4)
				$\left(\frac{P}{P_u}\right)$	$\left(\frac{M}{M_u}\right)_{IPB}$	$\left(\frac{M}{M_u}\right)_{OPB}$				
S	N4	0.77	10.6	1.06	0.16	—	0.02	0.03	1.27	0.05
P	N6	0.77	10.6	0.94	0.38	—	0.13	0.14	1.13	0.14
A	N7	0.77	10.6	0.95	0.38	—	0.13	0.14	1.14	0.14
R	J3	0.66	11.4	0.81	0.09	—	0.01	0.01	1.08	0.01
R	J7	0.66	11.4	0.66	0.88	—	0.76	0.77	0.88	1.05
O	K3	0.66	10.6	1.00	0.08	—	0.01	0.01	1.35	0.02
W	K4	0.66	10.6	0.96	0.13	—	0.01	0.02	1.30	0.04
	K5	0.66	10.6	0.96	0.19	—	0.02	0.04	1.30	0.08
	K6	0.66	10.6	0.98	0.35	—	0.13	0.12	1.32	0.28
	C3	0.42	10.6	1.11	0.12	—	0.01	0.02	1.06	0.01
	C4	0.42	10.6	1.09	0.15	—	0.02	0.02	1.04	0.01
(41)	C5	0.42	10.6	1.08	0.21	—	0.04	0.04	1.03	0.03

Notes:

(1) $= \left(\frac{M}{M_u}\right)^{2.1}_{IPB} + \left(\frac{M}{M_u}\right)^{1.2}_{OPB}$

(2) $= \left(\frac{M}{M_u}\right)^{2}_{IPB} + \left(\frac{M}{M_u}\right)^{1.0}_{OPB}$

(3) $= \left(\frac{P}{P_k}\right)$

(4) $= \left(\frac{M}{M_k}\right)^{2.0}_{IPB} + \left(\frac{M}{M_k}\right)^{1.0}_{OPB}$

TABLE B.3 – T JOINTS – DATABASE FOR BRACE LOAD INTERACTION EFFECTS FROM INSTITUTE TNO AND KINGSTON POLYTECHNIC

Results

Reference	Specimen	β	Y	$\left(\dfrac{P}{P_u}\right)$	$\left(\dfrac{M}{M_u}\right)_{IPB}$	$\left(\dfrac{M}{M_u}\right)_{OPB}$	(1)	(2)	(3)	(4)
	3	0.36	8	-	1.00	-	1.00	1.00	-	2.31
	24	0.36	8	0.39	0.98	-	0.96	0.96	0.45	2.22
	25	0.36	8	0.82	0.50	-	0.23	0.25	0.96	0.58
	5	0.36	8	1.00	-	-	-	-	1.17	-
	26	0.36	8	0.68	-	0.66	0.66	0.66	0.80	0.78
	4	0.36	8	-	-	1.00	1.00	1.00	-	1.18
	54	0.36	8	0.50	0.70	0.70	1.12	1.19	0.57	1.95
	27	0.36	8	-	0.80	0.80	1.39	1.44	0	2.41
S	69	0.68	8	1.00	-	-	-	-	1.18	-
	70	0.68	8	-	1.00	-	1.00	1.00	-	1.99
T	71	0.68	8	-	-	1.00	1.00	1.00	-	1.16
	76	0.68	8	-	0.70	0.60	1.01	1.09	-	1.66
	77	0.68	8	0.42	0.45	0.45	0.57	0.65	0.49	0.92
O	72	0.68	8	0.80	0.50	-	0.23	0.25	0.94	0.49
	37	0.68	8	0.40	0.88	-	0.76	0.77	0.48	1.51
L	75	0.68	8	0.70	-	0.37	0.30	0.37	0.83	0.43
(40)	74	0.68	8	0.37	-	0.64	0.58	0.64	0.44	0.74
	1	0.36	15	-	1.00	-	1.00	1.00	-	1.39
	23	0.36	15	-	0.79	0.68	1.24	1.30	-	1.72
	2	0.36	15	-	-	1.00	1.00	1.00	-	1.24
	21	0.36	15	0.40	-	0.70	0.65	0.70	0.42	0.87
	22	0.36	15	0.80	-	0.51	0.45	0.51	0.84	0.63
	6	0.36	15	1.00	-	-	-	-	1.06	-
	7	0.36	15	0.73	0.56	-	0.30	0.31	0.77	0.45
	8	0.36	15	0.37	0.88	-	0.76	0.77	0.39	1.08

TABLE B.3 - (Continued)

Results

Reference	Specimen	β	γ	$\left(\frac{P}{P_u}\right)$	$\left(\frac{M}{M_u}\right)_{IPB}$	$\left(\frac{M}{M_u}\right)_{OPB}$	(1)	(2)	(3)	(4)
S T O L (40)	10	0.68	15	-	1.00	-	1.00	1.00	-	0.85
	32	0.68	15	-	0.92	0.46	1.23	1.31	-	1.17
	33	0.68	15	-	0.48	0.95	1.15	1.18	-	1.10
	11	0.68	15	-	-	1.00	1.00	1.00	-	0.95
	31	0.68	15	0.35	-	0.78	0.74	0.78	0.41	0.74
	30	0.68	15	0.7	-	0.40	0.33	0.40	0.83	0.38
	9	0.68	15	1.00	-	-	-	-	1.19	-
	28	0.68	15	0.70	0.39	-	0.14	0.15	0.83	0.13
	29	0.68	15	0.37	0.78	-	0.59	0.61	0.44	0.53
	57	0.68	15	0.45	0.50	0.50	0.67	0.75	0.54	0.69
	58	0.68	15	0.62	0.33	0.50	0.53	0.61	0.73	0.57
	61	1.00	15	-	1.00	-	1.00	1.00	-	1.44
	67	1.00	15	-	0.80	0.78	1.37	1.42	-	1.68
	62	1.00	15	-	-	1.00	1.00	1.00	-	0.94
	66	1.00	15	0.44	-	0.87	0.85	0.87	0.43	0.82
	65	1.00	15	0.90	-	0.47	0.40	0.47	0.89	0.44
	60	1.00	15	1.00	-	-	-	-	0.99	-
	63	1.00	15	0.90	0.45	-	0.19	0.20	0.89	0.29
	64	1.00	15	0.44	0.87	-	0.75	0.76	0.43	1.08
	68	1.00	15	0.53	0.58	0.55	0.81	0.89	0.52	1.00
	13	0.36	24	-	1.00	-	1.00	1.00	-	1.51
	38	0.36	24	-	0.35	0.85	0.93	0.97	-	1.39
	14	0.36	24	-	-	1.00	1.00	1.00	-	1.41
	37	0.36	24	0.31	-	0.79	0.75	0.79	0.43	1.11
	36	0.36	24	0.93	-	0.60	0.54	0.60	1.29	0.85
	12	0.36	24	1.00	-	-	-	-	1.39	-

TABLE B.3 (Continued)

Reference	Specimen	β	γ	Results (P/Pu)	Results (M/Mu)IPB	Results (M/Mu)OPB	(1)	(2)	(3)	(4)
	34	0.36	24	0.87	0.43	—	0.17	0.18	1.21	0.27
	35	0.36	24	0.40	0.85	—	0.71	0.72	0.56	1.10
	53	0.36	24	0.42	0.54	0.63	0.85	0.92	0.57	1.34
	16	0.68	24	—	1.00	—	1.00	1.00	—	1.28
	44	0.68	24	—	0.80	0.52	1.08	1.16	—	1.51
	43	0.68	24	—	0.35	0.90	0.99	1.02	—	1.37
S	17	0.68	24	—	—	1.00	1.00	1.00	—	1.36
	41	0.68	24	0.30	—	0.80	0.76	0.80	0.46	1.08
T	42	0.68	24	0.60	—	0.40	0.33	0.40	0.90	0.54
	15	0.68	24	1.00	—	—	—	—	1.51	—
O	40	0.68	24	0.82	0.40	—	0.15	0.16	1.23	0.20
	39	0.68	24	0.40	0.80	—	0.63	0.64	0.60	0.81
L (40)	55	0.68	24	0.40	0.40	0.56	0.64	0.72	0.60	0.96
	56	0.68	24	0.60	0.30	0.35	0.36	0.44	0.90	0.58
	19	1.00	24	—	1.00	—	1.00	1.00	—	1.64
	49	1.00	24	—	0.56	0.67	0.91	0.98	—	1.31
	20	1.00	24	—	—	1.00	1.00	1.00	—	1.18
	47	1.00	24	0.30	—	0.70	0.65	0.70	0.39	0.82
	48	1.00	24	0.58	—	0.40	0.33	0.40	0.76	0.47
	18	1.00	24	1.00	—	—	—	—	1.31	—
	45	1.00	24	0.74	0.37	—	0.12	0.14	0.97	0.23
	46	1.00	24	0.32	0.70	—	0.47	0.49	0.42	0.81
	59	1.00	24	0.42	0.37	0.48	0.54	0.62	0.55	0.80

TABLE B.3 — (Continued)

APPENDIX C

TABLE 2 EXPERIMENTAL AND NUMERICAL RESULTS - AXIALLY LOADED JOINTS																				
							TEST RESULTS				AVAILABLE FORMULAE				$F_{u,numerical}/F_{u,formulae}$				
JOINT	F_H	d_0	β	2γ	τ	$f_{y0,L}$ $f_{u0,L}$	F_u	Fail. Mode	$F_{u,num}$	$F_{u,test}$	Kurobane mean	IIW char.	API * 1.7	AWS * 1.8	Kurobane mean	IIW char.	API * 1.7	AWS * 1.8
	kN.	mm.				N/mm² N/mm²	kN.	(1)	kN.	$\dfrac{F_{u,test}}{F_{u,num}}$	kN.	kN.	kN.	kN.				
X1	-	408.0	0.6	40.0	1.0	331 435	430	1	446	1.04	439	385	387	383	1.02	1.16	1.15	1.16
XX2	0	408.0	0.6	40 0	1 0	331 435	532	2	565	1.06	-	-	-	383	-	-	-	1.48
XX3	+213	408 5	0.6	40 9	1 0	318 425	683	2	654	0.96	-	-	-	424	-	-	-	1.54
XX4	-231	408.5	0.6	40.9	1.0	318 425	422	2	414	0.98	-	-	-	304	-	-	-	1.36

(1) Modes of failure

1   Plastic deformation leading to failure of chord cross section
2   Plastic deformation leading to failure of chord cross section + initiation of cracks at the weld toe(s)
3   Plastic deformation leading to failure of chord cross section + through cracks at the weld toe(s)
4   Squash load or full plastic moment of the brace(s)

Table 2   Experimental and numerical results – axially loaded joints

TABLE 3 EXPERIMENTAL AND NUMERICAL RESULTS - JOINTS LOADED BY BENDING [1]

JOINT	F_H kN	d_0 mm.	β	2γ	τ	$f_{y0,L}$ N/mm²	$f_{u0,L}$ N/mm²	TEST RESULTS M_u kNm.	M_{Yura} kNm.	Fail. Mode [2]	$M_{num.Yura}$ kNm.	$\dfrac{M_{num,Yura}}{M_{test,Yura}}$	AVAILABLE FORMULAE [3] mean kNm.	[3] char. kNm.	API *1.7 kNm.	AWS *1.8 kNm.	$M_{num.,Yura}/M_{u,formulae}$ [3] mean kNm.	[3] char. kNm.	API *1.7 kNm.	AWS *1.8 kNm.
X5	-	408.5	0.6	40.9	1.0	318	425	133	132	2	126	0.96	125	114	93	84	1.01	1.11	1.36	1.50
XX6	0	408.0	0.6	40.0	1.0	331	435	145	145	2	140	0.96	·	·	·	·	·	·	·	·
XX7	+242	408.5	0.6	40.9	1.0	318	425	161	160	2 + 4	151	0.94	·	·	·	·	·	·	·	·
XX8	-213	408.5	0.6	40.4	1.0	268	395	111	110	2	104	0.95	·	·	·	·	·	·	·	·
X9	-	408.0	0.6	40.0	1.0	331	435	63	63	2	71	1.13	59	51	52	52	1.20	1.38	1.36	1.36
XX10	0	408.5	0.6	40.4	1.0	268	395	82	77	3	73	0.96	·	·	·	·	·	·	·	·
XX11	+213	408.5	0.6	40.4	1.0	268	395	77	·	3	73 [4]	0.95 [4]	·	·	·	·	·	·	·	·
XX12	-262	408.0	0.6	40.0	1.0	331	435	81	68	3	78	1.1·	·	·	·	·	·	·	·	·

(1) : All moments have been calculated at the intersection of the system lines ! For the moments at the crown intersection of the chord and brace, the moments have to be multiplied by 0.85.
M_{Yura} = moment at Yura's deformation limit

(2) : Modes of failure :

1 : Plastic deformation leading to failure of chord cross section
2 : Plastic deformation leading to failure of chord cross section + initiation of cracks at the weld toe(s)
3 : Plastic deformation leading to failure of chord cross section + through cracks at the weld toe(s)
4 : Squash load or full plastic moment of the brace(s)

(3) : Formulae recommended by Wardenier (1982)

(4) : For XX11, $M_{test,u}$ has been taken instead of $M_{test,Yura}$

Table 3   Experimental and numerical results – joints loaded by bending

joint	$F_{u,up}$		Multiplanar joints								$M_1 = 0.0$	
			Pre-load									
			$-0.6\,F_{u,up}$		0.0		$0.6\,F_{u,up}$		$F_{u,up}$			
	$F_{u,up}$ kN	$\dfrac{F_{u,up}}{f_{y,o}\cdot t_o^2}$	$M_{1,u,ipb}$ kNm	$\dfrac{M_{1,u,ipb}}{f_{y,o}\cdot t_o^2\cdot d_1}$	$M_{1,u,ipb}$ kNm	$\dfrac{M_{1,u,ipb}}{f_{y,o}\cdot t_o^2\cdot d_1}$	$M_{1,u,ipb}$ kNm	$\dfrac{M_{1,u,ipb}}{f_{y,o}\cdot t_o^2\cdot d_1}$	$M_{1,u,ipb}$ kNm	$\dfrac{M_{1,u,ipb}}{f_{y,o}\cdot t_o^2\cdot d_1}$	$F_{2,u}$ kN	$\dfrac{F_{2,u}}{f_{y,o}}$
XX1A3	289.	6.74	19.5	5.10	20.4	5.35	21.0	5.51			289.	6.
XX1A7	457.	10.63	55.4	7.82	64.5	9.09	68.9	9.72			454.	10
XX1A9	3215.	11.55	542.8	7.98	620.7	9.12	661.8	9.73			3962.	14
XX1A10	1195.	13.15	232.3	10.45	278.4	12.53	312.6	14.07			1401.	15
XX1A11	598.	13.93	124.4 **	11 84 **	153.9	14.66	180.4	17.18	115.3 *	10.98 *	679.	15
XX1A12	326.	14.35	74.6 **	13.43 **	92.8	16.70	111.3	20.03			362.	15

Remark :
* : the numerical analysis has been stopped before the rotation reached Yura's deformation limit
** : ultimate moment reached before the rotation exceeded Yura's deformation limit

Table 3 : Numerical results of the multiplanar XX-joints loaded by in-plane bending on the in-plane braces and axial forces on the out-of-plane

APPENDIX D

TABLE G.1 DATABASE FOR OVERLAPPING YT JOINTS

SPECIMEN	TYPE	D (mm)	d (mm)	T (mm)	θ_c°	θ_t°	$\zeta = g/D$	$\gamma = \frac{D}{2T}$	$\beta = \frac{d}{D}$	P_y (N/mm^2)	(1) (KN)	(2)	Qg
2	O/L YT	323.9	168.3	6.35	90	45	-0.127	25.504	0.520	289.6	929.6	79.6	5.47
3	O/L YT	323.9	168.3	6.35	90	45	-0.377	25.504	0.520	289.6	1232.1	105.5	7.25
II-2	OL/ YT	168.3	114.3	7.92	90	45	-0.319	10.625	0.679	312.3	865.1	44.2	2.30
II-4	O/L YT	168.3	88.9	5.60	90	45	-0.137	15.027	0.528	321.9	597.8	59.2	4.01
II-7	O/L YT	219.1	114.3	5.60	90	45	-0.129	19.563	0.522	311.6	581.8	59.5	4.07
II-8	O/L YT	219.1	141.3	5.60	90	45	-0.278	19.563	0.645	310.9	732.2	75.1	4.23
II-10	O/L YT	273.1	114.2	4.80	90	45	-0.005	28.448	0.419	306.1	220.2	31.2	2.59
II-11	O/L YT	273.1	141.3	4.80	90	45	-0.129	28.448	0.517	311.7	534.6	74.4	5.14
II-12	O/L YT	273.1	168.3	4.80	90	45	-0.146	28.448	0.616	321.9	678.1	91.4	5.39
II-14	O/L YT	219.1	88.9	5.60	90	45	-0.166	19.563	0.406	321.3	550.2	54.6	4.66
II-15	O/L YT	273.1	88.9	4.80	90	45	-0.143	28.448	0.326	317.9	566.2	77.3	7.95
II-16	O/L YT	273.1	114.3	4.80	90	45	-0.181	28.448	0.419	317.9	550.2	75.1	6.24
(45) II-17	O/L YT	273.1	141.3	4.80	90	45	-0.301	28.448	0.517	310.9	723.2	101.0	6.97
379	O/L YT	318.2	165.2	4.40	90	45	-0.130	36.159	0.519	419.5	438.42	54.0	3.72
413	O/L YT	219.1	95.3	4.65	90	45	-0.020	23.559	0.435	370.7	352.73	44.0	3.54
414	O/L YT	219.1	95.3	4.65	90	45	-0.260	23.539	0.435	370.7	424.47	53.0	4.26

(Row group labels in left margin: PAN et al (45) for specimens 2 through II-17; KUROBANE (7) for specimens 379, 413, 414.)

Notes:
(1) Measured ultimate load for compression brace. For Pan et al data the through and overlapping braces are not explicitly defined.

(2) Measured non-dimensional strength = $\dfrac{P_u \sin\theta}{F_y T^2}$

(3) Q_g = ratio of measured strength to that predicted for a simple T joint

(4) All joints have balanced axial loads